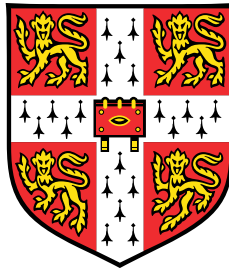


STOMATAL REGULATION IN C₄ PHOTOSYNTHESIS



Emmanuel L. Bernardo

Supervisor: Dr. Johannes Kromdijk

Department of Plant Sciences
University of Cambridge

This dissertation is submitted for the degree of
Doctor of Philosophy

Emmanuel College

October 2023

For my mother . . .

Declaration

I hereby declare that except where specific reference is made to the work of others, the contents of this dissertation are original and have not been submitted in whole or in part for consideration for any other degree or qualification in this, or any other university. This dissertation is my own work and contains nothing which is the outcome of work done in collaboration with others, except as specified in the text and Acknowledgements. This dissertation contains fewer than 65,000 words including appendices, bibliography, footnotes, tables and equations and has fewer than 150 figures.

Emmanuel L. Bernardo

October 2023

Abstract

Stomatal conductance in C₄ photosynthesis

Emmanuel L. Bernardo

The productivity of crops is largely determined by how efficiently they convert carbon dioxide (CO₂) into organic molecules through the process of photosynthesis. The exchange of gases between the atmosphere and the leaf intercellular spaces is facilitated by stomata, tiny pores found on the leaf epidermis. These pores act as gateways, allowing CO₂ to enter the leaf while water vapor exits through transpiration. The regulation of stomatal behavior results in a trade-off between CO₂ uptake and water loss in higher plants.

While genetic and biochemical analysis of stomatal regulation has focused heavily on the C₃ species *Arabidopsis thaliana*, it is well-known that stomatal regulation can vary between different species and different photosynthetic types. Therefore, this PhD project aimed to investigate stomatal regulation in C₃ and C₄ plants, comparing their responses to changes in light and CO₂. To control for potential confounding effects not related to photosynthetic type, three phylogenetically-controlled species from Cleomaceae, *Flaveria*, and *Alloteropsis* were used in the study.

Chapter focused on the response to blue and red light in C₃ and C₄ species. The study found that stomatal opening was highly responsive to blue light in a red light background in C₃ dicot species of Cleomaceae and *Flaveria*, which confirmed previous observations in *Arabidopsis*. However, stomatal conductance in C₄ dicot species was not responsive to the same treatment. In addition, stomatal opening in C₃ and C₄ species responded significantly to red light, while the intercellular CO₂ was kept constant. However, this response appeared to be largely species-specific, rather than associated with photosynthetic pathway.

The next chapter investigated stomatal regulation by [CO₂]. To distinguish responses linked to photosynthesis vs responses driven by mitochondrial respiration, CO₂ responses were assessed in darkness and under illumination with red light similar to growing condi-

tions. Whereas the C₃ species showed significant opening responses to sub-ambient CO₂ in darkness, C₄s were invariable. In contrast, the opening response to sub-ambient CO₂ under illumination was stronger in the C₄ species. Together with the differences in blue light response in Chapter 2, this may suggest that stomatal opening in the C₄ species relies more on guard cell photosynthesis and less on mitochondrial respiration, compared to the C₃ species.

Finally, in the last chapter of the thesis, using NADP-ME antisense lines of C₄ *F. bidentis*. It was hypothesized that perturbing the C₄ cycle, resulting in reduced carbon flux into the bundle sheath cells, may alter stomatal regulation. The study found that mutant plants had significantly increased operating C_i compared to control plants. When C_i was kept the same as the control plants a significant increase in stomatal opening was observed in the mutant lines, suggesting that disruption of the C₄ cycle disrupted stomatal sensitivity to CO₂. Further exploration of molecular factors known to be involved in the guard cell CO₂ response was performed, but turned out inconclusive.

Altogether, the work in this thesis shows that while stomatal regulation in response to CO₂ and light has remained qualitatively similar to the ancestral C₃ pathway, quantitative shifts in sensitivity may have supported further optimization of CO₂ assimilation and water use efficiency following evolution of the C₄ pathway.

Acknowledgements

Firstly, I want to express my sincere thanks to Wanne Kromdijk. I am deeply grateful for his generosity, patience, and encouragement during my time in the group, and the writing of this manuscript. I can only aspire to attain his sharp eye for detail and logic. Lastly, I express my most profound gratitude for his understanding, particularly during the numerous occasions when I fell short of being my best self.

Special thanks to Cristina Rodrigues Gabriel Sales, my postdoc partner for enduring my mood swings, guiding me through enzyme assays, and of course, for being never absent during my monthly meetings; your presence has been invaluable. My heartfelt acknowledgment goes to Julia for teaching me the basic tools of molecular biology, and for the myriad ways she supported me through the challenges of my PhD. And, of course, Rich, your generosity in troubleshooting the 6400XTs and your immense patience in the face of my mishaps with those machines have not gone unnoticed. My sincere thanks to Lucia for taking care of our *Alloteropsis* and generously sharing her plants whenever mine were less than thriving. To Georgia Taylor and Alice Robijns, for the engaging science chats and for listening to my PhD rants. I am grateful to Jessica Royles, our lab manager, for keeping the lab in order and our experiments possible, and to fellow members of the Kromdijk Group, Angie Burnett, John Fergusson, Lee Cacket, Alistair Leverett, Rohan Richard. A special shoutout to Weng Yik, my favorite Asian in the group, for joining me for lunch (even if it was primarily motivated by Emma's generous portions and top-notch meals and desserts).

I extend my gratitude to Professor Julian Hibberd and the members of his group, both past and present, for generously sharing their expertise and providing invaluable assistance throughout the execution of my experiments. Special thanks are due to Ivan Reyna-Llorens, Zhengao Di, Connor Simpson, Pallavi Singh, Gregory Reeves, Haiyan Xiong, Tina Schreier, Leonie Luginbuehl, Kumari Billakurthi, Patrick Dickinson, Susan Stanley, and Tianshu Sun for their technical support, and for the welcoming environment in Lab 101.

Thanks to Rachel Wong, from the Griffiths Group, for her friendship, as well as for generously allowing me to indulge in more than half of the cakes and pastries she brings to the office.

Thank you to The Philippine Council for Agriculture, Aquatic and Natural Resources Research and Development (PCAARRD) and Department of Science and Technology – Science Education Institute for funding my PhD Research.

Thank you to the Institute of Crop Science, College of Agriculture and Food Science, UPLB, for allowing me to pursue my PhD.

I am thankful for Nigel Boulding, Emma Jackson, and Mark Johns at the PGF, and to the Department of Plant Sciences for granting me hardship funding whilst I wrapped up my experiments.

Thank you to Emmanuel College for the additional funds to support my extended stay in Cambridge.

I would like to thank my family and friends, here and overseas. Special mention goes to my mother, Elena, to whom I dedicate this work; my father, Edison, and my siblings, Edelson, Ellaine, Eric, and Edileen. The presence of my nephew, Lorcan, and my niece, Yona, has given me renewed appreciation not to over-complicate life, for which I'm truly thankful.

Table of contents

List of figures	xvii
List of tables	xxi
1 Introduction	1
1.1 Sustainable Crop Production and the Global Carbon and Water Cycles	1
1.2 Stomata control carbon and water exchange between plants and the atmosphere	2
1.3 Environmental regulation of stomatal conductance	4
1.3.1 Regulation of stomatal movement by light	4
1.4 Regulation of stomatal movement by CO ₂	6
1.5 Stomatal regulation between C ₃ and C ₄ photosynthesis	6
1.5.1 C ₃ versus C ₄ photosynthesis	6
1.6 Phylogenetically-controlled experimental models to compare C ₃ and C ₄ . .	8
1.6.1 Cleomaceae family	8
1.6.2 <i>Flaveria</i> genus	9
1.6.3 <i>Alloteropsis</i> subspecies	9
1.7 Transgenic plants with altered photosynthetic activities	10
1.8 Hypotheses and Thesis Objectives	11
1.8.1 Hypotheses	11
1.8.2 Research Aims	11

Table of contents

2	A comparison of stomatal conductance responses to blue and red light between C₃ and C₄ photosynthetic species in three phylogenetically-controlled experiments	13
2.1	Introduction	13
2.2	Materials and Methods	15
2.2.1	Plant materials	15
2.2.2	Growth conditions	15
2.2.3	Gas exchange measurements	16
2.2.4	Determination of the red light response	17
2.2.5	Stomatal morphology and density using epidermal impressions . . .	18
2.2.6	Experimental design and data analysis	18
2.3	Results	19
2.3.1	Stomatal sensitivity to blue light is lower in C ₄ dicots compared to their C ₃ counterparts	19
2.3.2	C ₃ and C ₄ subspecies of the monocot <i>A. semialata</i> display the canonical blue light response	30
2.3.3	Red light response in phylogenetically-close pairs of C ₃ and C ₄ dicots and monocots, at constant C _i	35
2.3.4	Stomatal morphology and density	43
2.4	Discussion	50
2.4.1	C ₄ dicots are less sensitive to blue light than C ₃ dicots	51
2.4.2	Differences in stomatal red light response are determined by species, rather than photosynthetic pathway	52
2.4.3	Role of stomatal morphology and density on stomatal movements in response to light	53
2.5	Conclusion	55
3	Investigating stomatal responses to CO₂ in C₃ and C₄ pairs of congeneric dicot species	57

Table of contents

3.1	Introduction	57
3.2	Materials and Methods	59
3.2.1	Plant materials and growth conditions	59
3.2.2	Gas exchange measurements	59
3.2.3	Experimental design	59
3.2.4	Statistical analysis	60
3.3	Results	60
3.3.1	Cleomaceae, under increasing then decreasing CO ₂ concentration	60
3.3.2	g _s response curve of Cleomaceae under decreasing then increasing CO ₂ concentration	61
3.3.3	g _s response curve of <i>Flaveria</i> under increasing then decreasing CO ₂ concentration	64
3.3.4	g _s response curve of <i>Flaveria</i> , under decreasing then increasing CO ₂ concentration	64
3.3.5	Log-linear curve-fitting to systematically analyze responses to CO ₂ , light and presence of significant hysteresis	67
3.4	Discussion	77
3.4.1	Investigating g _s responses to varying CO ₂ concentrations	77
3.4.2	C ₄ stomata are relatively closed at ambient CO ₂ and remain closed at supra-ambient CO ₂	78
3.4.3	Stomata in C ₄ dicots are more sensitive to CO ₂ and showed limited stomatal movements in darkness than their C ₃ counterparts	79
3.5	Conclusion	80
4	Investigating g_s regulation in C₄ <i>Flaveria bidentis</i> with a diminished C₄ cycle	81
4.1	Introduction	81
4.2	Materials and Methods	84
4.2.1	Plant materials	84

Table of contents

4.2.2	Growth conditions	84
4.2.3	PCR confirmation and copy number estimation	84
4.2.4	SDS-PAGE and immunoblot analysis	85
4.2.5	Gas exchange measurements	86
4.2.6	Leaf harvesting and protein and chlorophyll contents	88
4.2.7	Enzyme activity assays	88
4.2.8	Extraction of epidermal peels for RT-qPCR	90
4.2.9	Stomatal morphology and density using impressions	90
4.2.10	Statistical analysis	90
4.3	Results	92
4.3.1	Transgenic <i>F. bidentis</i> with decreased NADP-ME activity	92
4.3.2	Enzyme activities and chlorophyll content	94
4.3.3	C_i is significantly increased in NADP-ME antisense lines of C_4 <i>F. bidentis</i>	96
4.3.4	g_s is elevated in NADP-ME antisense lines of C_4 <i>F. bidentis</i> at the C_i of the WT	98
4.3.5	Stomatal density and size remained unaltered in NADP-ME antisense lines	101
4.3.6	Gene expression analysis	102
4.4	Discussion	105
4.4.1	NADP-ME antisense construct did not have any pleiotropic effects.	106
4.4.2	Stomatal patterning and morphology can acclimate to CO_2 , but do not explain the observed differences in g_s in NADP-ME antisense lines.	107
4.4.3	Genes involved in stomatal CO_2 response and malate metabolism appear unchanged in NADP-ME mutants.	108
4.4.4	Could altered guard cell malate metabolism potentially explain the higher g_s observed in the antisense lines?	108

4.4.5 Conclusion	109
5 General Discussion	111
5.1 Thesis Summary	111
5.2 Discussion and Future work	112
5.2.1 Using phylogenetically-controlled comparisons is essential in understanding C ₄ photosynthesis.	112
5.2.2 Insensitivity to blue light and limited contributions from mitochondrial respiration may underlie stomatal movements in C ₄ dicot stomata.	113
5.2.3 The interaction between red light-induced stomatal opening and the CO ₂ response pathway is mediated both by C _i -dependent and C _i -independent mechanisms.	114
5.2.4 Do C ₄ dicot guard cells exhibit altered sensitivity to C _i , or do they perceive C _a instead of C _i ?	115
5.2.5 What is the functional role of CBC1/2 in CO ₂ sensing in Cleomaceae and <i>Flaveria</i> species?	116
References	119

List of figures

1.1	Stomatal traits vary between species.	3
2.1	Response of g_s in C_3 <i>T. hassleriana</i> and C_4 <i>G. gynandra</i> to R→RB→R and RB→R→RB light.	20
2.2	Time course of A in C_3 <i>T. hassleriana</i> and C_4 <i>G. gynandra</i> in response to a sequence of 100% red to 75% red + 25% blue light and vice versa.	22
2.3	Time course of g_s in C_3 and C_4 <i>Flaveria</i> species in response to a sequence of 75% red + 25% blue light and vice versa	24
2.4	Response of g_s in C_3 and C_4 <i>Flaveria</i> species to R→RB→R light.	27
2.5	Time course of A in C_3 and C_4 <i>Flaveria</i> species in response to a sequence of 75% red + 25% blue light and vice versa.	29
2.6	Response of g_s in C_3 and C_4 <i>Alloteropsis semialata</i> to R→RB→R and RB→R→RB light.	31
2.7	Time course of A in C_3 and C_4 <i>A. semialata</i> in response to a sequence of 75% red + 25% blue light and vice versa.	34
2.8	Response of g_s and A to red light PFD in C_3 <i>T. hassleriana</i> and C_4 <i>G. gynandra</i>	36
2.9	Response of g_s to red light PFD in C_3 and C_4 <i>Flaveria</i> species.	38
2.10	Response of A to red light PFD in C_3 and C_4 <i>Flaveria</i> species.	40
2.11	Red light response in C_3 and C_4 <i>Alloteropsis semialata subspecies</i>	42
2.12	Stomatal density and size per leaf surface in C_3 and C_4 pairs of Cleomaceae, <i>Flaveria</i> , and <i>Alloteropsis</i>	45

List of figures

2.13	Nail varnish impressions from leaf surfaces of C ₄ <i>G. gynandra</i> at x400 and C ₃ <i>T. hassleriana</i> at x600 used in the study.	46
2.14	Nail varnish impressions from leaf surfaces of <i>Flaveria</i> species used in the study.	48
2.15	Nail varnish impressions from leaf surfaces of <i>A. semialata</i> subspecies used in the study.	49
2.16	Stomatal size vs stomatal density in C ₃ and C ₄ pairs of Cleomaceae, <i>Flaveria</i> and <i>Alloteropsis</i> used in the study.	50
3.1	Response of g _s in Cleomaceae to recursive sequences of increasing or decreasing CO ₂	63
3.2	Response of g _s in <i>Flaveria</i> to recursive sequences of increasing or decreasing CO ₂	66
3.3	Plots of g _s as a function of C _i in C ₄ <i>G. gynandra</i> for all light and CO ₂ conditions.	68
3.4	Violin/box plots of the slope parameter from log-linear fits of the C ₄ <i>G. gynandra</i> and C ₃ <i>T. hassleriana</i> CO ₂ response curves.	69
3.5	Plots of g _s as a function of C _i in C ₃ <i>T. hassleriana</i> for all light and CO ₂ conditions.	70
3.6	Violin/box plots of the slope parameter from log-linear fits of the C ₃ <i>T. hassleriana</i> CO ₂ response curves.	71
3.7	Plots of g _s as a function of C _i in C ₄ <i>F. bidentis</i> for all light and CO ₂ conditions.	73
3.8	Slope parameter from log-linear fits of C ₄ <i>F. bidentis</i>	74
3.9	Plots of g _s as a function of C _i in C ₃ <i>F. cronquistii</i> for all light and CO ₂ conditions.	75
3.10	Slope parameter from log-linear fits of C ₃ <i>F. cronquistii</i>	76
4.1	NADP-ME protein expression in WT and antisense lines of C ₄ <i>F. bidentis</i>	93
4.2	Activities of NADP-ME (malic enzyme), PEPC, and Total Rubisco and Rubisco activation in WT and NADP-ME antisense lines of C ₄ <i>F. bidentis</i>	94

4.3	Total chlorophyll and total soluble protein contents from crude leaf extracts in 80%EtOH of 8-week-old plants.	95
4.4	Time course of g_s in WT and antisense lines of <i>F. bidentis</i>	97
4.5	Box plot of overall mean g_s and C_i in WT and three antisense lines of <i>F. bidentis</i>	98
4.6	Response g_s and A to red light PFD in WT and NADP-ME <i>F.bidentis</i> antisense lines	100
4.7	Stomatal density and size per leaf surface in WT and NADP-ME antisense lines of C_4 <i>F. bidentis</i>	101
4.8	Transcript levels of FbGASA9, FbOST1, FbHT1, and FbMPK12 in whole leaves, and abaxial and adaxial epidermises in WT and antisense lines of C_4 <i>F. bidentis</i>	103
4.9	Transcript abundance of key C_4 enzymes in whole leaves, and abaxial and adaxial epidermises in WT and antisense lines of C_4 <i>F. bidentis</i>	104

List of tables

2.1	Repeated measures (mixed-effects) ANOVA of g_s in Cleomeaceae under R→RB→R sequence (Fig. 2.1A, $R^2=0.96$, RMSE = 0.044).	21
2.2	Repeated measures (mixed-effects) ANOVA of g_s in Cleomeaceae under RB→R→RB sequence (Fig. 2.1B, $R^2=0.93$, RMSE = 0.029).	21
2.3	Repeated measures (mixed-effects) ANOVA of A in Cleomeaceae under R→RB→R sequence ($R^2=0.98$, RMSE = 0.397).	23
2.4	Repeated measures (mixed-effects) ANOVA of A in Cleomeaceae under RB→R→RB sequence ($R^2=0.93$, RMSE = 0.87).	23
2.5	Repeated measures (mixed-effects) ANOVA of g_s in three species of <i>Flaveria</i> under R→RB→R sequence ($R^2=0.97$, RMSE = 0.017).	25
2.6	Repeated measures (mixed-effects) ANOVA of g_s in three species of <i>Flaveria</i> under RB→R→RB sequence ($R^2=0.99$, RMSE = 0.014).	25
2.7	Repeated measures (mixed-effects) ANOVA of g_s in five species of <i>Flaveria</i> under R→RB→R sequence ($R^2=0.97$, RMSE = 0.0017). To carry out the analysis, g_s at the introduction or removal of blue light (t = 5 min and t =65 min, R→BR→R) or the reverse (t = 5 and t = 65, BR→R→BR), and the final g_s at t = 125 min were extracted from the gas exchange time series.	28
2.8	Repeated measures (mixed-effects) ANOVA of g_s in <i>Alloteropsis</i> under R→RB→R sequence ($R^2=0.91$, RMSE = 0.009).	32
2.9	Repeated measures (mixed-effects) ANOVA of g_s in <i>Alloteropsis</i> under RB→R→RB sequence ($R^2=0.87$, RMSE = 0.011).	32
2.10	Repeated measures (mixed-effects) ANOVA of A in <i>Alloteropsis</i> under R→RB→R sequence ($R^2=0.98$, RMSE = 0.510).	35

List of tables

2.11	Repeated measures (mixed-effects) ANOVA of A in <i>Alloteropsis</i> under RB->R->RB sequence ($R^2=0.90$, RMSE = 0.872).	35
2.12	Repeated measures (mixed-effects) ANOVA of A in Cleomaceae under varying intensities of red light ($R^2=0.024$, RMSE = 0.977).	37
2.13	Repeated measures (mixed-effects) ANOVA of g_s in Cleomaceae under varying intensities of red light ($R^2=1.825$, RMSE = 0.93).	37
2.14	Repeated measures (mixed-effects) ANOVA of g_s in <i>Flaveria</i> under varying intensities of red light ($R^2=0.027$, RMSE = 0.91).	39
2.15	Repeated measures (mixed-effects) ANOVA of g_s in <i>Flaveria</i> under varying intensities of red light ($R^2=1.926$, RMSE = 0.92).	41
2.16	Repeated measures (mixed-effects) ANOVA of g_s in <i>Alloteropsis</i> under varying intensities of red light ($R^2=0.99$, RMSE = 0.002).	42
2.17	Repeated measures (mixed-effects) ANOVA of A in <i>Alloteropsis</i> under varying intensities of red light ($R^2=0.88$, RMSE = 0.797).	43
3.1	Mixed-effects ANOVA of the slope parameter in C ₄ <i>G. gynandra</i> in all light and CO ₂ conditions.	69
3.2	Mixed-effects ANOVA of the slope parameter in C ₃ <i>T. hassleriana</i> in all light and CO ₂ conditions.	71
3.3	Mixed-effects ANOVA of the slope parameter in C ₄ <i>F. bidentis</i> in all light and CO ₂ conditions.	74
3.4	Mixed-effects ANOVA of the slope parameter in C ₃ <i>F. cronquistii</i> in all light and CO ₂ conditions.	76
4.1	Primers pairs used in phenotyping and copy number estimation, and in determining relative transcript abundance of selected CO ₂ core signalling pathway genes.	87

Chapter 1

Introduction

1.1 Sustainable Crop Production and the Global Carbon and Water Cycles

The Sustainable Development Goals (SDGs) are a set of 17 global goals adopted by all United Nations Member States in 2015 as part of the 2030 Agenda for Sustainable Development. These goals represent a framework designed to address a range of global challenges, including climate change and environmental degradation, which directly impact global crop production and availability of water resources [133].

SDG 2 is "Zero Hunger" and aims to end hunger, achieve food security, improve nutrition, and promote sustainable agriculture [133]. By 2050, the world population is expected to reach the 10 billion mark according to a projection by the UN [89], from its current 8 billion. Thus, to feed a growing global population, agricultural productivity needs to increase while promoting responsible and efficient resource management. However, current crop production practices at a global scale are placing significant strain on both water and land resources in many places. The unprecedented rate at which the world is heating up is also putting intense pressure on these precious resources, severely impacting global food supply.

In the context of modern crop production, maximum plant productivity is determined by the efficiency with which plants transform carbon dioxide into organic molecules through photosynthesis and release water back into the atmosphere through a process called transpiration. This trade-off of carbon dioxide and water molecules is facilitated by tiny pores found on leaf surfaces, termed stomata. Stomata therefore control plant water status,

Introduction

leaf temperature, and carbon assimilation rates [61]. The ease with which stomata allow CO₂ into or water out of the leaf is called stomatal conductance (g_s), which adjusts depending on stomatal aperture. Stomatal aperture, in turn, is governed by changes in osmotic potential and turgor pressure in guard cells (GCs) surrounding the stomatal pore in response to a variety of cues [53]. Arguably, the two main environmental drivers of stomatal responses are light and [CO₂].

Enhancing plant productivity and water use efficiency (WUE, the amount of carbon gained for every water loss) requires a comprehensive understanding of steady state g_s and stomatal dynamics in response to light and CO₂. Not surprisingly, as the gateway of CO₂ and water, stomata play a central role in addressing the question of how to increase the amount of carbon fixed per unit of water lost through transpiration from a crop. However, despite the vast researches dedicated to this topic over the course of the last century, a lot of open questions and knowledge gaps remain.

The task of a crop scientist of our times is elegantly summed up in the following passage,

"...that whoever could make two ears of corn, or two blades of grass, to grow on a spot of ground where one grew before, would deserve better of mankind and do more essential service to his country..." -Jonathan Swift

1.2 Stomata control carbon and water exchange between plants and the atmosphere

The epidermis of the plant leaf has small pores on its surface that act as physical gateways to let CO₂ into the leaf and allow the escape of water vapour. Individual pores are termed a "stoma" (stomata, *pl.*), from the Latin meaning "mouth". Specialised turgor-operated "guard" cells surround a stoma, and together, a stoma and pair of guard cells form a stomatal complex.

Stomatal pores are not passive and are instead highly regulated by endogenous and exogenous cues. Abscisic acid and high internal [CO₂] are well-known signals that induce stomatal closing. Irradiance, low [CO₂], and high humidity meanwhile triggers opening responses. Stomatal movements operate by perceiving a signal and adjusting the turgor pressure in the guard cell. Stomatal opening involves the accumulation of solute, mainly K⁺, Cl⁻ and malate, as well as sugars, upon activation of H⁺-ATPases and ion-selective channels.

1.2 Stomata control carbon and water exchange between plants and the atmosphere

The closing response is a reversal of this process, which involves metabolising the solutes, or releasing them to the apoplast [59, 50]

Stomata display a wide range of morphology, size, and distribution (Fig.1.1). For most dicots, stomata are defined by a pair of elliptic-shaped guard cells. In monocots, stomata are dumbbell-shaped with additional subsidiary cells flanking the guard cells, such as those found among grasses. The contrasting morphology of grass stomata facilitates more rapid responses to short-term and long-term perturbations [42, 15] which may have contributed to their fast colonisation of semi-arid and arid niches [125, 126].

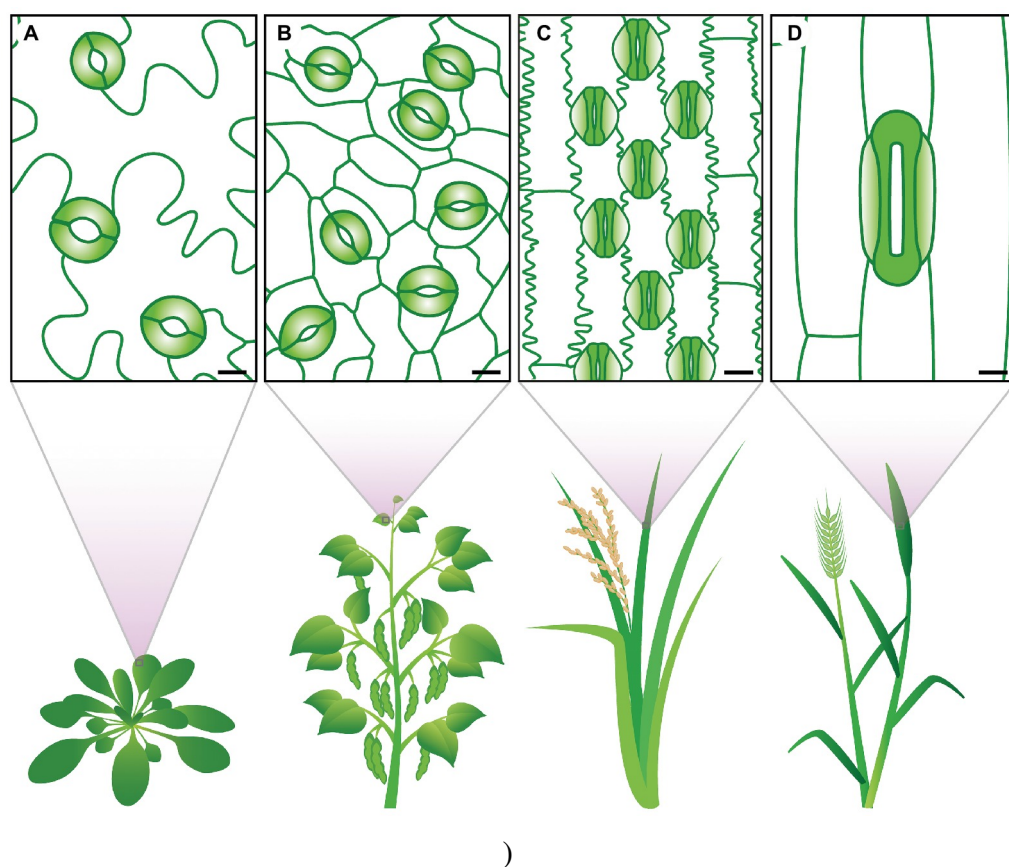


Fig. 1.1 Stomatal traits vary between species. The eudicots (A) *Arabidopsis thaliana* and (B) *Phaseolus vulgaris* display kidney-shaped guard cells (colored in green). The grasses (C) *Orzya sativa* and (D) *Triticum aestivum* show dumbbell-shaped guard cells (solid green) and specialized subsidiary cells (light green gradient). Clear differences in stomatal size and stomatal density can be observed. Scale bars 10 μ M. (Image and caption from [10])

1.3 Environmental regulation of stomatal conductance

Efficient coordination of carbon gain versus water loss by stomata is achieved by a range of responses to environmental factors, most notably light and CO₂. Signals are either perceived directly in the guard cells, or indirectly via signals derived from the underlying mesophyll.

1.3.1 Regulation of stomatal movement by light

Blue light perception and signaling

Blue light induces the opening of stomata. This observation was first reported in *Phaseolus vulgaris* [102] where two varieties grown in full sun or shade showed a distinct stomatal response to BL. The implication was that species with contrasting growth habits might also utilise the stomatal response of BL differently depending on the habitat and its role in the ecophysiology of the leaves [143].

BL activates rapid stomatal opening via a pathway that is independent of photosynthesis and saturates at relatively low fluence rates [117]. Blue light has a direct and independent effect through autophosphorylation of phototropins, PHOT1 and PHOT2. Upon perception of blue light, PHOT1 is autophosphorylated and leads to a transient increase in Ca²⁺. PHOT2, a homologue of PHOT1, functions redundantly via their substrate BLUS1 (BLUE LIGHT SIGNALING 1) [49, 122] and CBC1/2 (CONVERGENCE OF BLUE LIGHT AND CO₂) kinases, which inhibit S-type anion channels [43]. Following membrane hyperpolarization, the activation of inwardly-rectifying K⁺ channels leads to the uptake of K⁺ [58]. Additionally, blue light induces the accumulation of malate and sucrose through starch breakdown or biosynthesis. Both of these processes contribute to an elevated solute content within guard cells, The accumulation of K⁺ and other solutes such as Cl⁻, malate and/or soluble sugars drives the influx of water into the GCs and the resulting turgor change leads to stomatal opening [123, 124].

The red light response

Red light can also stimulate stomatal opening. However, unlike blue light-induced opening, stomatal opening under red light requires higher flux rates and continuous illumination. The increase in g_s is directly proportional to increasing light intensity [8, 116] and is eliminated by inhibitors of photosynthetic electron transport, including 3-(3,4-dichlorophenyl)-1,1-

1.3 Environmental regulation of stomatal conductance

dimethylurea (DCMU), indicating that it is photosynthesis dependent, and indicating that chlorophyll could be the receptor [79]. This is supported by the observation that the stomata in albino leaf patches of *Vicia faba* and *Chlorophytum comosum* remained unresponsive to red light, while still exhibiting stomatal opening when exposed to blue light [104]. Stomatal opening is triggered by red light by driving mesophyll photosynthesis, reducing C_i . The reduction in C_i due to red light could be observed when large areas of a leaf are illuminated, but not when a single beam of red light is projected onto guard cells only [103], implying that the red light-induced stomatal opening was an indirect response to the reduction of C_i by photosynthesis. This response to red light is seen as the primary mechanism linking stomatal behaviour with mesophyll demands.

However, this feedback loop does not appear to be the only mesophyll-derived signal perceived by stomata. A significant response to red light was still observed in experiments where C_i was kept constant [82]. In addition, epidermal peel experiments revealed that GCs response to red light are reversibly altered by the presence of the underlying mesophyll tissue. Lee and Bowling (1992) demonstrated that isolated epidermis of *Commelina communis*, incubated without mesophyll cells or with dark-adapted chloroplasts, exhibits limited stomatal opening. In contrast, when the epidermis is co-cultured with illuminated mesophyll cells or chloroplasts, stomata open fully [65]. Thus, a link between mesophyll photosynthesis and guard cell responses must exist [63]. Busch (2014) proposed an alternative signaling mechanism in which the redox state of the chloroplastic plastoquinone (PQ) pool, rather than a signal derived from photosynthesis, communicates with stomatal guard cells. However, additional work is required to investigate the connection between the PQ redox state and the regulation of stomatal movements triggered by red light [56].

Interestingly, red light enhances blue light-mediated stomatal opening. A weak blue light illumination with a background of strong red light induces rapid stomatal opening in *Arabidopsis*, whereas no opening occurs without red light [117]. The mechanism that leads to K^+ uptake that drives stomatal opening by red light is not yet known, but recent evidence shows involvement of the PM^+ -ATPase. In the case of *Arabidopsis*, red light triggers the photosynthesis-dependent phosphorylation of threonine, which is the penultimate residue of $PM H^+$ -ATPase. This biochemical process results in stomatal opening, as reported by Ando et al. (2018) [2]. In contrast, in the presence of red light, elevated CO_2 induces guard cell $PM H^+$ -ATPase dephosphorylation as well as stomatal closure [4]. Similar to the stomatal opening responses, many components of the closing signalling pathways are still unidentified.

1.4 Regulation of stomatal movement by CO₂

Higher WUE is generally associated with stomatal morphological traits. For example, decreasing stomatal density (SD) or altering patterning has been seen as a promising strategy to develop crops with enhanced WUE, which could lead to improved crop productivity and reduced vulnerability to climate change-induced drought stress.

In addition to manipulating stomatal morphological traits, understanding how stomata regulate their apertures based on [CO₂] is also important. The response of the stomatal aperture to changes in [CO₂] is well defined in the C₃ *Arabidopsis thaliana* and other C₃ crops: stomata closes in response to higher than ambient CO₂ concentrations and opens at low CO₂ concentrations.

Firstly, guard cells respond to changes in CO₂ concentration. Stomatal aperture measured on individual stomatal complexes generally decreases when exposed to short-term elevated CO₂ and increases under low CO₂ both in darkness and light [140]. As mentioned above, guard cells appear to perceive the CO₂ concentration in the substomatal cavity (C_i) instead of that surrounding the leaf (C_a), which offers a direct feedback loop with photosynthetic activity in the mesophyll tissue [85, 86], where the rate of CO₂ assimilation directly affects C_i and thereby indirectly impacts stomatal conductance (g_s). However, this signal from the mesophyll may not be the only mesophyll signal that controls stomatal movement [82, 63, 78].

1.5 Stomatal regulation between C₃ and C₄ photosynthesis

Genetic and biochemical analysis of stomatal regulation has been strongly focused on the genetic model C₃ species *Arabidopsis thaliana*, driven by the abundance of genomic resources for this species. However, it is well-known that stomatal regulation can differ strongly between different species [80]. This might be especially true for species which differ in their photosynthetic pathway, as detailed below.

1.5.1 C₃ versus C₄ photosynthesis

Plants with C₄ photosynthesis are distinct from C₃ plants in anatomy and biochemistry. C₄ operates a CO₂-concentrating mechanism (CCM) between two morphologically different cell

1.5 Stomatal regulation between C₃ and C₄ photosynthesis

types, bundle sheath (BS) and mesophyll (M) cells. These cells form concentric circles around the vascular bundles in a wreath-like pattern called ‘Kranz anatomy’, after the German word for wreath. In this two-cell conformation the initial carboxylation of phospho-enol pyruvate to form oxaloacetic acid is catalysed by phosphoenol pyruvate carboxylase (PEPC) in the cytosol of M cells. In the BS cells, local decarboxylation of C₄ acids malate and aspartate releases CO₂-close to the site of Rubisco expression, thereby enhancing photosynthesis and suppressing photorespiration.

Aside from improved CO₂ capture, the CCM confers C₄ species with superior water use efficiency (WUE) compared with C₃ and C₃-C₄ intermediates. The higher WUE in C₄ plants is facilitated by the higher affinity of PEPC for inorganic carbon, compared to Rubisco, which allows the same rate of photosynthesis at lower intercellular CO₂. However, this likely requires altered guard cell sensitivity to C_i. C₄ photosynthesis does not saturate with light intensity as much as C₃ photosynthesis. Additionally, C₄ photosynthesis is typically (close to) CO₂-saturated, which may make CO₂ assimilation rates less dependent on stomatal conductance than in C₃ photosynthesis. Thus, the link between guard cell responses and photosynthesis of the underlying mesophyll tissue may be easier to deconvolute. And finally, C₄ photosynthesis requires higher vein density [105, 84], with typically a maximum of only three adjacent mesophyll cells. This drastically alters leaf hydraulic properties and likely stomatal conductance.

The C₄ CCMs are grouped based on the three major C₄ decarboxylases they utilise, solely or in conjunction with a secondary decarboxylase: nicotinamide adenine dinucleotide-malic enzyme (NAD-ME), nicotinamide adenine dinucleotide phosphate-malic enzyme (NADP-ME), and phosphoenolpyruvate carboxykinase (PCK). Each subtype, aside from leaf biochemistry, also differs in terms of anatomy, geographical distribution, and resource use [32].

Having a CCM alters the relationship of photosynthesis with CO₂ in C₄ species (Fig. 2B) which confers them photosynthetic advantage over C₃ species under saturating light conditions and hot environments. In these environments, C₄ species typically display higher intrinsic water use efficiency and net assimilation rates [105] compared to C₃ species. It can be argued that differential stomatal regulation is required to optimize photosynthetic capacity and water use efficiency between C₃ and C₄ species.

Species with C₄ photosynthesis are known to exhibit reduction in stomatal density as well as the size of the pore complex [10], however not much is known about altered stomatal sensitivities under various environmental conditions. The anatomical and biochemical

Introduction

features of C_4 photosynthesis both give reason to hypothesize that the regulation of stomatal conductance in response to these environmental factors must also have changed in C_4 photosynthesis.

1.6 Phylogenetically-controlled experimental models to compare C_3 and C_4

In evolutionary timescale, the C_4 syndrome is a recent occurrence. It developed at least 63 times independently in angiosperms ([108, 107, 109] suggesting that the transition from ancestral C_3 to the derived C_4 state is an easy one in a genetic sense. An evolutionary model that integrates various aspects of biochemistry, leaf morphology and anatomy and physiology of the pathway has been proposed. In this model, it takes seven distinctive phases that culminate in an *optimized* C_4 pathway [105]. The optimization model prescribes a modular, transitory, and sequential progression from C_3 to C_4 , which has been shown to be flexible [139] rather than one-directional [41] in acquiring C_4 traits.

1.6.1 Cleomaceae family

Comparing C_3 and C_4 species would typically be confounded by phylogenetic distance between the species, which would lead to differences not necessarily associated with the photosynthetic pathway. Closely related species or even subspecies with differing variations in the pathways offer a way around this issue, allowing a comparison between photosynthetic types while controlling for phylogenetic effects [84, 46]. C_3 - C_4 intermediate and C_4 species are all found in the genus Cleomaceae from the family Cleomaceae, a phylogenetic sister to Brassicaceae to which *A. thaliana* belongs. Cleomaceae is the largest genus in Cleomaceae and contains roughly 200 to 250 species [47]. *Tarenaya hassleriana* is a typical C_3 in this family [16] that is most abundant in South America [92]. Also within this genus is *Gynandropsis gynandra*, a recognized C_4 species [76]. Two other species, *C. angustifolia* and *C. oxalidea* also exhibit features of C_4 . All three are classified as NAD-ME subtype which makes for a complementary comparison to C_4 *Flaveria* species, which are of the NADP-ME type [36]. The C_3 - C_4 *C. paradoxa* and C_3 species *C. africana* are also contained in this lineage [55]. Cleomaceae is widespread geographically. Species can be found in arid areas of Latin America and Africa [47] to the pan- and subtropics, and in Australia [37].

1.6 Phylogenetically-controlled experimental models to compare C₃ and C₄

Since Cleomaceae is a close relative to *Arabidopsis* [92], it provides a unique opportunity to utilize the abundance of genomic data on *Arabidopsis*. Genome sequences of *G. gynandra* [7] and *T. hassleriana* [16] are both available.

1.6.2 *Flaveria* genus

The genus *Flaveria*, a dicot, is another recognized model to examine evolution and function of C₄ photosynthesis. The genus contains six NADP-ME C₄ types, three C₃ species, nine C₃-C₄ intermediates and three C₄-like species. C₄ *F. trinervia* and *F. bidentis* are widely distributed in Africa, in the Caribbean, South America, including the Middle East, and in almost every state of Mexico [81] while C₃-like *F. pringlei* is located from South central Mexico. *F. pringlei* has proto-Kranz [110] and is not a canonical C₃. A true C₃ in the *Flaveria* is *F. cronquistii* [96]. Empirical evidence supports that the C₃ species of *Flaveria* are ancestral to the C₃-C₄ and C₄-like intermediates, as well as the true C₄ species [73, 81], and therefore presents an opportunity to analyse a continuum from the ancestral C₃ to the C₄ state. The genus has also provided insights into PEPC regulation [11].

1.6.3 *Alloteropsis* subspecies

Alloteropsis semialata is the only grass species with individuals encompassing C₃ and C₄ species (Russell, 1983) and intermediate phenotypes [72]. C₄ *A. semialata* is functionally classified as an NADP-ME subtype, but it primarily engages PEPCK. In particular, C₃+C₄ intermediate plants display a “weak C₄ cycle” only having rudimentary anatomical and biochemical features of a characteristic C₄ plant (Dunning et al., 2019). It has been suggested that the C₃ *A. semialata* subspecies might represent a reversal from the C₃-C₄ intermediate state [70]. Since *A. semialata* is a grass, it is also a monocot. Interestingly, the *A. semialata* C₄ subspecies show a wide geographical distribution [71] including cooler regions [137], whereas the C₃ subspecies are confined to Southeast Africa [71]. This seems to be in contradiction with the general notion that C₄ photosynthesis may be less able to acclimate to contrasting climatic conditions than C₃ species [108]. These ecological distributions make *A. semialata* an especially interesting model to evaluate the general applicability of observations on the two other models.

1.7 Transgenic plants with altered photosynthetic activities

Transgenic and mutant plants have been instrumental in uncovering the mechanisms of guard cells, the molecules that sense stimuli, and the pathways of signal transduction. Additionally, they have been useful in understanding ion uptake and regulation of ion channels, both of which are essential for stomatal sensitivity and behaviour [64].

Impaired photosynthesis mutants in C_3 species have been previously used to study the coordination of g_s and CO_2 assimilation. Several studies have employed RNA antisense to manipulate the expression of key photosynthetic enzymes in C_4 *Flaveria bidentis*. To date, specific targets have included Rubisco [31], NADP-malate dehydrogenase [132], pyruvate phosphate dikinase [30], Rubisco activase [135], carbonic anhydrase [18], PEPC protein kinase [33], and NADP-ME [94]. Studies in C_3 transgenics with altered photosynthetic capacity showed similar stomatal conductance values in transgenic plants compared to wild-type controls, despite a severe reduction in A and higher $[C_i]$ [45, 60, 119], suggesting altered guard cell sensitivity to CO_2 . Nevertheless, as these experiments were conducted under either white light or a red/blue light source, the possibility of an equal and direct stimulation of opening by blue light in both wild-type and transgenic plants, independent of photosynthesis, cannot be ruled out. To address this issue, Baroli and colleagues (2008) used only red light and still observed lack of sensitivity of guard cells to C_i in transgenic tobacco plants with low Rubisco or cytochrome *b₆f* content, in conjunction with earlier reports that used white or red/blue light [98, 97, 136]. In another study, antisense SBPase tobacco plants opened when exposed to increasing red light when C_i was kept constant supporting a C_i -independent signal [62]. In general, these findings may suggest that the connection between mesophyll photosynthesis and the stomatal response to CO_2 is not as straightforward as previously believed.

In transgenic potato with low PEPC activity, a role for PEPC and malate activity was supported by a decrease in stomatal movement in guard cells with reduced PEPC, while the over-expressors showed accelerated opening [34]. These findings are supported by work on *Amaranthus edulis* where plants deficient in PEPC showed slower rates of stomatal opening and low final g_s values [19]. However, Lawson (2009) argued that since the Cauliflower mosaic virus (CAMv) promoters were used in most studies, it was assumed that a) all cells were antisensed in a similar way, and therefore may also have changed the dynamics of the malate pool, and b) the observed response was equivalent to steady state g_s [61].

Although numerous studies documented observations of g_s , in general, research on transgenics with decreased photosynthetic ability was not specifically carried out to investigate g_s [61]. Furthermore, the cell-autonomous nature of C_3 photosynthesis will inadvertently affect the photosynthetic assimilate supply in the guard cells as in the mesophyll. In C_4 cycle mutants, this could be less of an issue, but similar studies in C_4 that aimed to explore the link between CO_2 assimilation and stomatal responses to CO_2 are lacking.

1.8 Hypotheses and Thesis Objectives

1.8.1 Hypotheses

1. Aside from leaf anatomy and biochemistry, C_3 and C_4 plants differ in stomatal regulation under short-term changes to light and CO_2 .
2. Control over stomatal movements in response to short-term changes to light and CO_2 is shared between guard cells and the underlying mesophyll.

1.8.2 Research Aims

1. To investigate how C_4 photosynthesis impacts on short-term regulation of stomatal conductance in response to environmental factors such as light and CO_2 .
2. To study the role of guard cell physiology and mesophyll photosynthesis in stomatal responses to CO_2 and light in C_4 species.

Chapter 2

A comparison of stomatal conductance responses to blue and red light between C₃ and C₄ photosynthetic species in three phylogenetically-controlled experiments

Published as Bernardo et al. 2023 Frontiers in Plant Science 14: 1253976

2.1 Introduction

Efficient coordination of carbon gain versus water loss by stomata is achieved by a range of stomata responses to these environmental factors, most notably light and CO₂. Light stimulates stomatal opening via at least two distinct signaling pathways with contrasting action spectra [117], which are either perceived directly in the guard cells or indirectly via signals derived from the underlying mesophyll [63, 86].

Blue light (BL) is a potent signal for stomatal opening, and guard cells contain all the components required for the blue light signaling pathway [117, 120]. Blue light initiates rapid stomatal opening via a pathway that is independent of photosynthesis and saturates at relatively low fluence rates. Blue light triggers the autophosphorylation of phototropins, PHOT1 and PHOT2 via their substrate BLUS1 (BLUE LIGHT SIGNALING 1) [49, 122]. This sequentially triggers the activation of plasma membrane H⁺ ATPase pump, which

A comparison of stomatal conductance responses to blue and red light between C₃ and C₄ photosynthetic species in three phylogenetically-controlled experiments

hyperpolarizes the plasma membrane, leading to the uptake of K⁺ through inward-rectifying channels. The accumulation of K⁺ and other solutes drives the influx of water into the GCs and the resulting turgor change leads to stomatal opening [117].

Illumination with red light (or photosynthetically active wavelengths other than blue) also triggers stomatal opening but the quantum efficiency to stimulate opening is typically lower than blue light. An indirect effect of red light that is tied to CO₂ inside the leaf (C_i, intercellular CO₂), is triggered by high (red) light through mesophyll photosynthesis, which reduces C_i, and consequently affects g_s. However, this feedback loop does not appear to be the only mesophyll-derived signal perceived by stomata. A significant response to red light was still observed in experiments where C_i was kept constant [82]. In addition, epidermal peel experiments revealed that GC responses to red light are reversibly altered by the presence of the underlying mesophyll tissue. Thus, an additional link between mesophyll photosynthesis and guard cell responses may exist [63]. The identity of the mesophyll signal however remains unresolved.

Plants with C₄ photosynthesis are distinct from C₃ plants in anatomy and biochemistry. C₄ operates a CO₂-concentrating mechanism (CCM) between two morphologically different cell types, bundle sheath cells (BSC) and mesophyll (M) cells [105]. Having a CCM alters the relationship of photosynthesis with CO₂ in C₄ species which confers them a photosynthetic advantage over C₃ species under saturating light conditions and hot environments [13]. In these environments, C₄ species typically display higher intrinsic water use efficiency and net assimilation rates [105] compared to C₃ species [59]. It can therefore be argued that differential stomatal regulation is required to optimize photosynthetic capacity and water use efficiency between C₃ and C₄ species. And that the mesophyll signal argued above may be different between C₃ and C₄ species. However, not much is known about stomatal sensitivities with regard to photosynthetic types under various light and CO₂ environments.

Comparisons between C₄ and C₃ species are easily be confounded by phylogenetic distance between the species, which would lead to differences not necessarily associated with the photosynthetic pathway [84]. For instance, contrasting blue light responses in C₃ and C₄ were observed in crop species [146], but the findings could not be directly linked to photosynthetic type alone because the species examined were separated by considerable phylogenetic distance. Closely related species or even subspecies with differing photosynthetic pathways offer a way around this issue, allowing a comparison between photosynthetic types while controlling for phylogenetic effects [84, 46].

In this study, blue and red-light stomatal responses were studied in three phylogenetically-controlled experiments, using closely related species from the Cleomaceae (*Tarenaya* and *Gynandropsis*), Asteraceae (*Flaveria*), and Poaceae (*Alloteropsis*) that use either C₃ or C₄ photosynthesis. The results show a striking lack of sensitivity to blue light in C₄ dicots, compared to their C₃ counterparts, which exhibited significant blue light responses. In contrast, in the monocot *A. semialata*, a weak blue light response was observed regardless of photosynthetic type. The quantitative red light response varied across species, and variation within-species was also observed as in the case of *Flaveria*. However, the presence or absence of a significant stomatal red light response was not related to differences in photosynthetic pathway.

2.2 Materials and Methods

2.2.1 Plant materials

Stomatal responses were compared across closely related C₃ and C₄ species from the Cleomaceae (*Cleome*), Asteraceae (*Flaveria*), and Poaceae (*Alloteropsis*), with considerable phylogenetic distance separating each of the controlled comparisons. From the genus *Cleome*, *Tarenaya hassleriana* (C₃) was compared with *Gynandropsis gynandra* (C₄). Seeds of C₃ *T. hassleriana* (Cleomaceae) were obtained from Prof. Julian Hibberd's group (Cambridge, UK). From the genus *Flaveria*, *F. cronquistii* and *F. robusta* (C₃) were compared with *Flaveria pringlei* (C₃-like) and with *Flaveria trinervia* and *Flaveria bidentis* (C₄). Seeds of *F. bidentis*, *F. trinervia*, and *F. pringlei* were a gift from Dr. Peter Westhoff (University of Dusseldorf, Germany). Clonal plants of *F. cronquistii* and *F. robusta* were a kind gift from Dr. Marjorie Lundgren (Lancaster University, UK) and Prof. Julian Hibberd (Cambridge University, UK), respectively. Finally, from the genus *Alloteropsis*, *A. semialata* subsp. *eckloniana* GMT (C₃) and *A. semialata* subsp. *semialata* MDG and MAJ (both C₄) were a gift from Prof. Pascal-Antoine Christin (University of Sheffield, UK).

2.2.2 Growth conditions

Seeds of C₃ *T. hassleriana* were germinated on moistened filter paper (Whatman, Grade 1) in a plastic Petri plate (90 mm x 150 mm). The plates containing the seeds were kept in a growth cabinet maintained at 27°C for 16 h during the day and were placed in an undisturbed

A comparison of stomatal conductance responses to blue and red light between C₃ and C₄ photosynthetic species in three phylogenetically-controlled experiments

part of the laboratory overnight to attain a nighttime temperature differential of at least 10°C for 5-7 days, or until the radicle emerged. Individual seedlings of *T. hassleriana* were then transplanted into 24-cell trays for 2-3 weeks before replanting them into 10 cm H x 9 cm L x 9 cm W plastic pots with M3 compost (Levington®, Evergreen Garden Care (UK) Ltd.). Gas exchange data were collected from the youngest recently expanded leaf from plants with 4-5 sets of mature leaves. Seeds of C₄ *G. gynandra* were sown in a community pot, also in M3 compost. Once the first true set of leaves appeared in two weeks the plants were transferred to individual 24-cell trays where the seedlings were allowed to develop for two more weeks until they were finally transferred to 10 cm H x 9 cm L x 9 cm W plastic pots. As with *T. hassleriana*, gas exchange measurements were taken from the youngest recently expanded leaf from plants with 4-5 sets of mature leaves.

Seeds of C₄ *F. bidentis*, C₄ *F. trinervia*, and C₃-like *F. pringlei* were germinated on M3 compost. After 1 week, seedlings with a pair of true leaves were individually transplanted to 24-cell seed trays where they were allowed to develop for 2 to 3 weeks before being transferred to 10 cm H x 9 cm L x 9 cm W plastic pots containing M3 compost. Clonal plants of C₃ *F. cronquistii* and C₃ *F. robusta* were propagated from cuttings. All gas exchange measurements were taken from plants with 4-5 sets of mature leaves.

The Cleomaceae and *Flaveria* were grown in an environmentally-controlled growth room at the Plant Growth Facility (PGF), Department of Plant Sciences, University of Cambridge. Photoperiod was kept at 16 hours (6:00 to 22:00) of light supplied by fluorescent lamps with a PPFD of 300 $\mu\text{mol m}^{-2} \text{s}^{-1}$. The growth room was maintained at day and night temperatures of 20°C and 60% RH at ambient CO₂. The *Alloteropsis* accessions were grown at the Cambridge Botanic Gardens Glasshouse. Plants were vegetatively propagated to contain 2-3 tillers per 1 L pots filled with 4:1 M3 compost: coarse vermiculite and 5 g controlled-release fertilizer (Osmocote®). Supplemental light from sodium halide lamps (140-160 W m⁻²) was provided from 4:00 to 20:00. Greenhouse set point temperature was at 18°C, while nighttime temperatures were at 15°C. CO₂ and RH were at ambient.

2.2.3 Gas exchange measurements

An open gas exchange system (LI-6400XT, LI-COR, Lincoln, NE, USA) with an integrated fluorometer and light source (LI-6400-40, LI-COR) was used to measure stomatal conductance (g_s) and assimilation rate (A).

Red and Blue light Switchover experiment

To characterize stomatal responses to light of different spectral compositions, a series of switchover protocols were designed comprising sequential changes between 100% red and 75% red + 25% blue light, while keeping the total photosynthetic photon flux density (PPFD) equal. In Sequence R→RB→R, leaves were first acclimated under 100% red light, and then switched to 75% red and 25% blue light, and then back to the original light environment of 100% red light. 500 $\mu\text{mol m}^{-2} \text{s}^{-1}$ PPFD was maintained throughout the time course for this experiment and the complementary sequence (RB→R→RB). Each switchover experiment was initiated when steady state was reached (typically after 2 h). Gas exchange measurements were logged every 60 s throughout the protocol. After logging the first 5 min (in Cleomaceae and *Alloteropsis*) and 10 min (in *Flaveria*) of the steady state condition, the light composition was switched to either red or red+blue, followed finally by a switch back to the initial light composition. During each phase gas exchange parameters were logged for 60 mins (in the Cleomaceae and *Alloteropsis*) and 50 mins (in *Flaveria*). Thus, for each measurement series, 125 mins were recorded for *Cleomaceae* and *Alloteropsis* subspecies and 100 mins for *Flaveria*. The initial experiment in *Flaveria* was performed using C₃-like *F. pringlei*, C₄ *F. trinervia* and C₄ *F. bidentis*. However, because C₃-like *F. pringlei* has proto-Kranz [37], it is not considered a canonical C₃. Therefore, a repeat experiment in *Flaveria* was performed to include two true C₃ species, *F. cronquistii* and *F. robusta*. For this experiment, only sequence R→RB→R was repeated, since the previous experiments had shown that both sequences yielded very similar results. Reference CO₂ during the experiment was controlled at 400 $\mu\text{mol mol}^{-1}$, block temperature was kept at 25°C and average VPD was ca. 1.2 kPa. All measurements were taken between 10:00 and 16:00 h.

2.2.4 Determination of the red light response

To characterize the red-light response of stomatal conductance, the protocol by Messinger et al. (2006) was adopted. This protocol measures the stomatal response to red light, while controlling for the potentially confounding effect of the stomatal CO₂ response by maintaining a constant intercellular CO₂ concentration (C_i) at each light intensity. Briefly, the Messinger protocol [31] involved illuminating the leaf segment clamped inside the cuvette with 800 $\mu\text{mol m}^{-2} \text{s}^{-1}$ red light to steady state. Subsequently, the PFD was lowered step-wise from 800 to 600, 400, 200, 0 $\mu\text{mol m}^{-2} \text{s}^{-1}$, each change was initiated once steady state of stomatal conductance was achieved. As A and g_s changed in response to the new light

A comparison of stomatal conductance responses to blue and red light between C₃ and C₄ photosynthetic species in three phylogenetically-controlled experiments

environment, CO₂ was manually adjusted using the mixer millivolt signal to keep C_i at the value observed at 800 μmol m⁻² s⁻¹.

2.2.5 Stomatal morphology and density using epidermal impressions

Epidermal imprints from all species, except for *Flaveria trinervia*, were taken from adaxial and abaxial layers using clear nail varnish (Rimmel, London) using the same leaves used for gas exchange measurements. Dried nail varnish was lifted from the leaf using sticky tape (Sellotape) and affixed onto glass slides. Images were captured using a Nikon microscope (Olympus BX41, Japan) fitted with a CCD camera (U-TV0.5zc- 3/Micropublisher 3.3 RTV, Olympus, Japan) and installed with (Q-Capture Pro 7 imaging software). Total magnifications of x200 and x400 (Olympus WHB 10x/20 eyepiece x Olympus PN 20x/0.40 or PCN 60x/0.80 objectives) were used for stomatal density counting and investigation of stomatal anatomical parameters, respectively, unless stated otherwise. For *Flaveria trinervia* the quality of nail varnish impressions was not sufficient to collect stomatal anatomical parameters, data were instead collected from epidermal peels, using the same microscopy set up with a total magnification of x400. Therefore, these data were not from the same leaf as was used for gas exchange but instead were taken from other leaves at the same developmental stage.

To assess stomatal size (SS), guard cell width (GCW) and guard cell length (GCL), were measured using FiJi software [115]. SS was calculated using the formula for the area of an ellipse. Stomatal density (SD) was calculated as the number of stomata per unit area (-mm²). A stoma was counted if >50% was located within the field of view. Four random microscopic fields of view each from the adaxial and abaxial surfaces were collected from 3-5 biological replicates, giving >300 stomata per species. Logarithmic models were fitted using the 'drc' package [100] in the RStudio environment to examine the relationship between SS and SD between photosynthetic types.

2.2.6 Experimental design and data analysis

For the red and red+blue light switchover experiments, pairs of C₃ and C₄ species were measured in parallel between 10:00 and 16:00 h to control for the effect of circadian rhythms on stomatal conductance. Each phylogenetically-controlled comparison was an independent experiment. To estimate the impact of light on stomatal conductance resulting from the shift from one light environment to the next, a linear mixed-effects model was used. Light was the

within-subject factor and species was the between-subject factor. Biological replicates were treated as random variables.

To carry out the analysis, g_s and A at the introduction or removal of blue light ($t = 5$ min and $t = 65$ min, $R \rightarrow BR \rightarrow R$) or the reverse ($t = 5$ and $t = 65$, $BR \rightarrow R \rightarrow BR$), and the final g_s at $t = 125$ min were extracted from the gas exchange time series. These values were used to assess the differences between g_s end-point values under R versus BR illumination via linear mixed-effects modelling.

Linear mixed-effects model was also fitted to the red light response data set. Red light PFD and species were assigned as within- and between-subject variables, respectively, while individual biological replicates were treated as random variables.

For every genus, the density of stomata and size of stomata on the abaxial and adaxial surfaces were analysed using a two-way ANOVA post-hoc comparisons were carried out using Tukey's HSD at an $\alpha=0.05$.

The statistical tests were carried out using R, version 4.2.1 and RStudio, version 2022.07.1 and JMP Pro 17 (SAS Institute).

Graphs were plotted using R, version 4.2.1 and RStudio, version 2022.07.1 and the *ggplot2* package [138]. Figures were compiled using the *ggpubr* package [51].

2.3 Results

2.3.1 Stomatal sensitivity to blue light is lower in C₄ dicots compared to their C₃ counterparts

To compare the sensitivity of stomatal opening to blue light relative to red light of equal intensity between C₃ and C₄ species, gas exchange was measured in response to a sequence of 75% red:25% blue (RB) light to 100% red (R) with a total PAR of 500 $\mu\text{mol photons m}^{-2} \text{s}^{-1}$ as well as the reverse sequence. Following steady state g_s of 0.49 $\text{mol H}_2\text{O m}^{-2} \text{s}^{-1}$ at R light, g_s in the C₃ species *T. hassleriana* increased gradually to 0.64 $\text{mol H}_2\text{O m}^{-2} \text{s}^{-1}$ upon shifting to RB light and the effect was rapidly reversed when the light was returned to R (Fig. 1.A.1). Similarly, when moving from $RB \rightarrow R$ in the reverse sequence, C₃ *T. hassleriana* rapidly declined from 0.38 to 0.20 $\text{mol H}_2\text{O m}^{-2} \text{s}^{-1}$, and gradually increased again by the

A comparison of stomatal conductance responses to blue and red light between C₃ and C₄ photosynthetic species in three phylogenetically-controlled experiments

switch from R→RB over the course of an hour (Fig. 1.B.1). In contrast, no effects of the R→RB→R sequence, nor the reverse RB→R→RB sequence were observed on g_s in the C₄ species *G. gynandra*, which remained invariable at 0.19 mol H₂O m⁻² s⁻¹ (Figs 1.A.2 and 1.B.2). It is also worth noting that the strong stomatal movements in C₃ *T. hassleriana* did not correspond to parallel responses in A (Fig.2.2A & B), which instead was not significantly impacted by the changes in light composition in either of the *Cleome* species (Fig.2.2).

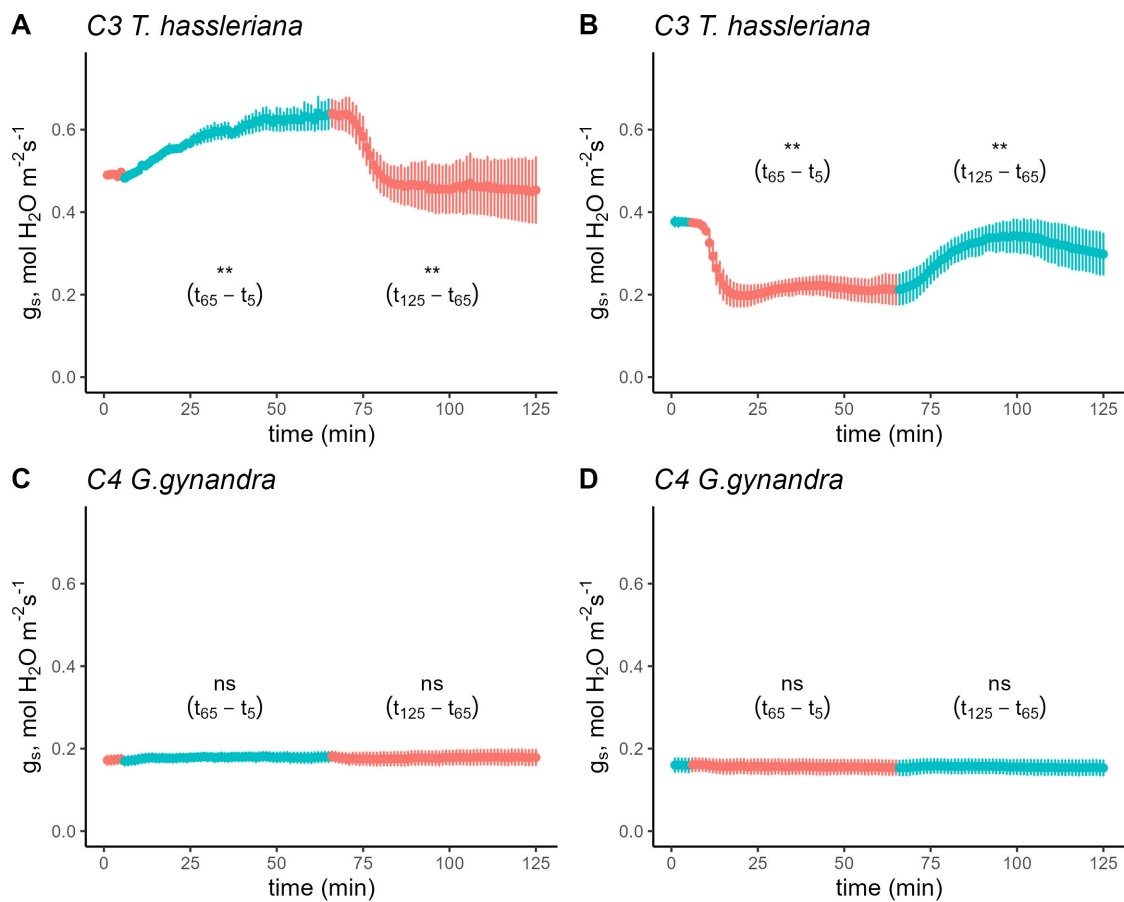


Fig. 2.1 Time course of g_s in C₃ *T. hassleriana* (A and B) and C₄ *G. gynandra* (C and D) in response to a sequence of 75% red + 25% blue light and vice versa. Leaves were initially acclimated in either 100% red or 75% red+25% blue light until steady-state was achieved. Subsequently, the light environment was switched depending on the initial light condition while maintaining an intensity of 500 $\mu\text{mol m}^{-2} \text{s}^{-1}$. Subsequently, the leaves were acclimated to the new light condition for 1 hr before returning it back to the original condition. Light conditions were reversed at t_6 and t_{65} . Reference CO₂ was maintained at 400 $\mu\text{mol mol}^{-1}$, block temperature was kept at 25°C and average VPD was 1.2 kPa. Data points represent mean \pm se (n=4-5). Asterisks indicate significant difference at the end of blue or red light sequence from the imposition of treatment.

Table 2.1 Repeated measures (mixed-effects) ANOVA of g_s in Cleomeaceae under R→RB→R sequence (Fig. 2.1A, $R^2=0.96$, RMSE = 0.044).

Source	DF	F ratio	Pr(>F)
Species	1	85.88	0.0002
Light	2	8.90	0.0060
Species x Light	2	8.10	0.0082

Table 2.2 Repeated measures (mixed-effects) ANOVA of g_s in Cleomeaceae under RB→R→RB sequence (Fig. 2.1B, $R^2=0.93$, RMSE = 0.029).

Source	DF	F ratio	Pr(>F)
Species	1	16.99	0.0092
Light	2	14.45	0.0011
Species x Light	2	12.52	0.0019

A comparison of stomatal conductance responses to blue and red light between C₃ and C₄ photosynthetic species in three phylogenetically-controlled experiments

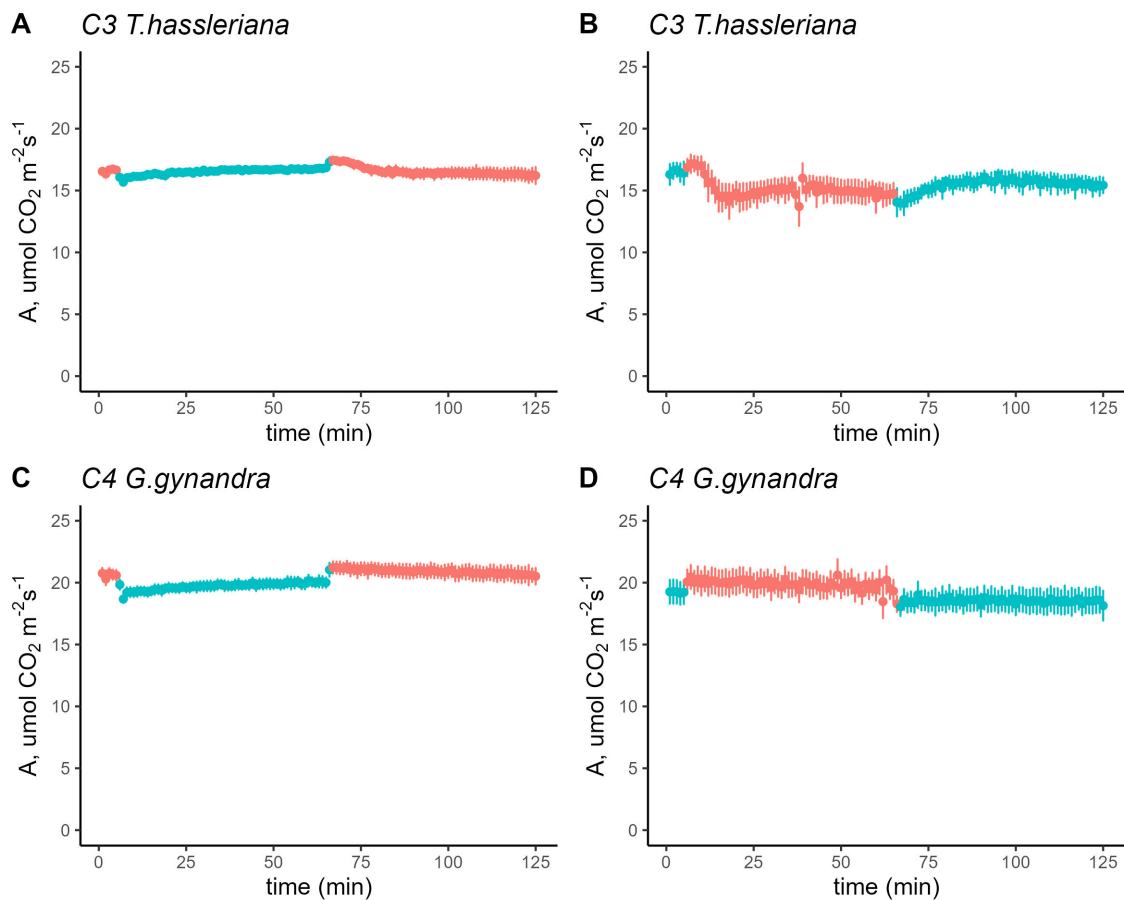


Fig. 2.2 Time course of A in C₃ *T. hassleriana* (A and B) and C₄ *G. gynandra* (C and D) in response to a sequence of 100% red to 75% red + 25% blue light and vice versa. Leaves were initially acclimated in either 100% red or 75% red+25% blue light until steady state was achieved. The light environment was switched depending on the initial light condition while maintaining $500 \mu\text{mol m}^{-2} \text{ s}^{-1}$. The leaves were acclimated in the new light condition for 1 hr before returning it back to the original condition. Light conditions were changed at t_6 and t_{65} . Reference CO₂ was maintained at $400 \mu\text{mol mol}^{-1}$, block temperature was kept at 25°C and average VPD was 1.2 kPa. Data points represent $n = 3-4 \pm \text{se}$.

Fitting the g_s data to a mixed-effects model revealed highly significant interaction effect for both R→RB→R (Table 2.1) and RB→R→RB sequences (Table 2.2). There was no evidence for a similar relationship in A, however (Tables 2.3 and 2.4).

Table 2.3 Repeated measures (mixed-effects) ANOVA of A in Cleomeaceae under R→RB→R sequence ($R^2=0.98$, RMSE = 0.397).

Source	DF	F ratio	Pr(>F)
Species	1	24.43	0.0043
Light	2	7.379	0.0108
Species x Light	2	0.9126	0.4325

Table 2.4 Repeated measures (mixed-effects) ANOVA of A in Cleomeaceae under RB→R→RB sequence ($R^2=0.93$, RMSE = 0.87).

Source	DF	F ratio	Pr(>F)
Species	1	1.519	0.2832
Light	2	2.275	0.1395
Species x Light	2	1.167	0.3792

To find out if these differences between C_3 and C_4 *Cleome* species were representative of general differences in stomatal responses between photosynthetic pathways, the R→RB→R sequence was also performed on *Flaveria*, another genus which contains C_3 , C_3 - C_4 , and C_4 species (Fig. 2.3). Following steady state g_s of $0.35 \text{ mol H}_2\text{O m}^{-2} \text{ s}^{-1}$ at R light in the C_3 -like *F. pringlei* (proto-kranz) g_s increased gradually to $0.40 \text{ mol H}_2\text{O m}^{-2} \text{ s}^{-1}$ upon the addition of blue light (Fig. 2.3E). When light was returned to R, g_s decreased rapidly to $0.29 \text{ mol H}_2\text{O m}^{-2} \text{ s}^{-1}$. Similarly, when moving from RB→R, C_3 -like *F. pringlei* rapidly declined from 0.37 to $0.32 \text{ mol H}_2\text{O m}^{-2} \text{ s}^{-1}$, which was gradually reversed by the switch from R→RB over the course of 40 mins (Fig. 2.3). In contrast, no effects of the R→RB→R sequence, nor the reverse RB→R→RB sequence were observed on g_s in both C_4 *F. trinervia* and C_4 *F. bidentis*, which stayed at 0.10 and $0.19 \text{ mol H}_2\text{O m}^{-2} \text{ s}^{-1}$ in both sequences.

Significant species by light interaction was detected for R→RB→R (Table 2.5, $p=0.0005$), but not for the reverse sequence, RB→R→RB (Table 2.6), where the main effects were marginally significant (Light, $p=0.0529$; Species, $p=0.0717$).

A comparison of stomatal conductance responses to blue and red light between C₃ and C₄ photosynthetic species in three phylogenetically-controlled experiments

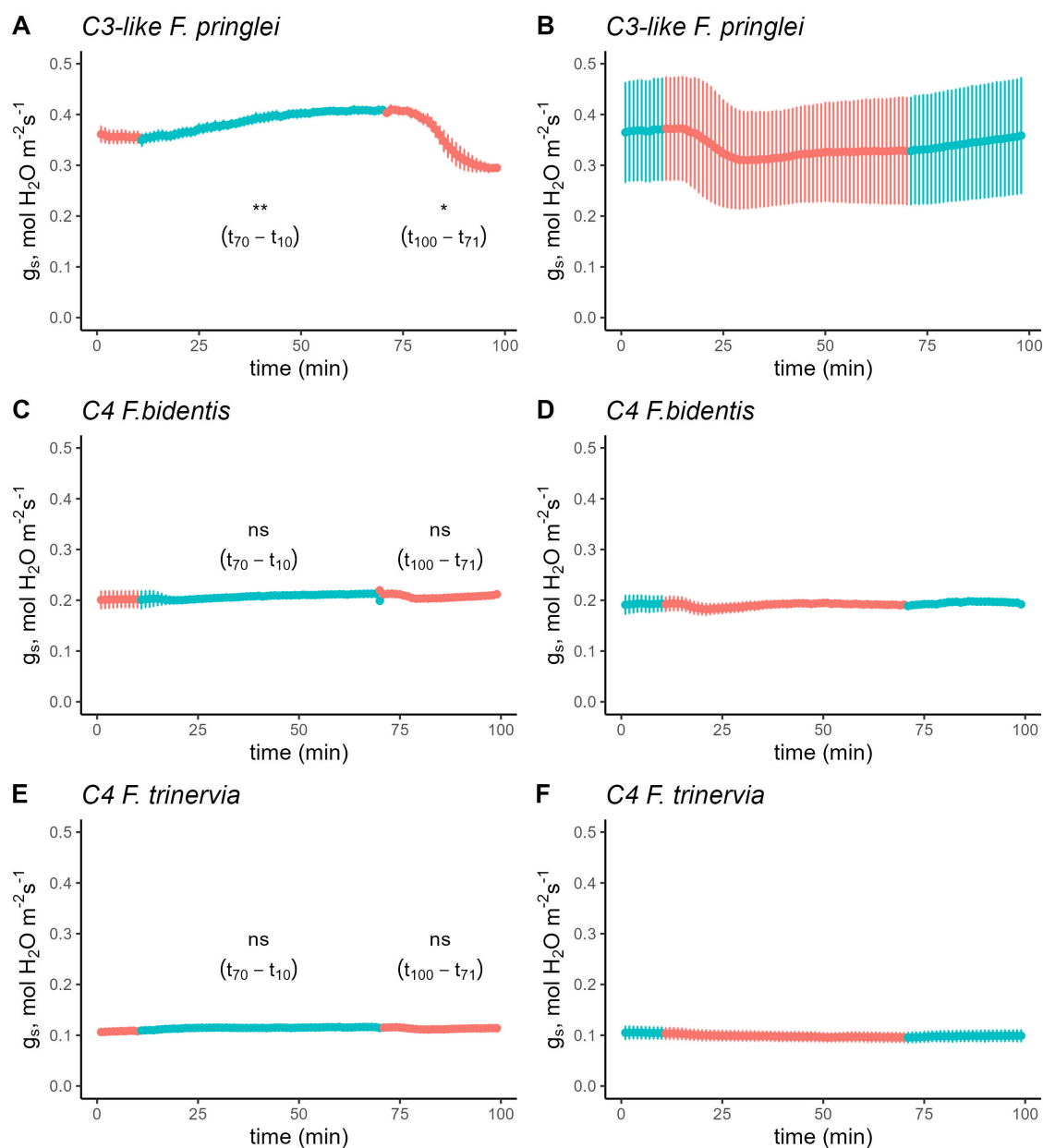


Fig. 2.3 Time course of g_s in C₃-like *F. pringlei* (A and B), C₄ *F. bidentis* (C and D), and C₄ *F. trinervia* (E and F) in response to a sequence of 75% red + 25% blue light and vice versa. Leaves were initially acclimated in either 100% red or 75% red+25% blue light until steady state was achieved. Subsequently, the light environment was switched depending on the initial light condition while maintaining $500 \mu\text{mol m}^{-2} \text{s}^{-1}$. The leaves were acclimated in the new light condition for 60 min before returning it back to the original condition for another 30 mins before terminating the experiment. Light conditions were reversed at t_{10} and t_{70} . Reference CO₂ was maintained at $400 \mu\text{mol mol}^{-1}$, block temperature was kept at 25°C and average VPD was 1.2 kPa. Data points represent $n=3 \pm \text{se}$. Data points represent mean $\pm \text{se}$ ($n=4-5$). Asterisks indicate significant difference at the end of blue or red light sequence from the imposition of treatment.

Table 2.5 Repeated measures (mixed-effects) ANOVA of g_s in three species of *Flaveria* under R→RB→R sequence ($R^2=0.97$, RMSE = 0.017).

Source	DF	F ratio	Pr(>F)
Species	2	711.862	<0.0001
Light	2	12.635	0.0011
Species x Light	4	11.340	0.0005

Table 2.6 Repeated measures (mixed-effects) ANOVA of g_s in three species of *Flaveria* under RB→R→RB sequence ($R^2=0.99$, RMSE = 0.014).

Source	DF	F ratio	Pr(>F)
Species	2	4.22	0.0717
Light	2	3.793	0.0529
Species x Light	4	2.2190	0.1285

The results in Fig.2.3 show the differences in blue light response between C_3 and C_4 species were also present in *Flaveria*. However, to account for the fact that the first set of *Flaveria* experiments used the proto-kranz C_3 -like species *F. pringlei* as the C_3 representative, the experiment was repeated with the inclusion of two other C_3 *Flaveria* species. Because the complementary sequence RB→R→RB yielded the similar results as the R→RB→R sequence, only the latter was repeated (Fig.2.4) on two ‘true’ C_3 species, *F. robusta* (Fig.2.4A) and *F. cronquistii* (Fig.2.4B), as well as the two C_4 species, *F. trinervia* (Fig.2.4C) and *F. bidentis* (Fig.2.4D) and C_3 -like *F. pringlei* (Fig.2.4E). After reaching steady state in R, g_s increased significantly from 0.22 mol H₂O m⁻² s⁻¹ to 0.28 (Fig.2.4A) mol H₂O m⁻² s⁻¹ in *F. robusta* upon the switch to RB and from 0.30 mol H₂O m⁻² s⁻¹ to 0.36 mol H₂O m⁻² s⁻¹ in C_3 *F. cronquistii* (Fig.2.4B). On the other hand, g_s in C_4 *F. trinervia* showed only a slight non-significant increase from 0.11 mol H₂O m⁻² s⁻¹ to 0.13 mol H₂O m⁻² s⁻¹ under RB light (2.4C), and similarly g_s in C_4 *F. bidentis* remained unchanged at 0.13 mol H₂O m⁻² s⁻¹ (Fig.2.4D). Finally, in C_3 -like *F. pringlei*, from an initial g_s of 0.16 mol H₂O m⁻² s⁻¹ it rose to 0.19 mol H₂O m⁻² s⁻¹ under BR (Fig. 2.4E). Further, the stimulating effects on g_s of the R→RB switch in the C_3 and C_3 -like species were largely reversed by the switch back to R light, but again g_s remained unaffected in the C_4 species. Similar to the first experiment with three *Flaveria* species, a significant interaction effect between species and light composition

A comparison of stomatal conductance responses to blue and red light between C₃ and C₄ photosynthetic species in three phylogenetically-controlled experiments

was present (Table 2.7). The light composition switches did not significantly affect the rate of net CO₂ assimilation in any of the species (Fig. 2.5), as was found in Cleomaceae.

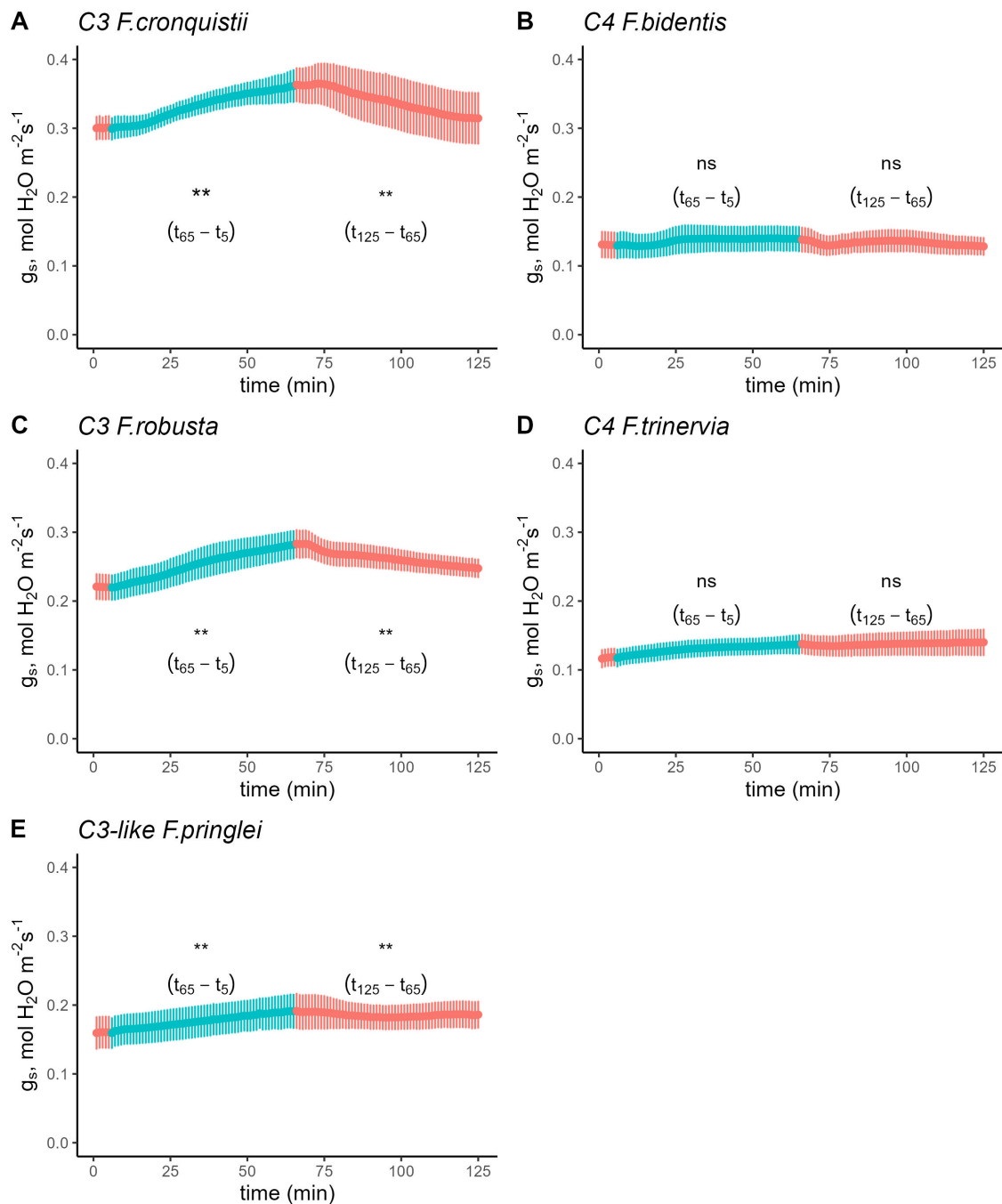


Fig. 2.4 Time course of g_s in *C3 F. robusta* (A), *C3 F. cronquistii* (B), *C4 F. trinervia* (C), *C4 F. bidentis* (D), and *C3-like F. pringlei* (E) in response to a sequence of 75% red + 25% blue light and vice versa. Leaves were initially acclimated in either 100% red or 75% red+25% blue light until steady state was achieved. Subsequently, the light environment was switched depending on the initial light condition while maintaining an intensity of $500 \mu\text{mol m}^{-2} \text{s}^{-1}$. The leaves were acclimated to the new light condition for 60 min before returning them back to the original condition for another 60 mins before terminating the experiment. Light conditions were reversed at t_6 and t_{65} . Reference CO_2 was maintained at $410 \mu\text{mol mol}^{-1}$, block temperature was kept at 25°C and average VPD was 1.2 kPa. Data points represent $n=4-5 \pm \text{s.e.}$. Asterisks indicate significant difference at the end of blue or red light sequence from the imposition of treatment.

A comparison of stomatal conductance responses to blue and red light between C₃ and C₄ photosynthetic species in three phylogenetically-controlled experiments

Table 2.7 Repeated measures (mixed-effects) ANOVA of g_s in five species of *Flaveria* under R→RB→R sequence ($R^2=0.97$, RMSE = 0.0017). To carry out the analysis, g_s at the introduction or removal of blue light (t = 5 min and t = 65 min, R→BR→R) or the reverse (t = 5 and t = 65, BR→R→BR), and the final g_s at t = 125 min were extracted from the gas exchange time series.

Source	DF	F ratio	Pr(>F)
Species	4	85.88	0.0002
Light	2	8.90	0.0001
Species x Light	8	8.08	0.0048

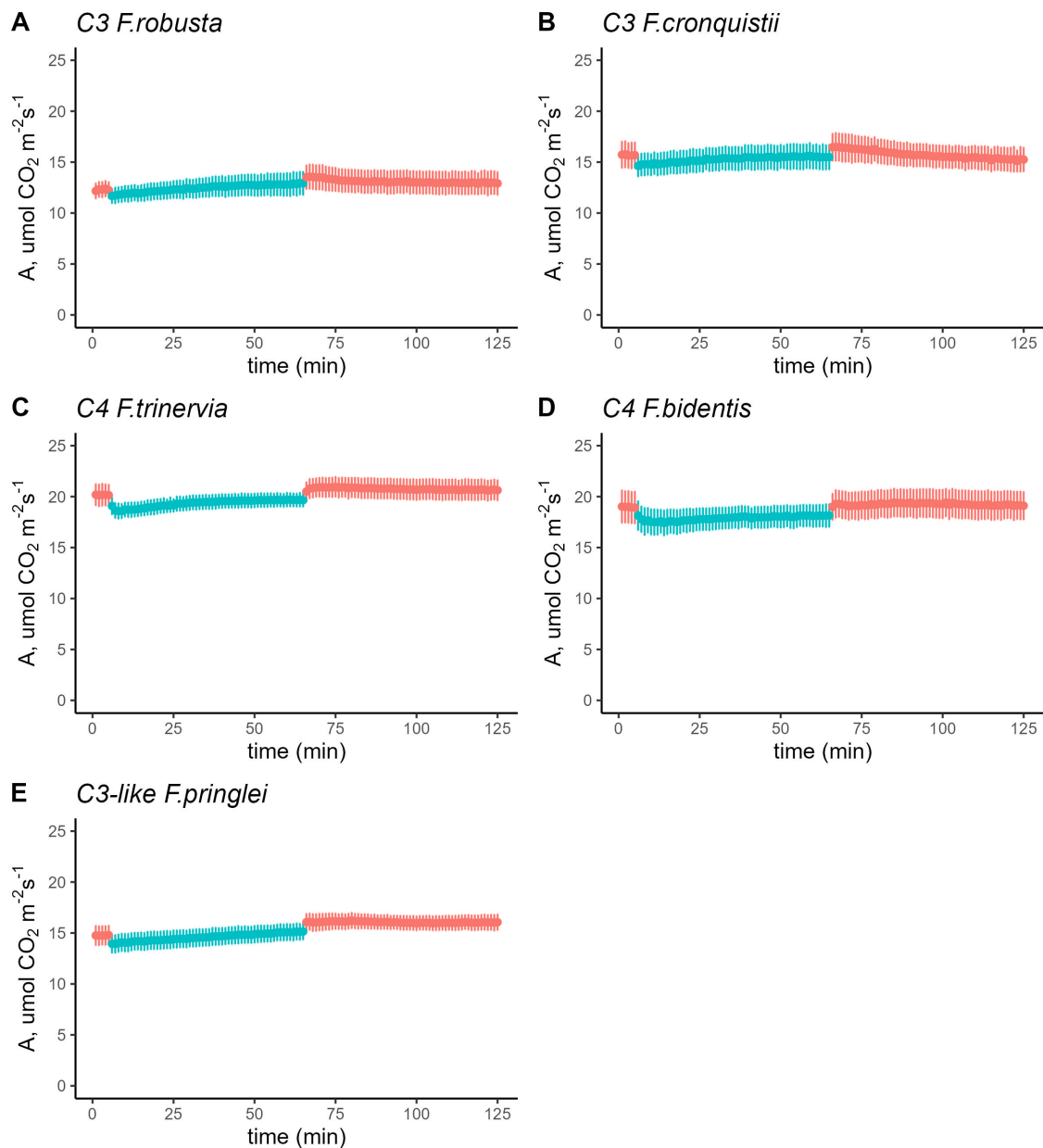


Fig. 2.5 Time course of A in C_3 *F.robusta* (A), C_3 *F. cronquistii* (B), C_4 *F. trinervia* (C), C_4 *F. bidentis* (D), and C_3 -like *F. pringlei* (E) in response to a sequence of 75% red + 25% blue light and vice versa. Leaves were initially acclimated in either 100% red or 75% red+25% blue light until steady state was achieved. Subsequently, the light environment was switched depending on the initial light condition while maintaining an intensity of $500 \mu\text{mol m}^{-2} \text{s}^{-1}$. The leaves were acclimated to the new light condition for 60 min before returning them back to the original condition for another 60 mins before terminating the experiment. Light conditions were reversed at t_6 and t_{65} . Reference CO_2 was maintained at $410 \mu\text{mol mol}^{-1}$, block temperature was kept at 25°C and average VPD was 1.2 kPa. Data points represent $n=4-5 \pm \text{s.e.}$

A comparison of stomatal conductance responses to blue and red light between C₃ and C₄ photosynthetic species in three phylogenetically-controlled experiments

To make sure that the stomata in C₄ dicots were not already at their maximum aperture when the switchover experiments were performed, an independent experiment using 200 ppm CO₂ showed increasing g_s in *Cleome* and in C₄ *F. bidentis* under the same 500 $\mu\text{mol m}^{-2} \text{s}^{-1}$ RB light combination. The results indicate that the stomata were not already at maximum opening in the switch over experiment.

2.3.2 C₃ and C₄ subspecies of the monocot *A. semialata* display the canonical blue light response

Cleome and *Flaveria* are both dicotyledonous species, but C₄ photosynthesis is also quite prevalent in the monocots [105]. Monocot species have stomatal features distinctly different from dicots [10]. To determine if the differences in stomatal responses to blue light described above also extend to monocots, the R→RB→R switchover experiment was also performed on C₃ and C₄ *A. semialata* subspecies (Fig.2.6). In this case, significant stimulation of g_s in response to the R→RB switch was observed across both C₃ and C₄ subspecies, increasing from 0.05 to 0.07 mol H₂O m⁻² s⁻¹ and returning to 0.05 mol H₂O m⁻² s⁻¹ in response to the RB→R switch.

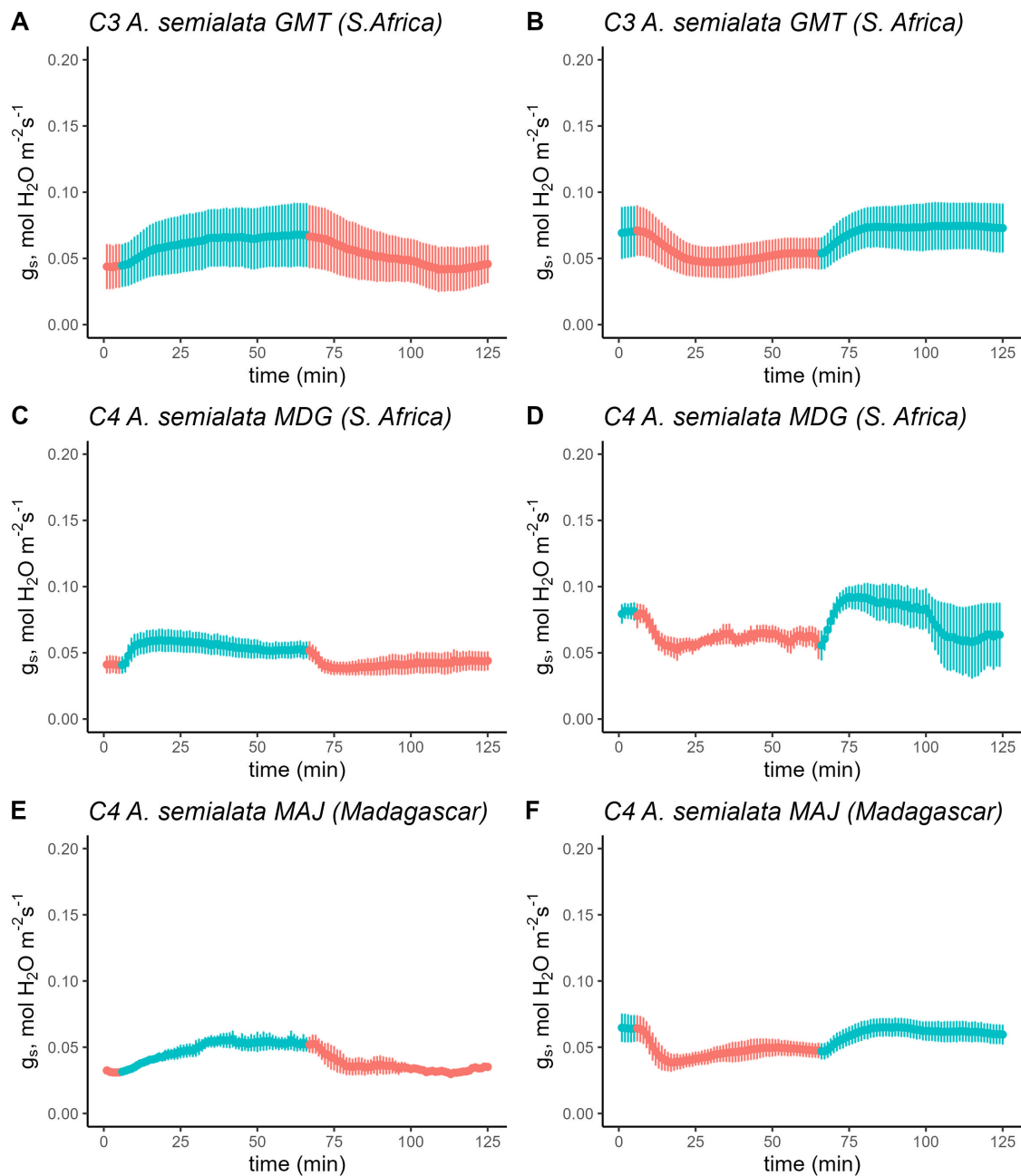


Fig. 2.6 Time course of g_s in C_3 *A. semialata* subsp. *eckloniana* ‘GMT’ (A and B), C_4 *A. semialata* subsp. *semialata* ‘MDG’ (C and D) and C_4 *A. semialata* subsp. *semialata* ‘MAJ’ (E and F) in response to a sequence of 75% red + 25% blue light and vice versa. Leaves were initially acclimated in either 100% red or 75% red+25% blue light until steady-state was achieved. The light environment was switched depending on the initial light condition while maintaining $500 \mu\text{mol m}^{-2} \text{s}^{-1}$. The leaves were acclimated to the new light condition for 40 min before returning it back to the original light condition. Reference CO_2 was maintained at $410 \mu\text{mol mol}^{-1}$, block temperature was kept at 25°C and average VPD was 1.2 kPa. Data points represent $n=3-4 \pm \text{s.e.}$

A comparison of stomatal conductance responses to blue and red light between C₃ and C₄ photosynthetic species in three phylogenetically-controlled experiments

Table 2.8 Repeated measures (mixed-effects) ANOVA of g_s in *Alloteropsis* under R→RB→R sequence ($R^2=0.91$, RMSE = 0.009).

Source	DF	F ratio	Pr(>F)
Species	2	0.252	0.7837
Light	2	12.72	0.0007
Species x Light	4	0.635	0.6457

Table 2.9 Repeated measures (mixed-effects) ANOVA of g_s in *Alloteropsis* under RB→R→RB sequence ($R^2=0.87$, RMSE = 0.011).

Source	DF	F ratio	Pr(>F)
Species	2	0.123	0.8859
Light	2	7.53	0.0060
Species x Light	4	0.482	0.7486

After reaching steady state in R, g_s increased significantly from 0.05 mol H₂O m⁻² s⁻¹ to 0.07 mol H₂O m⁻² s⁻¹ in C₃ *A. semialata* 'GMT' upon the switch to RB, and then returned to 0.05 mol H₂O m⁻² s⁻¹ when the light was shifted back to R. On the other hand, Both C₄ *A. semialata* ('MDG' and 'MAJ') also showed an increase from 0.04 mol H₂O m⁻² s⁻¹ to 0.05 mol H₂O m⁻² s⁻¹ under RB, and back to 0.04 when the light was reverse to R.

In the reverse sequence, g_s followed a similar pattern. In C₃ *A. semialata* 'GMT', g_s was 0.07 mol H₂O m⁻² s⁻¹ at the start of R, which then dropped to 0.05 mol H₂O m⁻² s⁻¹ under R, and returned to 0.07 mol H₂O m⁻² s⁻¹ when light was changed to RB. Following steady state, the initial g_s in C₄ *A. semialata* 'MDG' under BR was 0.08 mol H₂O m⁻² s⁻¹, which rapidly declined to 0.06 mol H₂O m⁻² s⁻¹, with a final g_s of 0.06 mol H₂O m⁻² s⁻¹. Similarly, g_s in C₄ *A. semialata* 'MAJ' started at 0.07 mol H₂O m⁻² s⁻¹ under RB, decreased to 0.05 mol H₂O m⁻² s⁻¹ under R and returned to 0.06 mol H₂O m⁻² s⁻¹ under RB.

Under R→RB→R and the reverse sequence, RB→R→RB, fitting the g_s data to a linear mixed-effects model showed a highly significant effect of light (Table 2.8, $p=0.0007$; Table 2.9, $p=0.0060$), but the main effect of species (R-RB-R, $p=0.7837$; RB-R-RB, $p=0.8859$) and its interaction with light (R-RB-R, $p=0.6456$; RB-R-RB, $p=0.7486$) were not significantly different.

Linear mixed-effects model analysis of A under R→RB→R showed a significant main effect of light (Table 2.10, $p=0.0013$), but the general trends suggested that A was insensitive to the changes in light composition, similar to the Cleomaceae and *Flaveria* results. Indeed, analysis of the reverse sequence found no significant effects of species, light or their interaction on A (Table 2.11).

A comparison of stomatal conductance responses to blue and red light between C₃ and C₄ photosynthetic species in three phylogenetically-controlled experiments

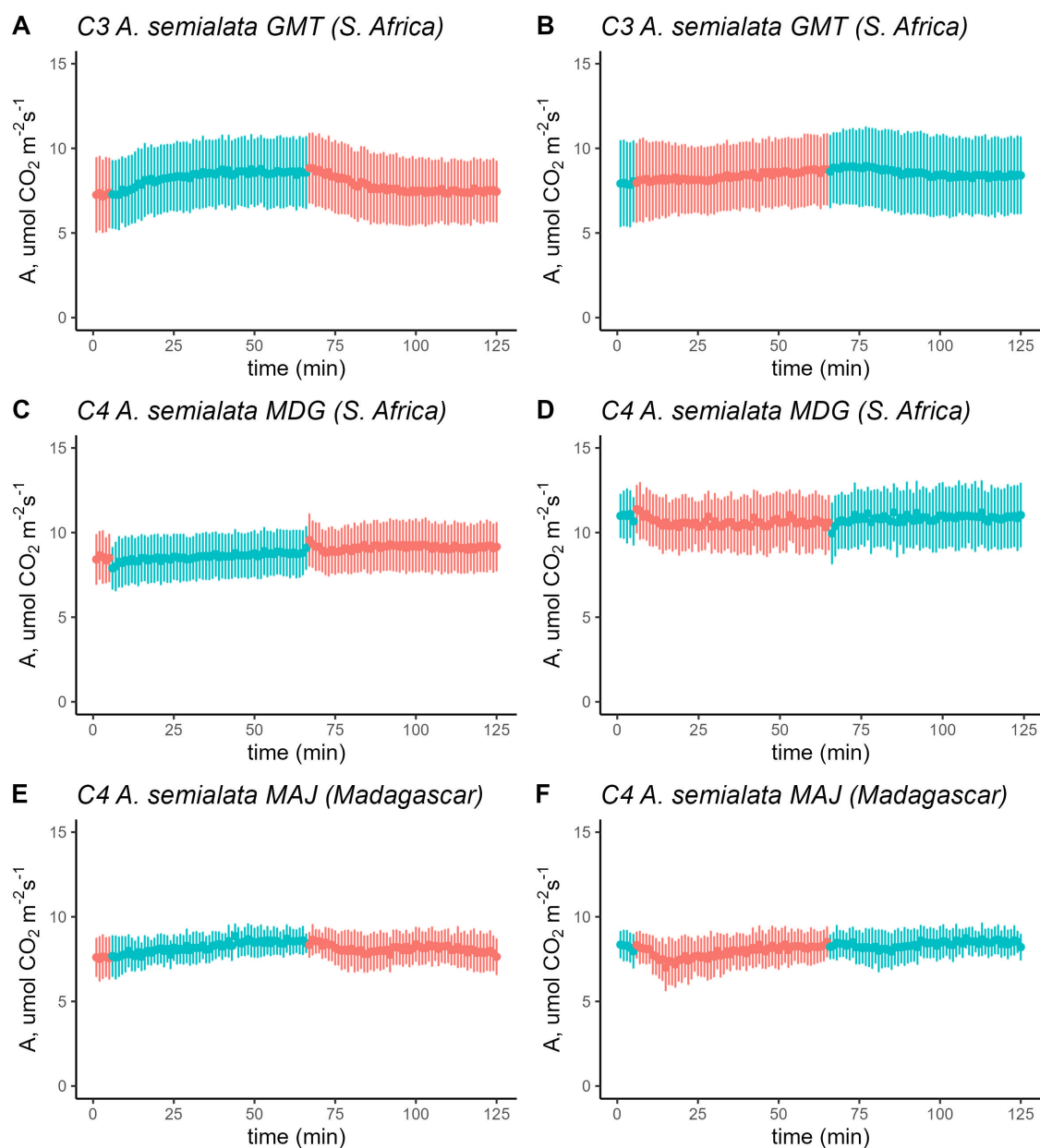


Fig. 2.7 Time course of A in C₃ *A. semialata* subsp. *eckloniana* ‘GMT’ (A and B), C₄ *A. semialata* subsp. *semialata* ‘MDG’ (C and D) and C₄ *A. semialata* subsp. *semialata* ‘MAJ’ (E and F) in response to a sequence of 75% red + 25% blue light and vice versa. Leaves were initially acclimated in either 100% red or 75% red+25% blue light until steady state was achieved. Subsequently, the light environment was switched depending on the initial light condition while maintaining an intensity of $500 \mu\text{mol m}^{-2} \text{s}^{-1}$. The leaves were acclimated to the new light condition for 60 min before returning them back to the original condition for another 60 mins before terminating the experiment. Light conditions were reversed at t_6 and t_{65} . Reference CO₂ was maintained at $410 \mu\text{mol mol}^{-1}$, block temperature was kept at 25°C and average VPD was 1.2 kPa. Data points represent $n=3-4 \pm \text{s.e.}$

Table 2.10 Repeated measures (mixed-effects) ANOVA of A in *Alloteropsis* under R→RB→R sequence ($R^2=0.98$, RMSE = 0.510).

Source	DF	F ratio	Pr(>F)
Species	2	0.094	0.9117
Light	2	11.11	0.0013
Species x Light	4	1.968	0.1550

Table 2.11 Repeated measures (mixed-effects) ANOVA of A in *Alloteropsis* under RB→R→RB sequence ($R^2=0.90$, RMSE = 0.872).

Source	DF	F ratio	Pr(>F)
Species	2	1.519	0.2832
Light	2	2.273	0.1395
Species x Light	4	1.1378	0.3792

2.3.3 Red light response in phylogenetically-close pairs of C₃ and C₄ dicots and monocots, at constant C_i

To evaluate the quantitative "red" light stomatal response, stomatal responses were evaluated at different red PFDs. The depletion of CO₂ in the mesophyll can give rise to an apparent red light response [103] which was not the focus of the experiments here, therefore the stomatal response to red light was evaluated under constant C_i.

In *Cleome*, C₃ *T. hassleriana* showed a drop in steady state g_s from 0.42 mol H₂O m⁻² s⁻¹ to 0.26 mol H₂O m⁻² s⁻¹ when red light intensity was reduced from 800 μmol m⁻² s⁻¹ to 200 μmol red photons m⁻² s⁻¹ (Fig.2.8A) and C_i maintained at 288 μmol CO₂ mol⁻¹(Fig.2.8 gs). g_s in C₄ *G. gynandra* remained consistent around 0.15 mol H₂O m⁻² s⁻¹ at the starting light intensity of 800 μmol m⁻² s⁻¹ red light (Fig.2.8C), while C_i was held constant at 173 μmol CO₂ mol⁻¹ (Fig.2.8D) and only slightly decreased to 0.12 mol H₂O m⁻² s⁻¹ when light was set to 200 μmol red photons m⁻² s⁻¹.

A comparison of stomatal conductance responses to blue and red light between C₃ and C₄ photosynthetic species in three phylogenetically-controlled experiments

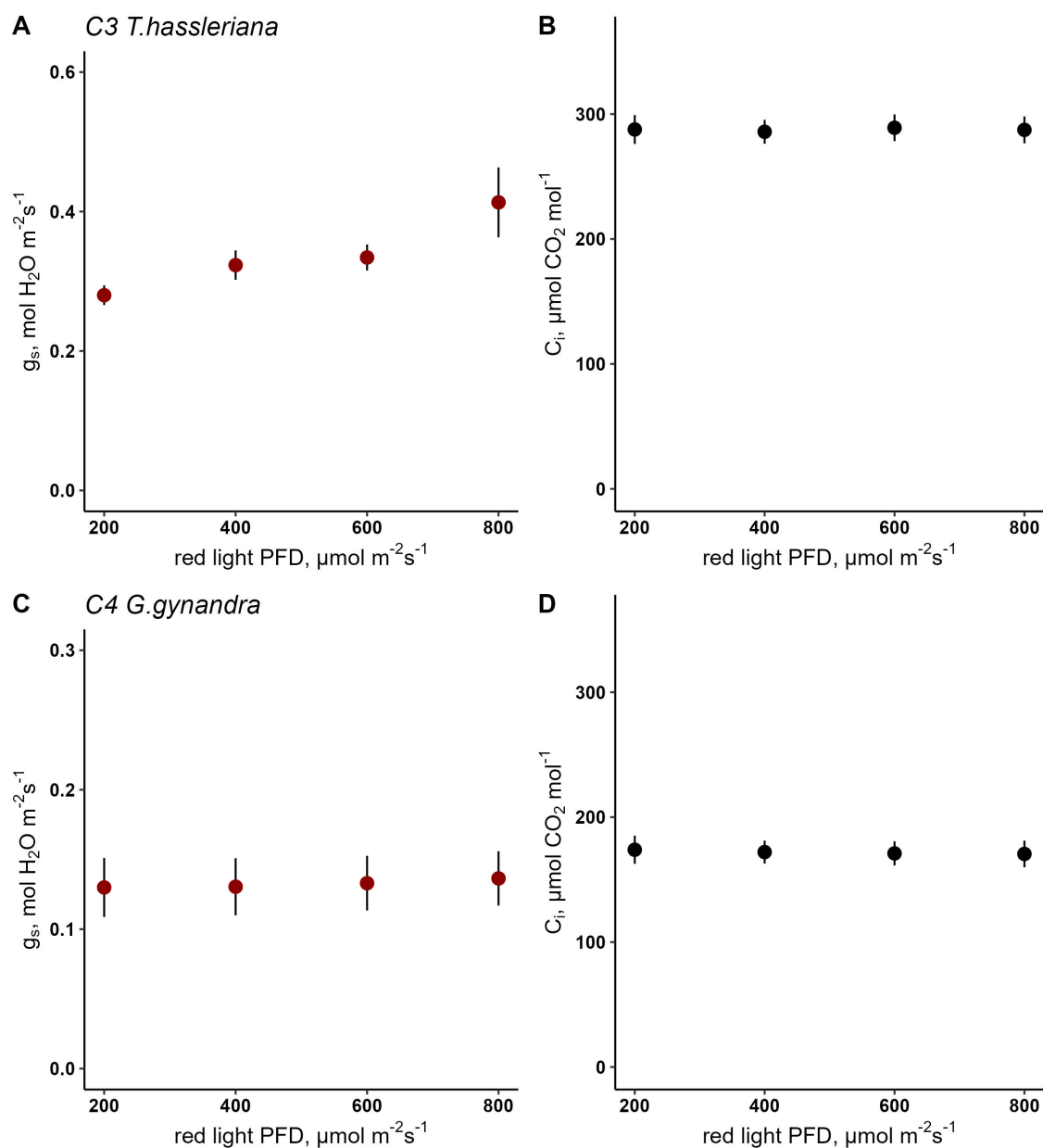


Fig. 2.8 Response of g_s and A to red light PFD in C₃ *T. hassleriana* (A, B, and E, n=4) and C₄ *G. gynandra* (C, D and F, n=4). A linear mixed-effects model analysis was carried out to test if photosynthetic type influences the response to red light in congeneric species belonging to Cleomaceae. Data points represent the mean \pm s.e.

Using a linear mixed-effects model, the interaction of photosynthetic type and red PFD on g_s was found to be significant (Table 2.12, $p < 0.0291$), with C₄ *G. gynandra* differing from C₃ *T. hassleriana*. In both species CO₂ assimilation rate also responded significantly to red light PFD (Table 2.13, $p = 0.0437$).

Table 2.12 Repeated measures (mixed-effects) ANOVA of A in Cleomaceae under varying intensities of red light ($R^2=0.024$, RMSE = 0.977).

Source	DF	F ratio	Pr(>F)
Species	1	45.21	0.0005
PPFD	1	10.09	0.0192
Species x PPFD	1	8.148	0.0291

Table 2.13 Repeated measures (mixed-effects) ANOVA of g_s in Cleomaceae under varying intensities of red light ($R^2=1.825$, RMSE = 0.93).

Source	DF	F ratio	Pr(>F)
Species	1	6.49	0.0437
PPFD	1	169.26	<0.0001
Species x PPFD	1	4.42	0.0802

In *Flaveria*, C_3 *F. cronquistii* showed an average g_s of $0.36 \text{ mol H}_2\text{O m}^{-2} \text{ s}^{-1}$ at $800 \mu\text{mol photons m}^{-2} \text{ s}^{-1}$ which decreased to $0.27 \text{ mol H}_2\text{O m}^{-2} \text{ s}^{-1}$ at $0 \mu\text{mol photons m}^{-2} \text{ s}^{-1}$ while C_i was kept constant at $296 \mu\text{mol CO}_2 \text{ mol}^{-1}$ (Fig.2.9A). C_3 *F. robusta* had a lower overall g_s , which started from $0.17 \text{ mol H}_2\text{O m}^{-2} \text{ s}^{-1}$ and decreased to $0.13 \text{ mol H}_2\text{O m}^{-2} \text{ s}^{-1}$ at a C_i of $247 \text{ mol CO}_2 \text{ mol}^{-1}$ (Fig.2.9B).

Meanwhile steady state g_s in C_4 *F. bidentis* under $800 \mu\text{mol red photons m}^{-2} \text{ s}^{-1}$ was $0.18 \text{ mol H}_2\text{O m}^{-2} \text{ s}^{-1}$ which slowly decreased to $0.13 \text{ mol H}_2\text{O m}^{-2} \text{ s}^{-1}$ with the decrease in light intensity (Fig. 2.9E), but while holding C_i constant at $157 \mu\text{mol CO}_2 \text{ mol}^{-1}$ (Fig.2.9F). g_s in C_4 *F. trinervia* was practically unchanged in response to red light intensity ranging between 0.12 and $0.10 \text{ H}_2\text{O m}^{-2} \text{ s}^{-1}$ (Fig.2.9G). Finally, C_3 -like *F. pringlei* had a g_s of $0.19 \text{ mol H}_2\text{O m}^{-2} \text{ s}^{-1}$ which decreased to $0.15 \text{ mol H}_2\text{O m}^{-2} \text{ s}^{-1}$ (Fig. 2.9I) as light intensity was reduced while keeping C_i at $240 \mu\text{mol CO}_2 \text{ mol}^{-1}$ (Fig.2.9J).

Fitting the g_s data to a linear mixed-effects model (Table 2.14) showed a highly significant species ($p<0.0001$) and red light PPFD ($p<0.0001$) main effects, and but a non-significant interaction effect ($p=0.6789$). The significance of the red light effect demonstrates that despite the limited range of the response, stomata did respond significantly to red light across some of these species. The strong significance of the species effect demonstrates that the absolute values of stomatal conductance differed significantly between *Flaveria* species in

A comparison of stomatal conductance responses to blue and red light between C₃ and C₄ photosynthetic species in three phylogenetically-controlled experiments

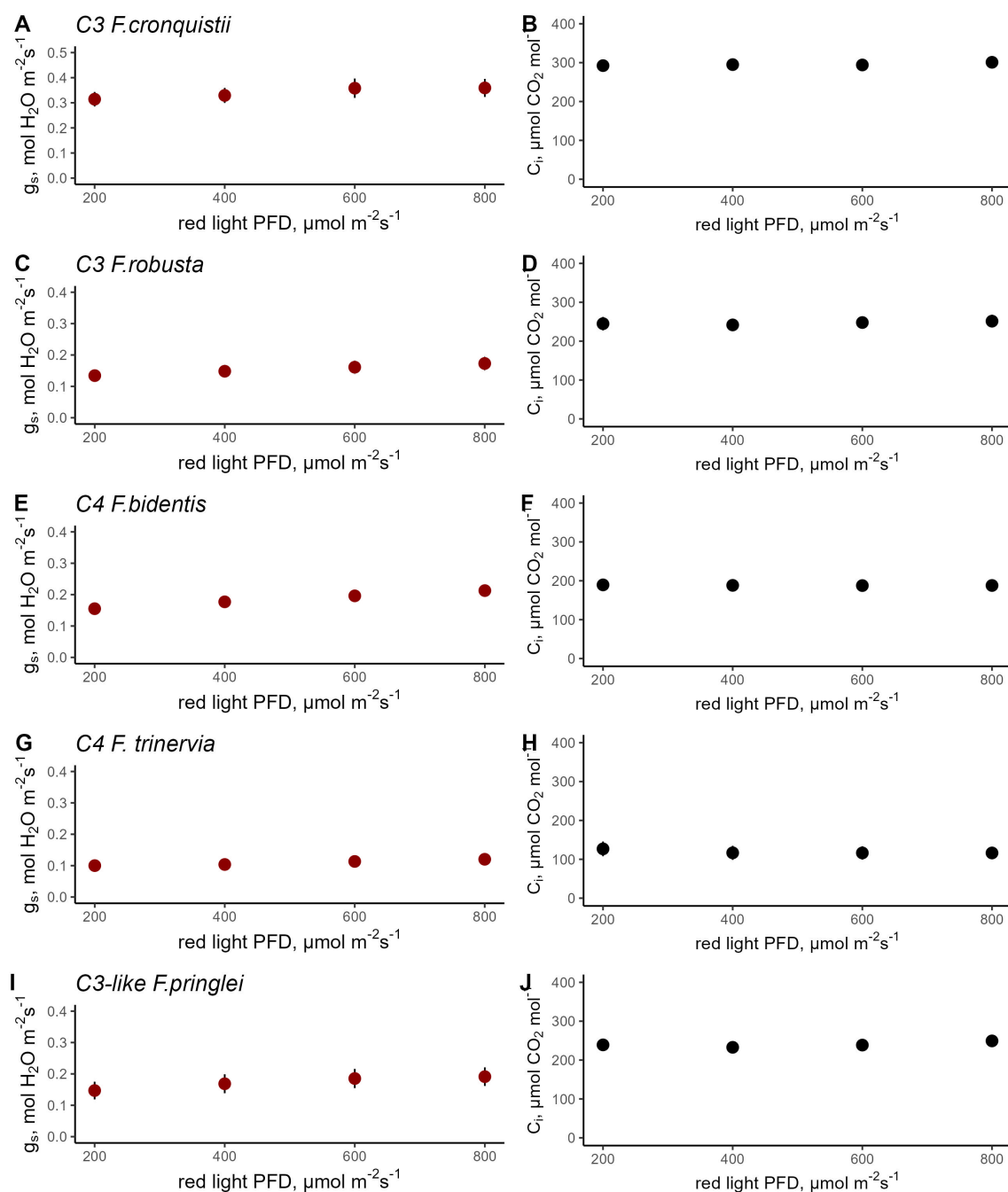


Fig. 2.9 Response of g_s to red light PFD in C₃ *F. cronquistii* (A, n=4) and C₃ *F. robusta* (B, n=5), C₄ *F. bidentis* (C, n=8), C₄ *F. trinervia* (D, n=5), and C₃-like *F. pringlei* (E, n=5). A linear mixed-effects model analysis was carried out to test if photosynthetic type influences the response to red light in congeneric species belonging to *Flaveria*. Data points represent the mean \pm s.e.

line with photosynthetic type. However, the absence of a significant interaction between species and red light demonstrates that the magnitude of the stomatal red light response did not differ significantly between these species.

Table 2.14 Repeated measures (mixed-effects) ANOVA of g_s in *Flaveria* under varying intensities of red light ($R^2=0.027$, RMSE = 0.91).

Source	DF	F ratio	Pr(>F)
Species	4	14.88	<0.0001
PPFD	1	59.608	<0.0001
Species x PPFD	1	0.506	0.6789

Not surprisingly, CO_2 assimilation rate responded strongly to light intensity in all five species (Fig. 2.10 and Table 2.15), suggesting that the significant stomatal red light response in these species may serve to fine-tune coordination between stomatal conductance and photosynthesis, in concert with the stomatal CO_2 response.

A comparison of stomatal conductance responses to blue and red light between C₃ and C₄ photosynthetic species in three phylogenetically-controlled experiments

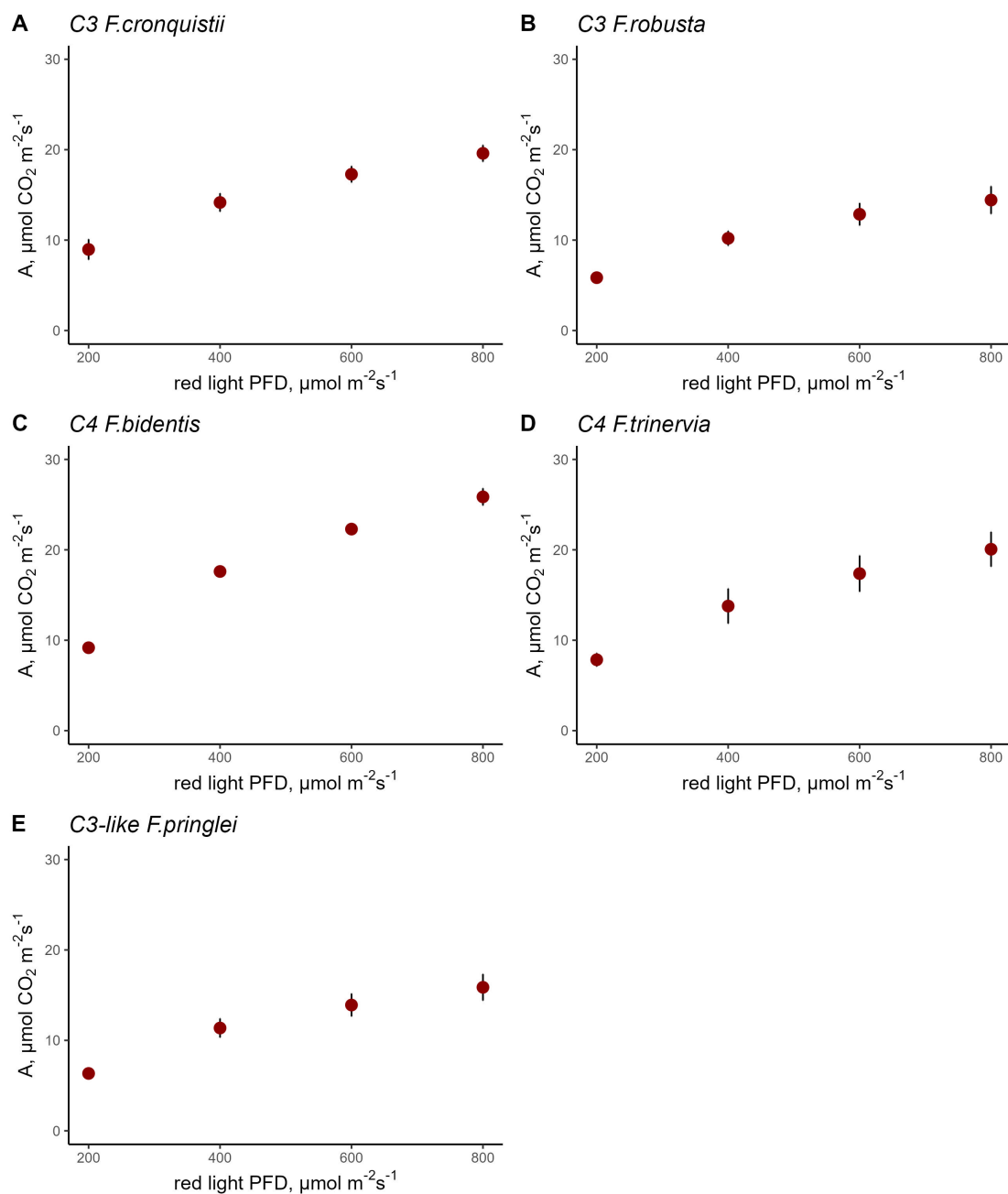


Fig. 2.10 Response of A to red light PFD in C₃ *F. cronquistii* (A, n=4) and C₃ *F. robusta* (B, n=5), C₄ *F. bidentis* (C, n=8), C₄ *F. trinervia* (D, n=5), and C₃-like *F. pringlei* (E, n=5). A linear mixed-effects model analysis was carried out to test if photosynthetic type influences the response to red light in congeneric species belonging to *Flaveria*. Data points represent the mean ± s.e.

Table 2.15 Repeated measures (mixed-effects) ANOVA of g_s in *Flaveria* under varying intensities of red light ($R^2=1.926$, RMSE = 0.92).

Source	DF	F ratio	Pr(>F)
Species	4	10.37	0.0002
PPFD	1	516.72	<0.0001
Species x PPFD	1	11.42	<0.0001

The stomatal red-light response was also characterized for C₃ *A. semialata* subsp. *eckloniana* and C₄ *A. semialata* subsp. *semialata* (Figs. 2.11A and C). When PPFD was reduced from 800 to 200 $\mu\text{mol red photons m}^{-2} \text{s}^{-1}$ for C₃ *A. semialata* subsp. *eckloniana*, g_s changed very little from 0.07 to 0.05 $\text{mol H}_2\text{O m}^{-2} \text{s}^{-1}$ (Figs. 2.11A and B). Similarly, the C₄ *A. semialata* subsp. *semialata* kept g_s at approximately 0.07 $\text{mol H}_2\text{O m}^{-2} \text{s}^{-1}$ despite the decrease in red PPFD (Figs. 2.11C and D). Curiously, the C₄ subspecies (Figs.2.11D) had a higher C_i than the C₃ subspecies at 800 $\mu\text{mol red photons m}^{-2} \text{s}^{-1}$ (Figs.2.11C; 153 vs 193 $\mu\text{mol CO}_2 \text{mol}^{-1}$), which has been observed previously for this paired comparison [5]. A linear mixed-effects model (Table 2.16) detected a marginal effect of red PPFD ($p=0.0525$) but there was no evidence of the effect of subspecies ($p=0.3884$) and its interaction with red PPFD ($p=0.1979$). Meanwhile, a significant interaction effect was noted for A in *Alloteropsis* ($p=0.0182$), indicating that the rise in A is dependent on red light intensity (Table 2.17).

A comparison of stomatal conductance responses to blue and red light between C₃ and C₄ photosynthetic species in three phylogenetically-controlled experiments

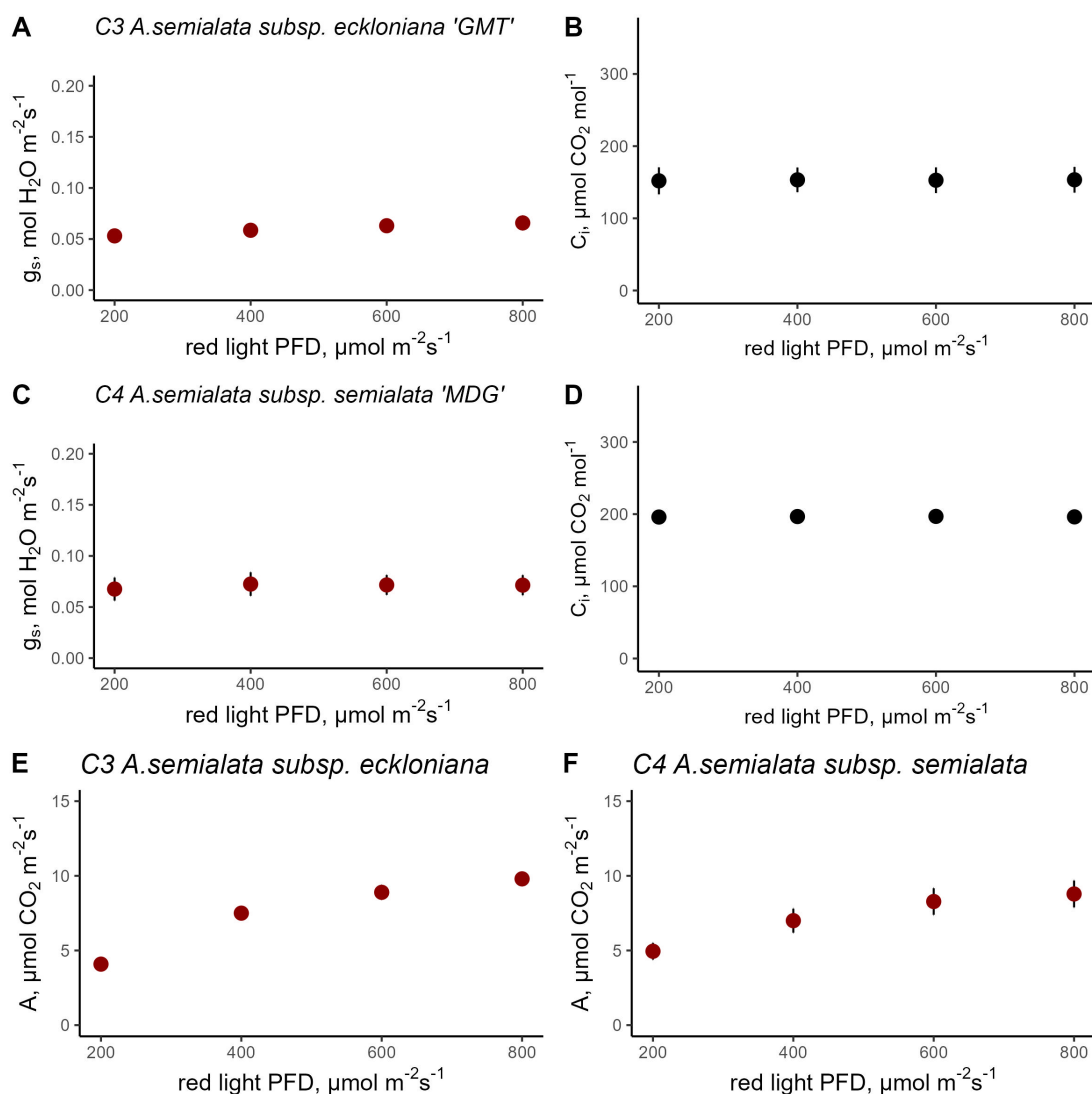


Fig. 2.11 Response of g_s and A_i in C₃ *A. semialata* subsp. *eckloniana* 'GMT' (A, B and E, n=4) and C₄ *A. semialata* subsp. *semialata* 'MDG' (C, D and F, n=5). Linear mixed-effects model analysis was carried out to test if photosynthetic type influences the response to red light in C₃ and C₄ subspecies belonging to *Alloteropsis*. Each data point represents the mean \pm s.e.

Table 2.16 Repeated measures (mixed-effects) ANOVA of g_s in *Alloteropsis* under varying intensities of red light ($R^2=0.99$, RMSE = 0.002).

Source	DF	F ratio	Pr(>F)
Species	1	0.864	0.3884
PPFD	1	5.814	0.0525
Species x PPFD	1	2.095	0.1979

Table 2.17 Repeated measures (mixed-effects) ANOVA of A in *Alloteropsis* under varying intensities of red light ($R^2=0.88$, RMSE = 0.797).

Source	DF	F ratio	Pr(>F)
Species	1	0.136	0.7255
PPFD	1	309.08	<0.0001
Species x PPFD	1	10.353	0.0182

Altogether, these data established a significant red light opening response to red light, independent of C_1 in *Cleome* and most *Flaveria* species, but only marginally in *Alloteropsis*. Thus the observed reduced stomatal sensitivity to red light in C_4 *G. gynandra* compared to C_3 *T. hassleriana* is unlikely to result from the hypothesized differences between C_3 and C_4 photosynthetic types. The differences observed among *Flaveria* species and the lack of these in *Alloteropsis* seem to suggest that these are more likely to be species-specific responses, rather than generic differences between photosynthetic pathways.

2.3.4 Stomatal morphology and density

Stomatal density and size were determined in conjunction with the gas exchange measurements described in the previous sections. In Cleomaceae, the overall stomatal density was higher in C_3 *T. hassleriana* (590 stomata mm^{-2}) than in C_4 *G. gynandra* (200 stomata mm^{-2}) (Species, $p < 0.0001$). The distribution of stomata on both leaf surfaces was also found to be significantly different, but in a species-dependent manner (Species x Leaf surface, $p < 0.0001$). The SD on the adaxial surface was almost two times higher than the abaxial surface in C_3 *T. hassleriana* (Fig. 2.12A and Figs. 2.13A and 2.13B). In contrast, in C_4 *G. gynandra*, SD was 25% higher on the adaxial compared to the abaxial surface (Fig. 2.12A and Figs. 2.13C and 2.13D).

While density varied depending on leaf surface in Cleomaceae, stomatal size was significantly larger on the abaxial than the adaxial surface (Leaf surface, $p < 0.0001$) (Fig. 2.12A). This SS difference was similar in both Cleomaceae species (Species x Leaf surface, $p = 0.4651$).

SD among *Flaveria* species (Figs. 2.12C and 2.14) were significantly different (Species, $p < 0.0001$), but the trend in SD was not consistent with the proposed progression of larger and fewer stomata in C_4 *Flaveria* than from smaller and more stomata in C_3 *Flaveria* [145].

A comparison of stomatal conductance responses to blue and red light between C₃ and C₄ photosynthetic species in three phylogenetically-controlled experiments

Instead, *F. cronquistii*, one of the two C₃ species, had the lowest SD whereas the highest SD was found for *F. bidentis*, one of the C₄ species. Thus, these differences in SD also appear to be species-dependent, but not determined by photosynthetic pathway. SD was similar between both leaf surfaces in both C₄ *Flaveria* species (Fig. 2.12C) as well as in the C₃ *F. cronquistii*, whereas the abaxial surface had higher SD in the C₃-like *F. pringlei* and the C₃ *F. robusta* (significant for the latter, $p < 0.05$). SS was higher on the abaxial side for all *Flaveria* species except for C₃ *F. cronquistii* resulting in an interaction effect of species x leaf surface which was highly significant ($p < 0.0001$) (Fig. 2.12D).

Meanwhile, there was no statistically significant difference in SD detected between the *Alloteropsis* subspecies (Species, $p = 0.338$) (Figs. 2.12E and 2.15), while SS was larger on the abaxial surface (Species x Leaf surface, $p = 0.05$) (Fig. 2.12F). Altogether, stomatal density, distribution and anatomical traits appeared to be largely determined by species effect, rather than photosynthetic pathway, although notably, all C₄ species had at equal SD on the adaxial and abaxial surfaces, whereas the more commonly found bias of SD towards the abaxial surface was only found in some of the C₃ species.

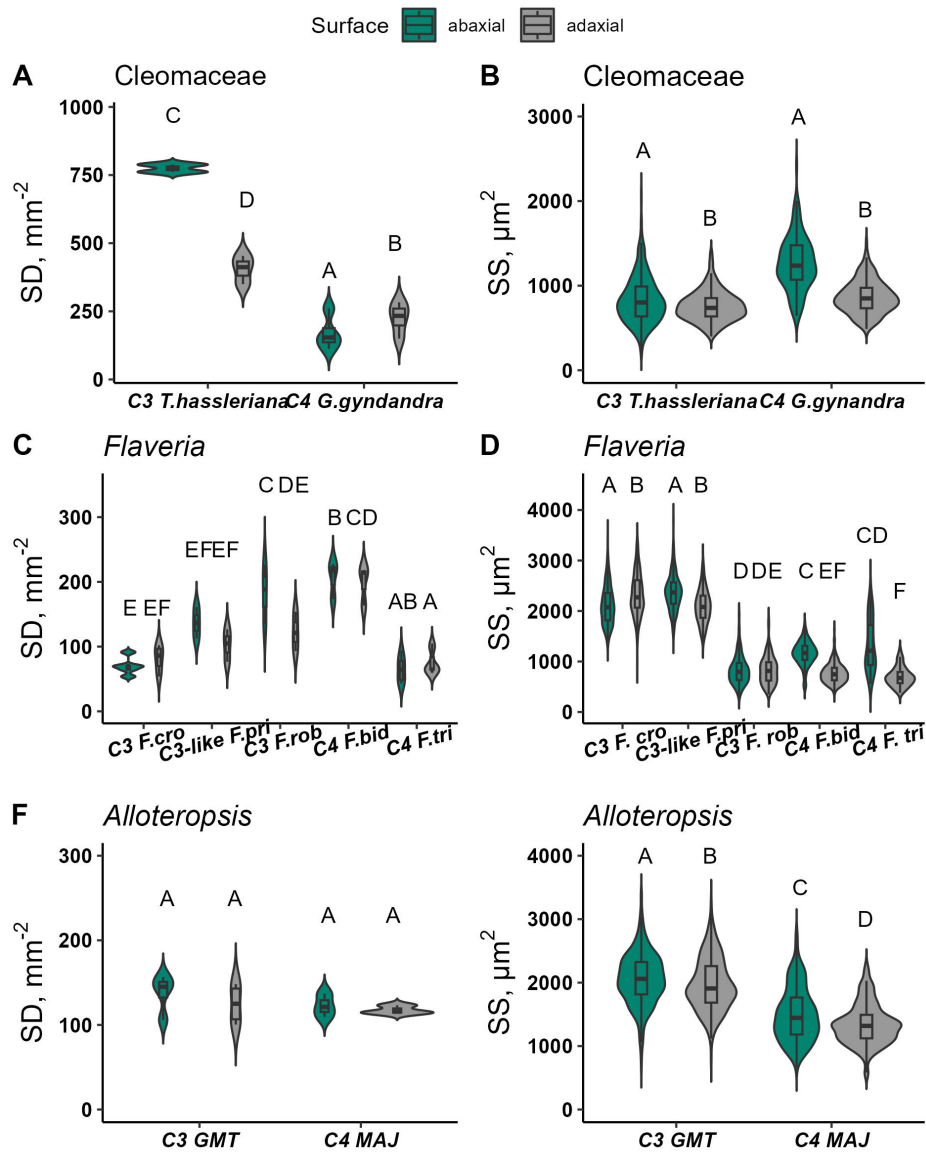


Fig. 2.12 Stomatal density (SD, stomata mm⁻²) and stomatal size (SS, μm²) on the abaxial and adaxial leaf surfaces of Cleomaceae (A and B), *Flaveria* (C and D), and *Alloteropsis* (E and F). Boxplots with the same letters are not significantly different at $\alpha = 0.05$ using Tukey's HSD test.

A comparison of stomatal conductance responses to blue and red light between C₃ and C₄ photosynthetic species in three phylogenetically-controlled experiments

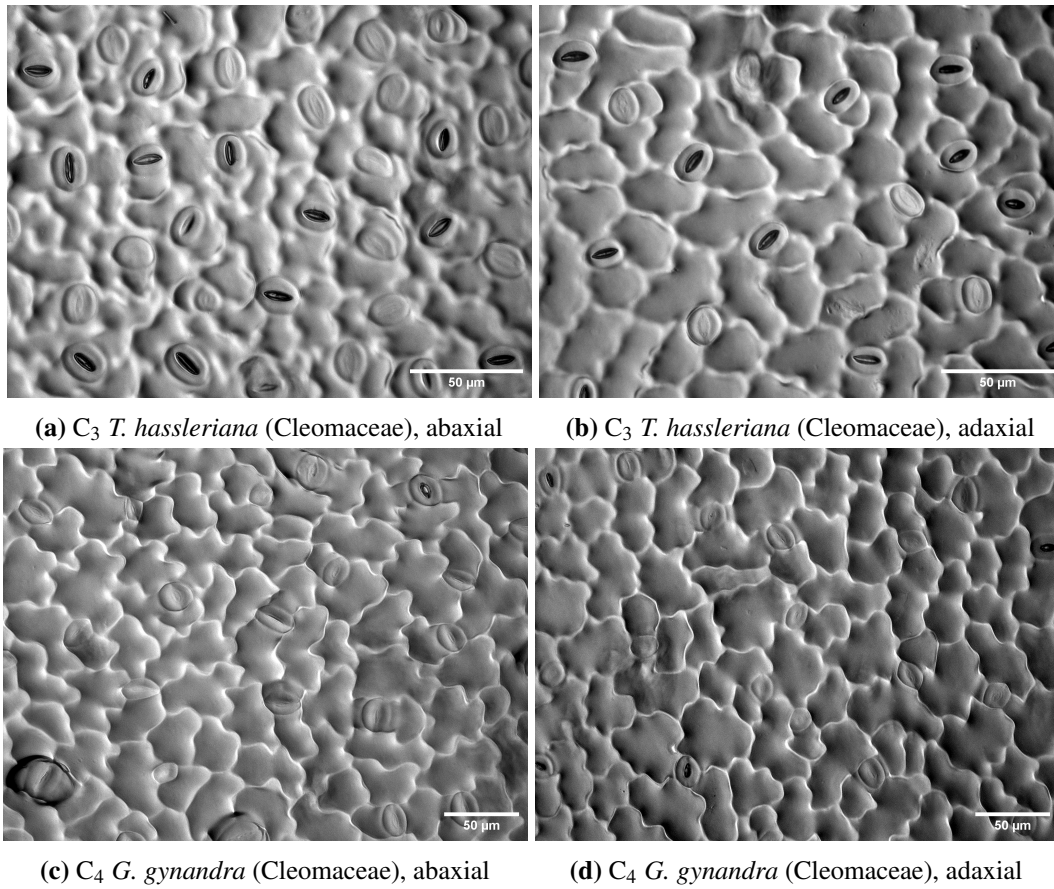
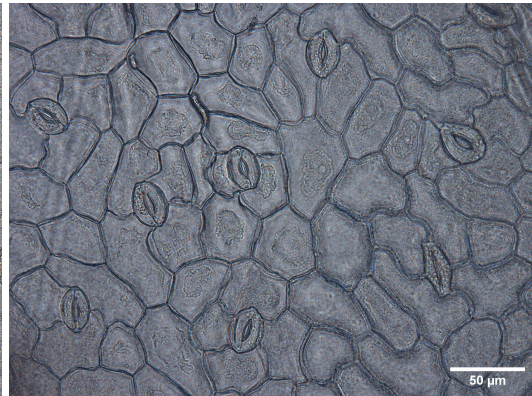


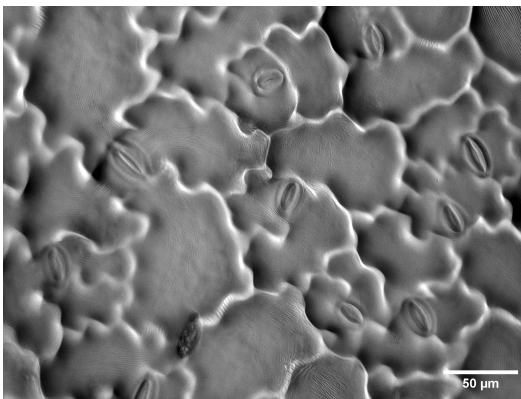
Fig. 2.13 Nail varnish impressions from leaf surfaces of C₄ *G. gynandra* at x400 and C₃ *T. hassleriana* at x600 used in the study. Photomicrographs were taken using Olympus microscope (BX41). Scale bar = 50 μm



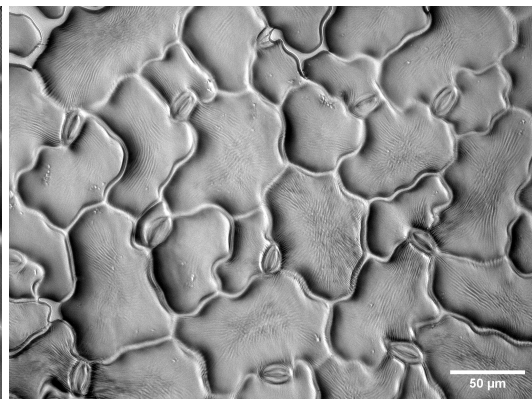
(a) C₃ *F. cronquistii*, abaxial



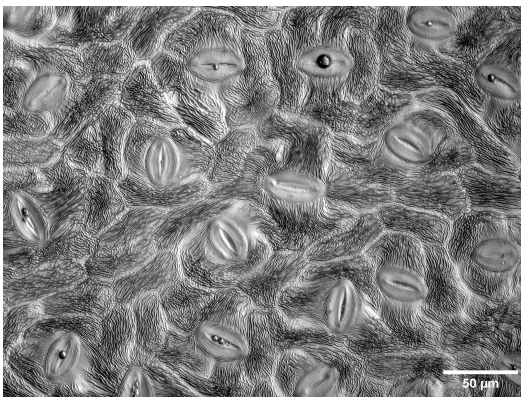
(b) C₃ *F. cronquistii*, adaxial



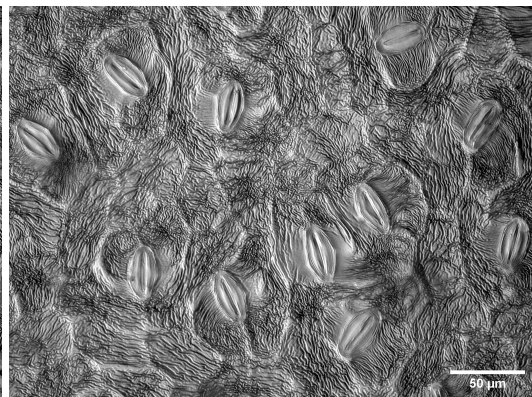
(c) C₄ *F. trinervia*, abaxial



(d) C₄ *F. trinervia*, adaxial



(e) C₃-like *F. pringlei*, abaxial



(f) C₃-like *F. pringlei*, adaxial

A comparison of stomatal conductance responses to blue and red light between C₃ and C₄ photosynthetic species in three phylogenetically-controlled experiments

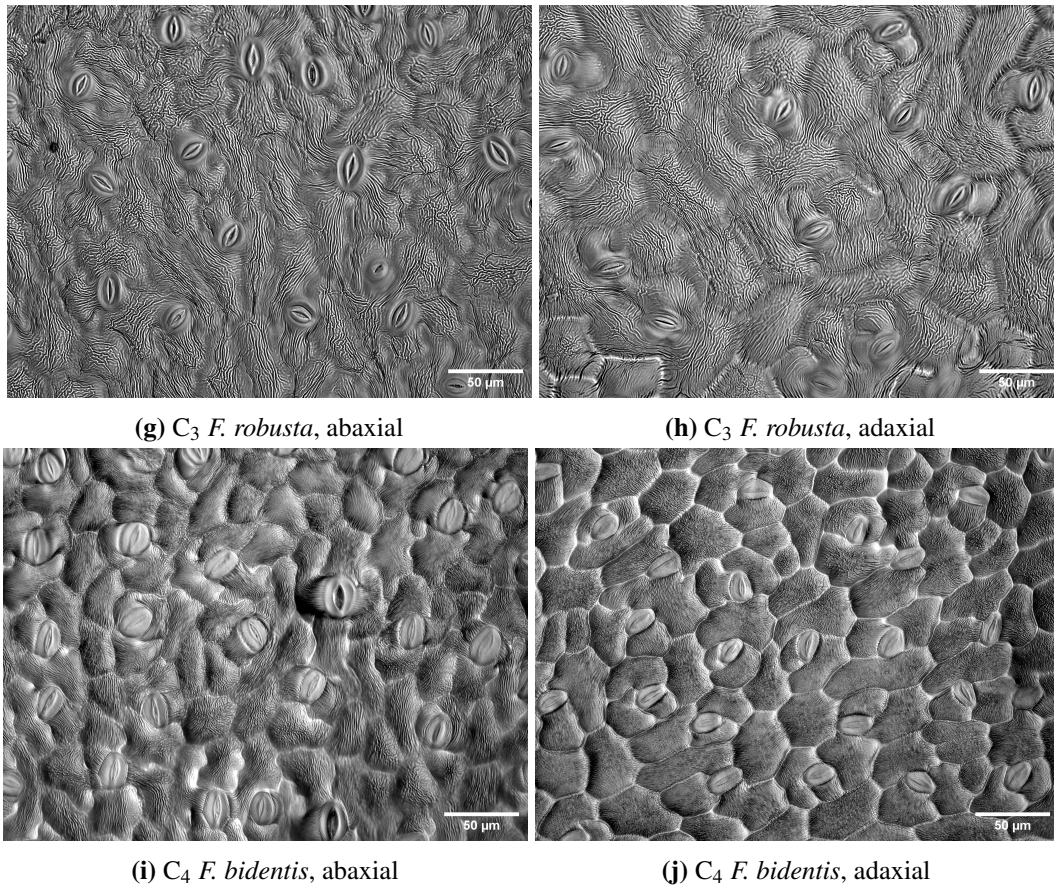


Fig. 2.14 Nail varnish impressions from leaf surfaces of *Flaveria* species used in the study. Photomicrographs were taken using Olympus microscope (BX41), at x400. Scale bar = 50 μm

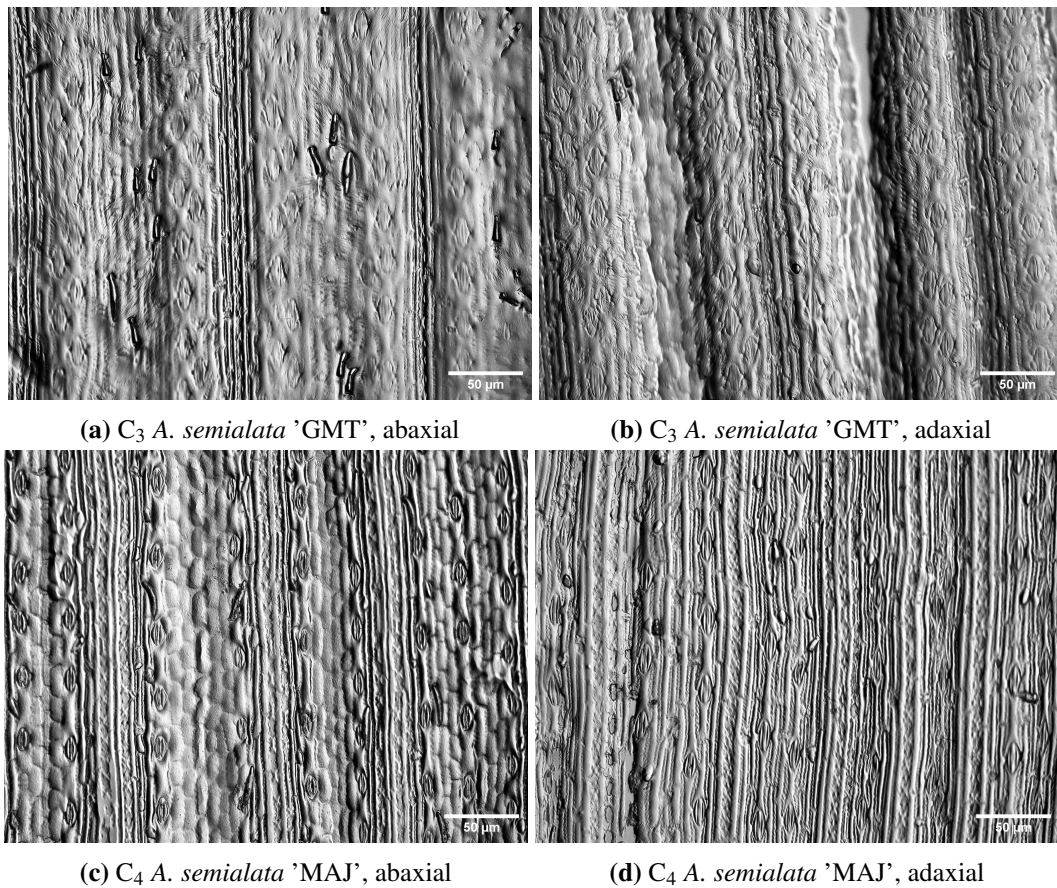


Fig. 2.15 Nail varnish impressions from leaf surfaces of *A. semialata* subspecies used in the study. Photomicrographs were taken using Olympus microscope (BX41), at $\times 400$. Scale bar = $50\ \mu\text{m}$

A comparison of stomatal conductance responses to blue and red light between C₃ and C₄ photosynthetic species in three phylogenetically-controlled experiments

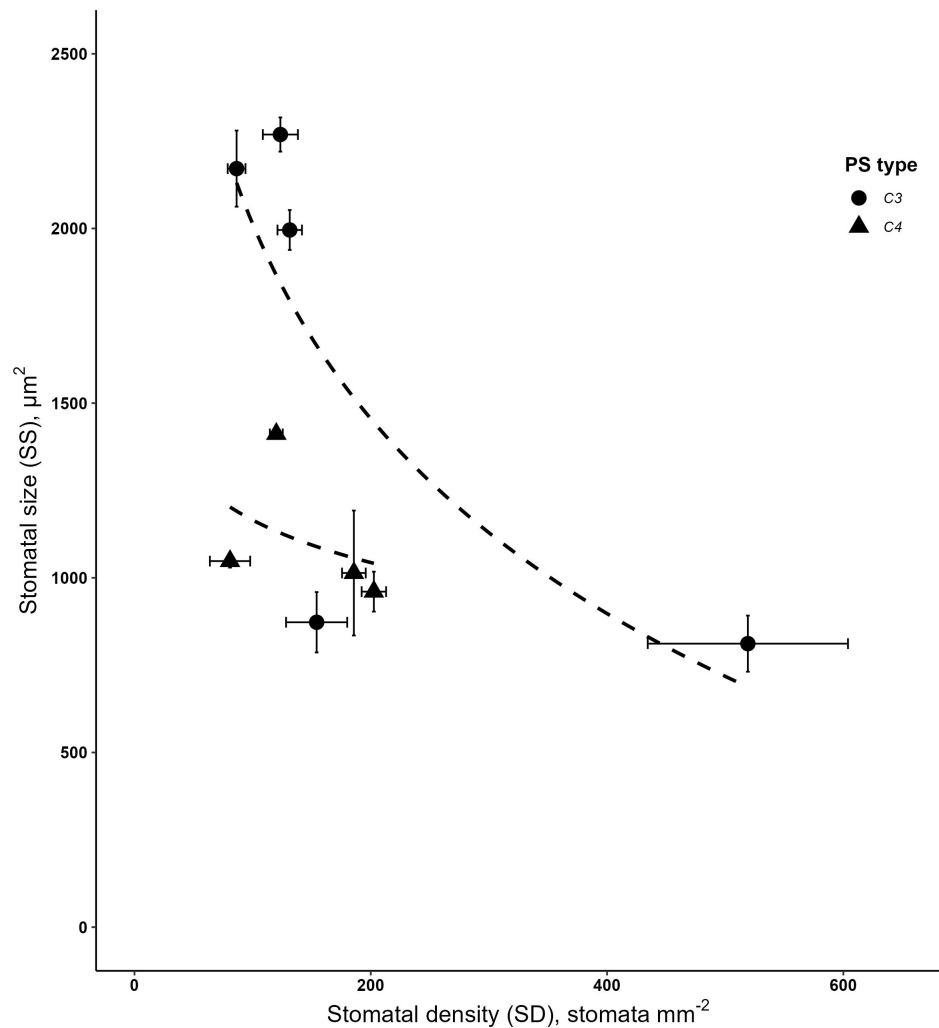


Fig. 2.16 Overall stomatal size (SS) was negatively correlated with stomatal density (SD), regardless of photosynthetic type. Logarithmic models describe the data for photosynthetic types.

Stomatal density and stomatal size (Fig. 2.16) were negatively correlated (pseudo $R^2 = 0.65$) in both C₃ and C₄ species represented in the study. The C₃ species tended to have bigger stomata, although C₃ *F. robusta* and C₃ *T. hassleriana*, were similar in size with C₄ species.

2.4 Discussion

In this chapter, leaf-level g_s responses to light quantity and spectral composition were compared between C₃ and C₄ species from *Cleome*, *Flaveria*, and *Alloteropsis* genera. All three

groups are well-studied models in the quest to understand evolution of C₄ photosynthesis. Combining experimental comparisons within all three genera allowed for a global comparison of stomatal light responses between C₃ and C₄ photosynthetic types while controlling for the effects of phylogenetic distance within each genus. The C₃ and C₄ species under the red and blue light treatments may be at different places in a light response curve such that the assimilation rate in C₄ may not have been fully light-saturated [5] at 500 $\mu\text{mol m}^{-2} \text{s}^{-1}$ PPFD.

2.4.1 C₄ dicots are less sensitive to blue light than C₃ dicots

BL promotes diverse physiological plant responses ranging from phototropism, chloroplast photorelocation movement, leaf flattening, leaf positioning, and stomatal opening [17, 49, 35]. Blue-light induced stomatal opening is probably the most well-characterised among these responses. However, the stomatal opening response to BL is not universal. Studies in model and non-model species provide strong evidence of the species-specificity of the BL stomatal opening response [134]. A recent study reported that C₄ crop species [146] displayed diminished stomatal opening to BL compared to C₃ crops. Indeed, in this study, C₄ dicots were found to be less sensitive to blue light-induced stomatal opening than close relatives operating the C₃ pathway. This observation demonstrates a clear difference between C₃ and C₄ opening response, as hypothesized.

In contrast, both the C₃ and C₄ accessions from the monocot *A. semialata* displayed blue light-dependent stomatal opening, which meant that the C₄ photosynthetic pathway *per se* does not determine this reduced blue light sensitivity. It should also be noted that the *A. semialata* had very low g_s values. When g_s is exceedingly low, accurate measurement becomes challenging, rendering C_i estimates more uncertain. Moreover, cuticular conductance can be disregarded with greater confidence at high g_s compared to low g_s , further amplifying the susceptibility of C_i calculations to error accumulation under low g_s conditions [38].

The decreased sensitivity of C₄ dicots to blue light may be a result of decreased guard cell expression of phototropins, the major blue light photoreceptor in plants. Analysis of transcript abundance in different cell types of C₄ *G. gynandra* showed that the transcript abundance of PHOT1 and PHOT2, as well as another blue light photoreceptor, CRY2, were lower in mesophyll and guard cells of C₄ *G. gynandra*, than in C₃ *T. hassleriana* [7]. In *Arabidopsis*, phototropins are expressed in almost every plant part [111], however the strongest expression in the epidermis is detected in guard cells, where photos are associated with the plasma membrane [111]. PHOT1 and 2 have partially overlapping roles. PHOT1 has been suggested

A comparison of stomatal conductance responses to blue and red light between C₃ and C₄ photosynthetic species in three phylogenetically-controlled experiments

to respond to lower PFD (0.1-50 $\mu\text{mol m}^{-2} \text{s}^{-1}$), while PHOT2 responds to PFD up to 250 $\mu\text{mol m}^{-2} \text{s}^{-1}$ in *Arabidopsis* [29]. Several hypotheses exist with regards to the function of the stomatal blue light response. One putative role is to stimulate photosynthesis via enhanced stomatal opening in the morning hours when blue light is more prevalent. In the results presented here, PFD was kept equal during the spectral changes, and CO₂ assimilation rate was invariable, despite significant changes in stomatal conductance in C₃ *T. hassleriana*, C₃-like *F. pringlei*, C₃ *F. robusta*, C₃ *F. cronquistii* and both *A. semialata* subspecies. These observations do not seem consistent with an important role for blue-light induced stomatal opening for photosynthetic carbon gain.

Could there be other benefits to blue sensitivity of stomatal movements? An alternative hypothesis to explain the differential sensitivity to blue light could be related to leaf thermoregulation. Stomatal opening in response to blue light has been suggested to work as a proxy for high-intensity sunlight [145] and function primarily to cool the leaf via transpiration [125]. Furthermore, photorespiration increases with temperature in C₃ species but is diminished in C₄ species [62, 6]. Hence, net CO₂ assimilation rate in C₄ species has a higher optimum temperature than in C₃ species [140], and a slight elevation of leaf temperature can substantially increase the photosynthesis rate in C₄, whereas the temperature response between 20°C and 30°C in C₃ species is almost negligible. Based on these differences, the presence of stomatal blue light response may help to cool the leaves of the C₃ dicot species studied here, and thus keep photorespiration lower, while the lack of the stomatal blue light response in the C₄ dicots may help elevate leaf temperature and thereby stimulate CO₂ assimilation rate.

Interestingly, this would also be consistent with the putative involvement of diminished PHOT expression, since PHOTs also perform thermosensory roles [29] and promote evapotranspiration and leaf cooling at high temperatures in *Arabidopsis* [54].

2.4.2 Differences in stomatal red light response are determined by species, rather than photosynthetic pathway

The mechanism underlying the red light response remains unresolved. Unlike the blue light response, red light-induced stomatal opening does not seem to involve direct signal transduction from red light photoreceptors in the guard cells but rather relies on the decrease in C_i through the consumption of CO₂ via mesophyll photosynthesis [85, 103, 62]. However, g_s was also observed to increase with red light despite constant or high C_i or after achieving

steady-state photosynthesis [78], which implies other signals than C_i could also be involved [63, 27].

C_4 photosynthesis operates in a two-cell compartment system, such that a strong metabolite gradient is essential to run it efficiently [67, 6]. Precise coordination between the C_3 and C_4 cycles is crucial under varying irradiances and C_i to avoid excessive CO_2 leakage from the bundle sheath [57]. C_3 photosynthesis, on the other hand, is less complex. We therefore hypothesized that species with these contrasting mesophyll photosynthesis characteristics may also be expected to show a different stomatal response to red light.

However, the comparison between the red light response in C_3 and C_4 dicot species showed that although significant variation in the stomatal red light response was found between species, no structural differences between C_3 and C_4 species were found across the three phylogenetically controlled comparisons. Instead, a distinct red light response was found in C_3 *T. hassleriana*, and a weaker, but significant red light effect was also found across all *Flaveria* species, suggesting that these species support the coordination between stomatal conductance and photosynthesis via stomatal responses to both C_i and red light. In contrast, C_4 *G. gynandra* as well as both *A. semialata* subspecies appear to rely solely on the C_i response.

One aspect of the red light response debate is whether stomatal guard cells can independently respond to red light. Indeed, a recent metabolomics study reported a direct guard cell response to red light [147]. This finding could be consistent with a putative mechanism involving the phosphorylation of the guard cell plasma membrane H^+ ATPase leading to stomatal opening in intact leaves [2]. Consistent with this mechanism, it was demonstrated that H^+ ATPase activation by red light was dependent on fluence rate [3]. If this mechanism can be shown to play a significant role, it may offer an alternative explanation for the observed species differences in the red light response, not necessarily dependent on a mesophyll-derived signal.

2.4.3 Role of stomatal morphology and density on stomatal movements in response to light

Stomatal density and morphology are well-known to impact responses to light [39]. These traits varied significantly between species studied here (Fig. 2.12). For most dicots, such as Cleomaceae and *Flaveria*, stomata are defined by a pair of kidney-shaped guard cells. In contrast, stomata in the monocot *A. semialata* subspecies are dumbbell-shaped with

A comparison of stomatal conductance responses to blue and red light between C₃ and C₄ photosynthetic species in three phylogenetically-controlled experiments

additional subsidiary cells flanking the guard cells. The morphology and size of stomata in the grasses are often suggested to facilitate more rapid responses to short-term environmental perturbations [15], such as fluctuating light or acute changes to temperature or VPD [9]. However, there was no evidence in this study linking stomatal morphology nor size to blue light-induced opening or quantitative red light responses.

Within the dicots, C₃ *T. hassleriana* (Cleomaceae) had denser and smaller stomata than the C₄ species *G. gynandra*, which was consistent with earlier observations [7]. The higher SD on the abaxial surface could be responsible for the pronounced red light response, independent of C_i in C₃ *T. hassleriana*. However, measurements on intact leaves do not make it possible to derive whether these responses rely on signal perception in the guard cell, or in the underlying mesophyll.

Furthermore, in *Flaveria*, SD and SS varied between species. Unlike in the Cleomaceae species, SD or SS had no evident relationship to the red light response in *Flaveria*. Additionally, the observed between-species variability in SD and SS in *Flaveria* was inconsistent with the proposed trajectory of stomatal density and guard cell length (and therefore, size) changes during C₄ evolution, where C₃ *Flaveria* species tended to have smaller but more stomata, while C₄ *Flaveria* show increased stomatal size and decreased density [145]. In fact, C₃-like *F. pringlei* and C₃ *F. cronquistii*, were found to have larger stomata (Fig. 2.12D), whereas both C₄ *Flaveria* had smaller stomatal sizes. The discrepancy between this study and Zhao et al. (2022) might have stemmed from low sample sizes used by the latter. Stomatal parameters in Zhao et al. (2022) were measured from a minimum of 5 individual stoma, to at most 10 stomata per species, which, as shown in Fig. 2.12D, is insufficient to capture size differences among *Flaveria* species.

Another possible reason for these discrepancies is the potential impact of ecological adaptation in some of the *Flaveria* species. C₃ *F. cronquistii* had equal stomatal distribution on both leaf surfaces like the C₄ *Flaveria* species, but with twice larger stomatal size on either leaf surface. In terms of leaf shape, C₃ *F. cronquistii* has linear, elongated leaves, whereas the other *Flaveria* representatives display elliptic or ovate leaf shapes. At an ecological standpoint, narrower leaves such as those in C₃ *F. cronquistii* perhaps reflect an adaptation in minimizing excessive heat load [68] whilst maximising net carbon gain [83] and together with a uniform stomatal distribution and a larger proportion of large stomata allow it to sustain higher g_s rates to effect cooling.

2.5 Conclusion

Here we used three phylogenetically-controlled comparisons to assess differences between stomatal anatomy and stomatal responses to red and blue light. The C₄ species in the dicot genera in this study did not have a detectable blue light stomatal blue light response, unlike their C₄ counterparts. However, perhaps surprisingly, the results demonstrate that the impact of photosynthetic pathway and stomatal morphology and distribution were not as strong as initially hypothesized, but instead varied between genera. Similarly, the quantitative red light response showed significant species variation but no association with photosynthetic pathway. Altogether, the findings suggest that the evolution of C₄ photosynthesis in the dicots may have lead to a change in light-regulated stomatal movements, challenge the general nature of previously observed stomatal morphological differences between C₃ and C₄ species [145] and demonstrate the importance of controlling for evolutionary distance.

Chapter 3

Investigating stomatal responses to CO₂ in C₃ and C₄ pairs of congeneric dicot species

3.1 Introduction

C₄ plants have a unique CO₂-concentrating mechanism (CCM) that allows them to increase the concentration of CO₂ around the enzyme Ribulose-1,5-bisphosphate carboxylase/oxygenase (Rubisco) in the bundle sheath cells. This helps to suppress the oxygenation reaction and limit photorespiration, which results in improved efficiency of photosynthesis. In contrast, C₃ plants do not have a CCM and rely solely on the diffusion of CO₂ into the leaf for photosynthesis, leading to competitive inhibition of RuBP carboxylation by RuBP oxygenation, and requires phosphoglycolate detoxification via the photorespiration pathway, which leads to less efficient carbon fixation.

In C₄ species, the ability to raise CO₂ concentration in the bundle sheath cells reduces the need for increased stomatal aperture. As a result, C₄ species have lower stomatal conductance and lower transpiration rate than the C₃ species, even under similar light and temperature conditions. Additionally, C₄ photosynthesis is typically CO₂-saturated at ambient CO₂ concentrations, facilitated by the higher affinity of PEPC for inorganic carbon, compared to Rubisco, leading to a reduced dependence of CO₂ assimilation rates on stomatal conductance and consequently a lower operational C_i as compared to C₃ photosynthesis. This reduced stomatal conductance at a given rate of CO₂ assimilation in C₄ plants leads to a higher water

Investigating stomatal responses to CO₂ in C₃ and C₄ pairs of congeneric dicot species

use efficiency (WUE) compared to C₃ plants, as less water is lost by transpiration for each CO₂ fixed. As such, if stomata are designed to maximise WUE as is often assumed, this would suggest that C₄ stomata would already be relatively closed under ambient conditions, and would remain closed at CO₂ levels above ambient. Furthermore, because PEPC in C₄ photosynthesis is saturated at a much lower [C_i] than Rubisco, any decrease in g_s will decrease assimilation (A) rate in a C₃ species, whereas in C₄ species it will only affect A if C_i is lowered below 100-150 μmol mol⁻¹ [69], suggesting that C₄ plants will be more sensitive to changes in CO₂ concentrations in the sub-ambient range.

Both hypotheses above imply that the sensitivity of stomatal movements to both supra-ambient and sub-ambient CO₂ could be significantly altered in C₄ relative to C₃ species. Studies in *Arabidopsis* show that stomatal responses to CO₂ are regulated by distinct signal transduction pathways controlling stomatal movements in response to high or low CO₂. [144]. Interestingly, these pathways converge with the blue light response pathway through the action of the CBC1 and CBC2 (Convergence of Blue Light and CO₂) protein kinases, which interact with the HT1 kinase to impact the SLAC1 anion channel in response to both cues. Blue light is a potent signal to trigger stomatal opening [2]. According to Vialet-Chabrand and colleagues (2021), blue light functions to power stomatal movement through ATP and reducing power derived from mitochondrial respiration. Findings from the previous chapter of this thesis show that the two C₄ dicot species assessed in this thesis do not have a significant blue light response. This may imply also that they rely less on mitochondrial energy support for stomatal opening, compared to their C₃ relatives.

In this chapter, we investigated the CO₂-dependent regulation of stomatal movements in pairs of C₃ and C₄ dicots from Cleomaceae and *Flaveria*. We hypothesise that 1) because C₄ photosynthesis is typically CO₂-saturated that C₄ stomata would remain relatively closed at ambient and above ambient CO₂; 2) CO₂-dependent stomatal regulation in C₄ species will exhibit a high degree of sensitivity to CO₂ and stomatal control compared to C₃ species at sub-ambient CO₂ range; and, 3) species with weak blue light responses are less dependent on mitochondrial energy for stomatal movements, and thus, they are expected to be less responsive to CO₂ in darkness.

3.2 Materials and Methods

3.2.1 Plant materials and growth conditions

As in Chapter 2, the same phylogenetically-controlled comparisons from Cleomaceae (C_4 *Gynandropsis* and C_3 *Tarenaya*) and *Flaveria* (C_4 *F. bidentis* and C_3 *F. cronquistii*) were used. Plants were grown similarly in M3 compost as described in Chapter 2, except that a new formulation of M3 was used, which has reduced peat content. Environmental conditions were the same as in Chapter 2.

3.2.2 Gas exchange measurements

Gas exchange measurements were performed on recently expanded leaves using an open gas exchange system (LI-6400XT, LI-COR, Lincoln, NE, USA) with an integrated fluorometer light source (LI-6400-40, LI-COR). Leaves were either kept in darkness or illuminated with $350 \mu\text{mol m}^{-2} \text{s}^{-1}$ Red PFD and 410 ppm reference CO_2 (CO_2R) at a flow rate of $300 \mu\text{mol s}^{-1}$ and a block temperature of 25°C .

To characterise stomatal behaviour in response to different CO_2 levels, leaves were allowed to achieve steady state for 1.5-2 h and then exposed to two different ranges of CO_2 concentrations. The lower [CO_2] range varied from 410 to 75 and then to 410 ppm, while the upper [CO_2] range started at 410 ppm and increased to 1500 ppm before returning to 410 ppm. At each [CO_2], the leaves were exposed for 30 min, and [CO_2] were adjusted using a custom auto-program. Throughout the experiment, the assimilation rate and stomatal conductance were recorded every 5 minutes. VPD ranged from 1.0 to 1.5 kPa from the beginning of acclimatisation until the end of the auto-programme, which lasted between 6.5 and 7 h. Due to the lengthy protocol, only one set of measurements was collected per day for each biological replicate. All measurements were taken within 2 h after the start and 2 h before the end of the photoperiod.

3.2.3 Experimental design

The objective of the experiment was to determine whether g_s in C_3 and C_4 dicots respond differently to changes in CO_2 concentrations. CO_2 concentrations followed two simple step-wise patterns of decreasing then increasing (low CO_2 range) or increasing then decreasing

Investigating stomatal responses to CO₂ in C₃ and C₄ pairs of congeneric dicot species

(high CO₂ range) starting and ending at 410 ppm CO₂, equally spaced at 30 min intervals, and logged every 5 min. The treatment combinations (plant and light treatments) were assigned randomly to each gas exchange system to avoid non-random errors.

3.2.4 Statistical analysis

Timeseries data were first used to generate g_s/C_i curves. Log-transformed data were fitted with linear models following the form, $g_s = a + b \cdot \log(C_i)$ using the *drc* package [100] in the RStudio environment [95] to examine the relationship between g_s and C_i during the first and second half of the CO₂ response sequences. The slope parameter of the fitted linear equation were extracted and subjected to mixed-model analysis using JMP Pro version 17 (SAS Institute). The means were compared using Tukey's HSD at $\alpha = 0.05$.

CO₂ response curves and interaction plots were generated using *ggplot2* [138] and compiled using *ggpubr* [51] in R version 4.2.1 [99] using the RStudio environment, version 2022.07.1 [95].

3.3 Results

To evaluate CO₂-dependent changes in g_s , gas exchange was measured in response to step changes in CO₂ concentrations. CO₂ treatments were designed as ordered sequences of increasing or decreasing CO₂ concentrations performed independently on pairs of C₃ and C₄ of Cleomaceae and *Flaveria*. These treatments were performed under 350 PFD red light or with the lights switched off.

3.3.1 Cleomaceae, under increasing then decreasing CO₂ concentration

C₄ *G. gynandra*

In C₄ *G. gynandra*, steady state g_s under 100% red light was 0.122 ± 0.011 mol CO₂ m⁻² s⁻¹, which decreased to 0.112 ± 0.012 mol CO₂ m⁻² s⁻¹ after switching to 600 ppm CO₂, and decreased slightly to 0.109 ± 0.011 mol CO₂ m⁻² s⁻¹ after changing [CO₂] to 900 ppm (Figure 3.1A). g_s then remained around 0.096 ± 0.010 mol CO₂ m⁻² s⁻¹ to 0.100 ± 0.010 mol CO₂ m⁻² s⁻¹, between 1200 ppm CO₂ and 600 ppm CO₂, before rising to 0.109 ± 0.010 mol CO₂ m⁻² s⁻¹ at 410 ppm CO₂ at the end of the time course.

In the dark, steady state g_s was 0.085 ± 0.010 mol CO₂ m⁻² s⁻¹ at the beginning of treatment at 410 ppm CO₂, then decreased to 0.075 ± 0.007 mol CO₂ m⁻² s⁻¹ at 1500 ppm CO₂ and to 0.073 ± 0.006 mol CO₂ m⁻² s⁻¹ upon return to 410 ppm (Figure 3.1A).

C₃ *T. hassleriana*

In C₃ *T. hassleriana*, g_s under 100% red light decreased from 0.355 ± 0.027 mol CO₂ m⁻² s⁻¹ to 0.293 ± 0.023 mol CO₂ m⁻² s⁻¹ after changing [CO₂] to 600 ppm (Figure 3.1B). Subsequently, a more gradual decrease was observed from 900 to 1500 ppm CO₂ from 0.231 ± 0.018 mol CO₂ m⁻² s⁻¹ to 0.164 ± 0.014 mol CO₂ m⁻² s⁻¹. g_s continued to decrease to 0.153 ± 0.014 mol CO₂ m⁻² s⁻¹ to 0.146 ± 0.013 mol CO₂ m⁻² s⁻¹ before increasing slightly to 0.154 ± 0.013 mol CO₂ m⁻² s⁻¹ at 600 ppm and finally to 0.179 ± 0.013 mol CO₂ m⁻² s⁻¹ at the end of treatment. The final g_s value was 50% lower than the starting g_s of 0.355 ± 0.027 mol CO₂ m⁻² s⁻¹ suggesting a hysteretic effect.

In parallel treatment in darkness, g_s decreased from 0.076 ± 0.010 mol CO₂ m⁻² s⁻¹ to 0.058 ± 0.009 at 600 ppm CO₂ to 0.049 ± 0.006 at 900 ppm CO₂ after which g_s remained stable throughout the rest of treatment at an average g_s of 0.040 ± 0.005 mol CO₂ m⁻² s⁻¹ (Figure 3.1B).

3.3.2 g_s response curve of Cleomaceae under decreasing then increasing CO₂ concentration

C₄ *G. gynandra*

At low [CO₂], under 100% red light, g_s of C₄ *G. gynandra* gradually increased from 0.140 ± 0.018 mol CO₂ m⁻² s⁻¹ at 410 ppm CO₂, to 0.360 ± 0.056 mol CO₂ m⁻² s⁻¹ at 75 ppm CO₂ (Figure 3.1C). Maximum g_s was reached at 100 ppm CO₂, where g_s was 0.375 ± 0.056 mol CO₂ m⁻² s⁻¹, twice the starting g_s . In the second half of treatment, from 200 ppm CO₂ back to 410 ppm CO₂, g_s decreased rapidly from 0.324 ± 0.041 mol CO₂ m⁻² s⁻¹ to 0.214 ± 0.019 mol CO₂ m⁻² s⁻¹ at the end of the treatment. In the dark, g_s remained constant from the starting g_s of 0.041 ± 0.005 mol CO₂ m⁻² s⁻¹ to the end of treatment at 0.048 ± 0.003 mol CO₂ m⁻² s⁻¹, except for a small increase in the second half of treatment at 100 ppm CO₂, with a g_s of 0.058 ± 0.004 mol CO₂ m⁻² s⁻¹ (Figure 3.1C).

Investigating stomatal responses to CO₂ in C₃ and C₄ pairs of congeneric dicot species

C₃ *T. hassleriana*

At 100% red light g_s in C₃ *T. hassleriana* at 0.354 ± 0.051 mol CO₂ m⁻² s⁻¹ at 410 ppm CO₂. Subsequently, g_s reached the maximum g_s value of 0.462 ± 0.034 mol CO₂ m⁻² s⁻¹ at 75 ppm CO₂ (Figure 3.1D). On switching to higher [CO₂] g_s began to slowly decrease until a final g_s of 0.316 ± 0.049 mol CO₂ m⁻² s⁻¹ was reached at the end of the experiment at 410 ppm CO₂.

The beginning of g_s of C₃ *T. hassleriana* was 0.105 ± 0.019 mol CO₂ m⁻² s⁻¹ in the dark (Figure 3.1D). g_s increased to 0.238 ± 0.014 mol CO₂ m⁻² s⁻¹ reaching maximum values at 75 ppm CO₂. Subsequently, the change to 100 ppm CO₂ in the second half of treatment gave a g_s of 0.225 ± 0.019 mol CO₂ m⁻² s⁻¹ that continued to slowly decrease to 0.080 ± 0.014 mol CO₂ m⁻² s⁻¹ at the final CO₂ concentration of 410 ppm.

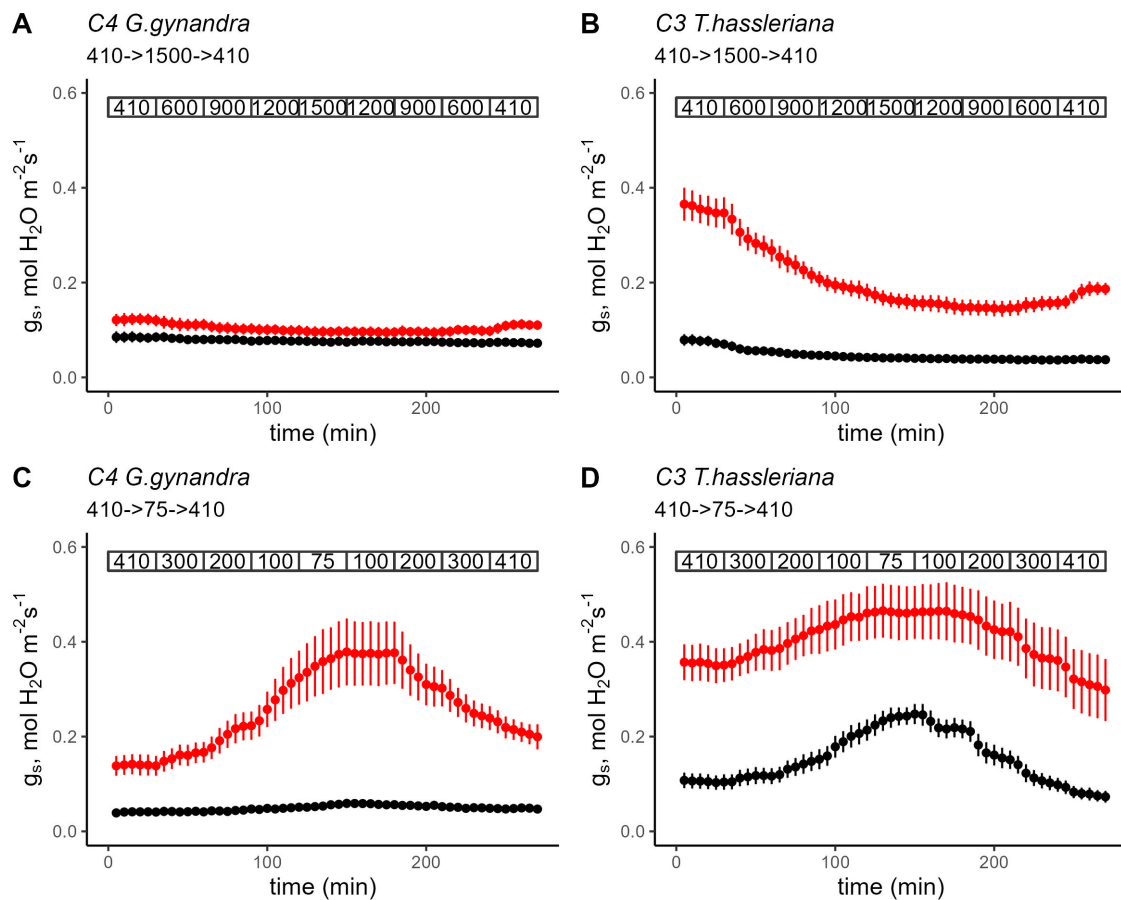


Fig. 3.1 Response of g_s in Cleomaceae to sequences of increasing (A,B) or decreasing (C,D) $[\text{CO}_2]$. To characterise stomatal behaviour in response to different CO_2 levels, leaves were allowed to achieve steady state at $350 \mu\text{mol m}^{-2} \text{s}^{-1}$ red light PPFD for 1.5-2 h and then exposed to two different ranges of $[\text{CO}_2]$. The lower $[\text{CO}_2]$ range varied from 410 to 75 and then to 410 ppm, while the upper $[\text{CO}_2]$ range started at 410 ppm and increased to 1500 ppm before returning to 410 ppm. At each $[\text{CO}_2]$, the leaves were exposed for 30 min, and $[\text{CO}_2]$ were adjusted using a custom auto-program. The assimilation rate and stomatal conductance were recorded every 5 minutes. VPD ranged from 1.0 to 1.5 kPa from the beginning of acclimatisation until the end of the auto-programme, which lasted between 6.5 and 7 h. Due to the lengthy protocol, only one set of measurements was collected per day for each biological replicate. All measurements were taken within 2 h after the start and 2 h before the end of the photoperiod.

Substantial stomatal movements were also observed in the dark, with g_s peaking at the lowest CO_2 concentration. g_s increased more than two-fold from steady state g_s of $0.105 \pm 0.043 \text{ mol CO}_2 \text{ m}^{-2} \text{ s}^{-1}$ at 410 ppm to $0.238 \pm 0.032 \text{ mol CO}_2 \text{ m}^{-2} \text{ s}^{-1}$ at 75 ppm.

3.3.3 g_s response curve of *Flaveria* under increasing then decreasing CO₂ concentration

C₄ F. bidentis

At 410 ppm CO₂ steady state g_s under 100% red light was 0.133 ± 0.012 mol CO₂ m⁻² s⁻¹ and decreased slightly to 0.094 ± 0.010 mol CO₂ m⁻² s⁻¹ at the highest [CO₂] of 1500 ppm. A stepwise reduction in CO₂ had no effect on g_s until the CO₂ concentration returned to its original level. In the dark, g_s showed a steady decrease with an initial steady state g_s of 0.084 ± 0.013 mol CO₂ m⁻² s⁻¹, to 0.060 ± 0.011 mol CO₂ m⁻² s⁻¹ at 1500 ppm, to the final [CO₂] of 410 ppm, with a g_s of 0.049 ± 0.008 mol CO₂ m⁻² s⁻¹.

C₃ F. cronquistii

Steady state under 100% g_s in C₃ *F. cronquistii* at 410 ppm started at 0.210 ± 0.029 mol CO₂ m⁻² s⁻¹ decreasing to 0.130 ± 0.026 mol CO₂ m⁻² s⁻¹ at 1500 ppm, further decreasing to 0.114 ± 0.027 mol CO₂ m⁻² s⁻¹ at 410 ppm at end of treatment. Similarly, in the dark, steady state g_s showed a steady decline from 0.157 ± 0.044 mol CO₂ m⁻² s⁻¹ at the beginning of treatment, slowly decreasing to 0.121 ± 0.032 mol CO₂ m⁻² s⁻¹ to 0.101 ± 0.030 mol CO₂ m⁻² s⁻¹ at the end of treatment.

3.3.4 g_s response curve of *Flaveria*, under decreasing then increasing CO₂ concentration

C₄ F. bidentis

C₄ F. bidentis steady state g_s under 100% red light was 0.155 ± 0.013 μmol CO₂ m⁻² s⁻¹ increasing by roughly 0.030 μmol CO₂ m⁻² s⁻¹ at every decrease in [CO₂]. At the lowest [CO₂] g_s was 0.414 ± 0.022 μmol CO₂ m⁻² s⁻¹. The highest g_s of 0.431 ± 0.021 μmol CO₂ m⁻² s⁻¹ was recorded in the second half of the treatment, at 100 ppm CO₂, with 0.431 ± 0.021 μmol CO₂ m⁻² s⁻¹.

The steady state g_s in the dark was 0.081 ± 0.013 μmol CO₂ m⁻² s⁻¹ at 410 ppm at the beginning of treatment. g_s decreased by 0.073 ± 0.012 μmol CO₂ m⁻² s⁻¹ at 410 ppm, before reaching 0.080 ± 0.012 μmol CO₂ m⁻² s⁻¹, which was practically starting g_s values, at 75

ppm CO₂. From the second half of the treatment, g_s decreased further from 0.075 ± 0.012 μmol CO₂ m⁻² s⁻¹ at 100 ppm CO₂ to 0.045 ± 0.010 μmol CO₂ m⁻² s⁻¹.

C₃ F. cronquistii

When exposed to 100% red light, *C₃ F. cronquistii* began with a steady state of g_s of 0.205 ± 0.023 μmol CO₂ m⁻² s⁻¹ and increased to 0.255 ± 0.026 μmol CO₂ m⁻² s⁻¹ at 75 ppm [CO₂]. The highest g_s values were observed in the second half of the time course, when the CO₂ level was at 100 ppm, with 0.260 ± 0.025 μmol CO₂ m⁻² s⁻¹. Subsequently, g_s decreased rapidly and eventually reached a final g_s of 0.142 ± 0.015 μmol CO₂ m⁻² s⁻¹ after returning at 410 ppm.

In darkness, the steady state g_s was 0.087 ± 0.014 μmol CO₂ m⁻² s⁻¹, which gradually increased to 0.103 ± 0.017 μmol CO₂ m⁻² s⁻¹ when [CO₂] was 75 ppm. During the second half of the treatment, when the [CO₂] was 100 ppm, g_s rose to 0.109 ± 0.017 μmol CO₂ m⁻² s⁻¹. Subsequently, g_s decreased to 0.060 ± 0.014 μmol CO₂ m⁻² s⁻¹ upon return at [CO₂] of 410 ppm at the end of the experiment.

Investigating stomatal responses to CO₂ in C₃ and C₄ pairs of congeneric dicot species

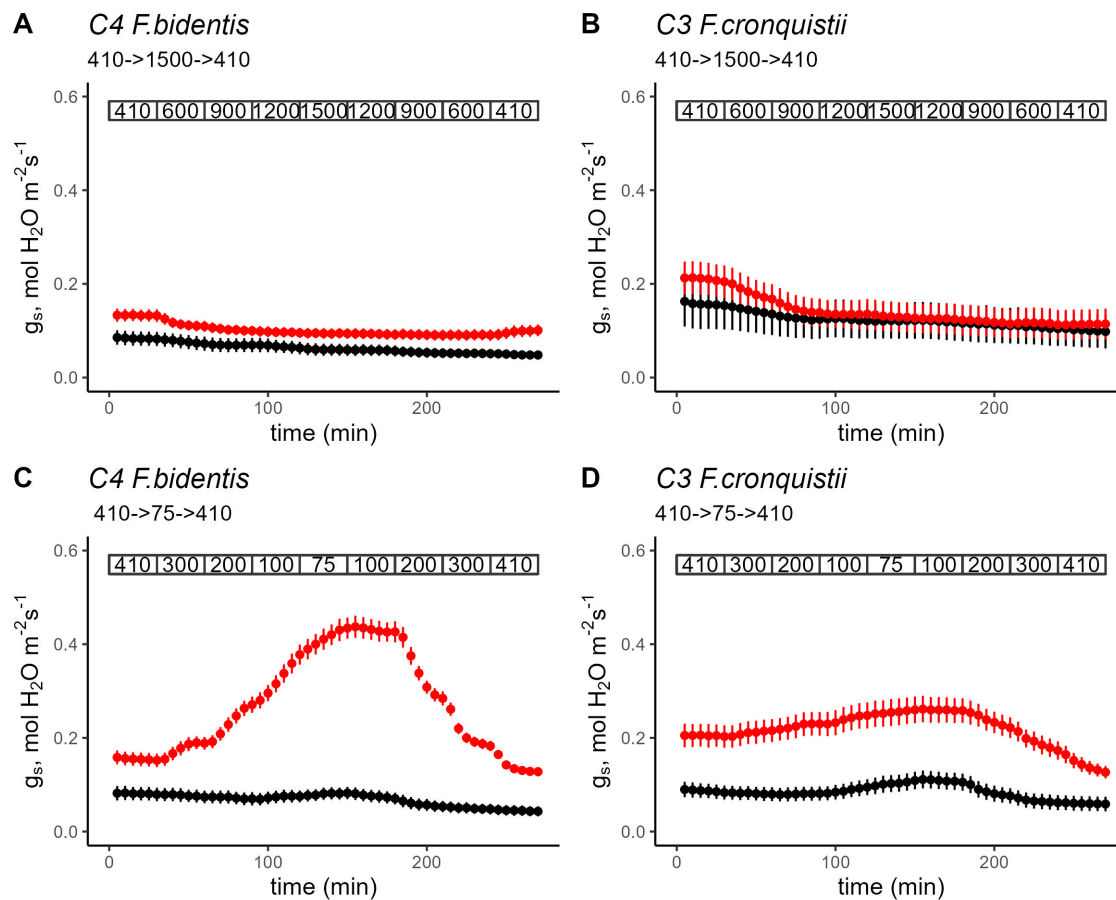


Fig. 3.2 Response of g_s in *Flaveria* to sequences of increasing (A,B) or decreasing (C,D) [CO₂]. To characterise stomatal behaviour in response to different CO₂ levels, leaves were allowed to achieve steady state at 350 $\mu\text{mol m}^{-2} \text{s}^{-1}$ red light PPFD for 1.5-2 h and then exposed to two different ranges of [CO₂]. The lower [CO₂] range varied from 410 to 75 and then to 410 ppm, while the upper [CO₂] range started at 410 ppm and increased to 1500 ppm before returning to 410 ppm. At each [CO₂], the leaves were exposed for 30 min, and [CO₂] were adjusted using a custom auto-program. The assimilation rate and stomatal conductance were recorded every 5 minutes. VPD ranged from 1.0 to 1.5 kPa from the beginning of acclimatisation until the end of the auto-programme, which lasted between 6.5 and 7 h. Due to the lengthy protocol, only one set of measurements was collected per day for each biological replicate. All measurements were taken within 2 h after the start and 2 h before the end of the photoperiod.

3.3.5 Log-linear curve-fitting to systematically analyze responses to CO₂, light and presence of significant hysteresis

Cleomaceae

To analyse the stomatal responses to CO₂ in the presence and absence of light in a more structured way, the g_s values were first plotted as a function of C_i (Figure 3.3 and Figure 3.5). Then, log-linear plots were fitted to the data and the resulting slope values were statistically compared between the four combinations (high/low CO₂ and light/darkness) (Figure 3.4 and Figure 3.6). In C₄ *G. gynandra*, a highly significant two-way interaction was found between the effects of light and CO₂ ($p < 0.0001$) Table (3.1). When the leaves were left in darkness or illuminated, the slope under high CO₂ condition was close to zero and not significantly different ($P < 0.05$). In contrast, at low CO₂, there was a significant difference ($P < 0.05$) in the slope parameter between leaves kept in darkness where it was still close to zero and those leaves which were illuminated where it was significantly more negative. These differences were present both during at the descending and ascending parts of the treatment. Thus, the effect of decreasing CO₂ on stomatal opening was only significant in the presence of light but not in darkness. Comparison of the slopes of log-linear fits between the ascending and descending parts of the experiment showed that there was no significant hysteresis in the stomatal responses observed in C₄ *G. gynandra* in any of the conditions.

Investigating stomatal responses to CO₂ in C₃ and C₄ pairs of congeneric dicot species

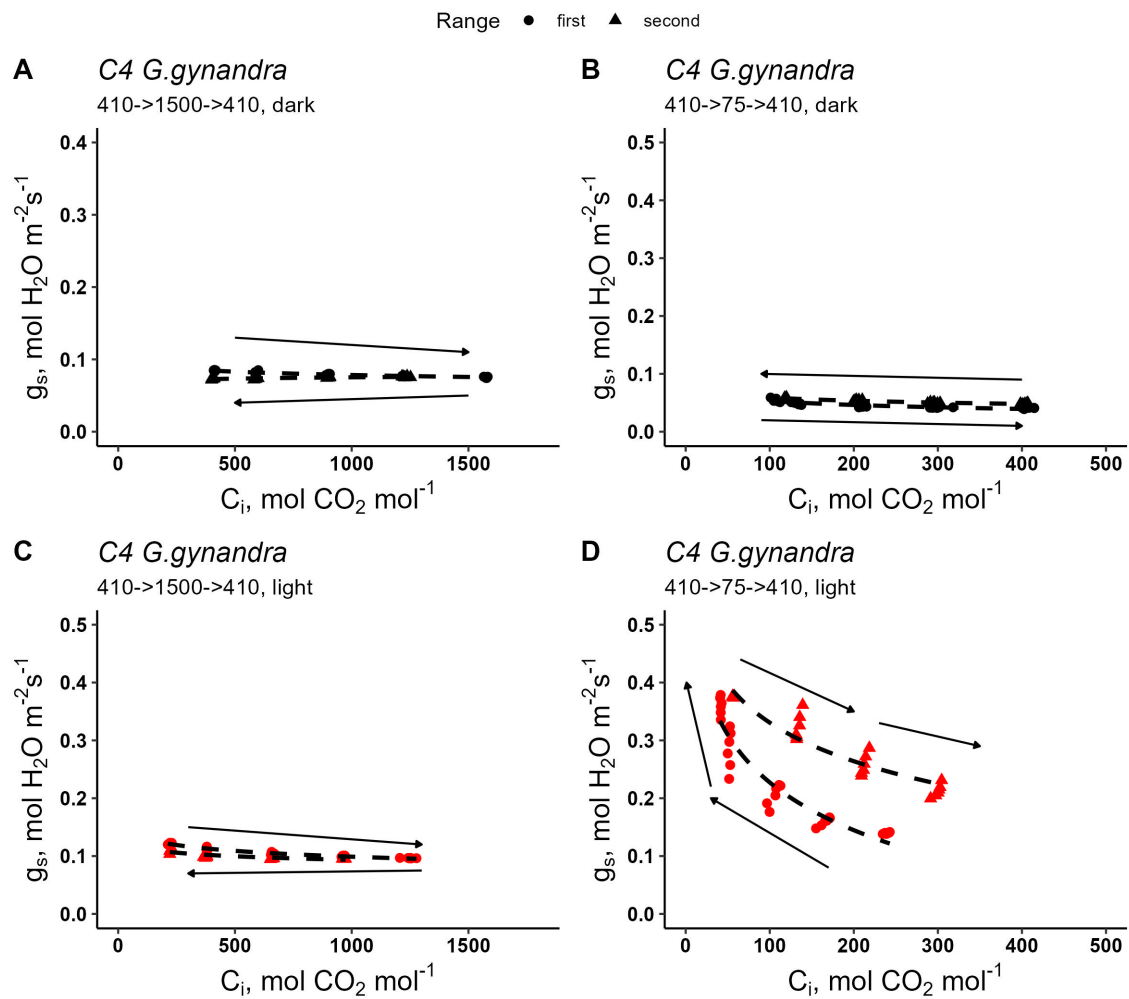


Fig. 3.3 Plots of g_s as a function of C_i in *C4 G. gynandra* for **A**) high CO₂, darkness, **B**) low CO₂, darkness, **C**) high CO₂, light; and **D**) low CO₂, light. First (circle) and second (triangle) portions of the CO₂ response curve indicate where CO₂ concentration was either increasing or decreasing. Arrows indicate the direction of the response. Data were taken from $n = 5-6$ biological replicates.

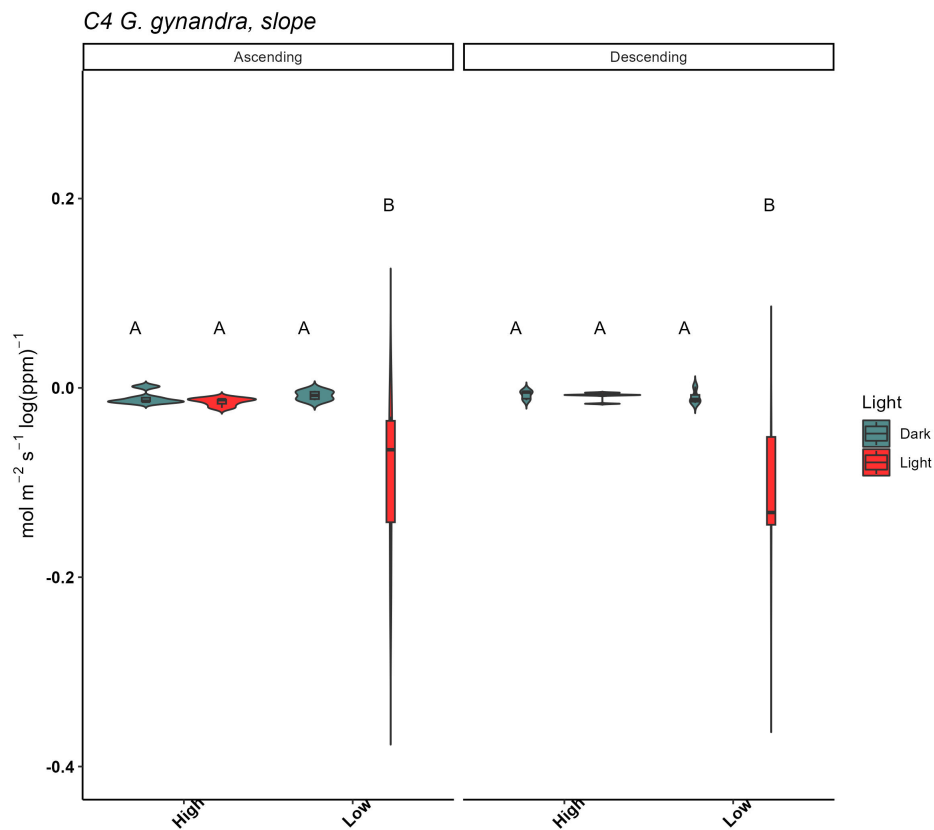


Fig. 3.4 Violin/box plots of the slope parameter from log-linear fits of the *C4 G. gynandra* and *C3 T. hassleriana* CO₂ response curves.

Table 3.1 Mixed-effects ANOVA of the slope parameter in *C4 G. gynandra* in all light and CO₂ conditions.

Source	DF	F ratio	Pr(>F)
Light	1	19.46	0.0002
CO ₂	1	15.08	0.0006
Light*CO ₂	1	17.47	0.0003
Range	1	0.0993	0.7552
Light*Range	1	0.1449	0.7066
CO ₂ *Range	1	0.4794	0.4949
Light*CO ₂ *Range	1	0.2364	0.6309

In *C3 T. hassleriana*, a highly significant interaction between the effects of light, CO₂, and CO₂ range (p=0.0360) was found Table (3.2). In leaves kept in darkness, slopes at

Investigating stomatal responses to CO₂ in C₃ and C₄ pairs of congeneric dicot species

high [CO₂] were not significantly different between the ascending (-0.0244) and descending (0.0017) portions of the treatment. Meanwhile, when leaves were illuminated, the slope was more negative (-0.1391) during the ascending part of the CO₂ response, while it was closer to zero (-0.0197) at descending CO₂ levels thus demonstrating significant hysteresis. At low CO₂, regardless of illumination, the slopes during the descending and ascending parts of the curve were more negative and not statistically significant from each other (P>0.05). Thus, in C₃ *T. hassleriana*, stomata responded significantly to changes in C_i in the subambient range, both in darkness and under illumination, whereas stomatal movements in response to C_i in the supra-ambient range were only significant in the presence of light.

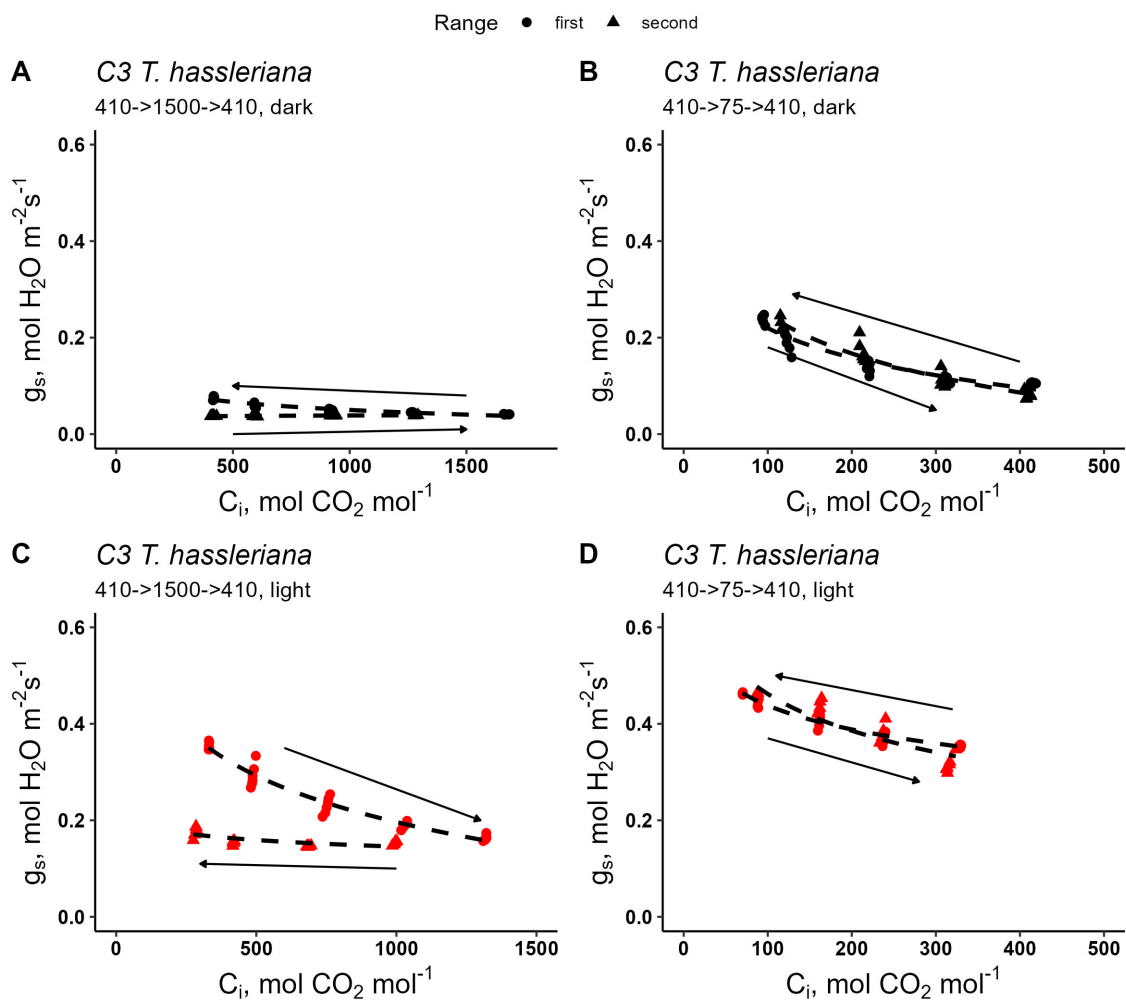


Fig. 3.5 Plots of g_s as a function of C_i in C₃ *T. hassleriana* for **A**) high CO₂, darkness, **B**) low CO₂, darkness, **C**) high CO₂, light; and **D**) low CO₂, light. First (circle) and second (triangle) portions of the CO₂ response curve indicate where CO₂ concentration was either increasing or decreasing. Arrows indicate the direction of the response. Data were taken from n = 5-6 biological replicates.

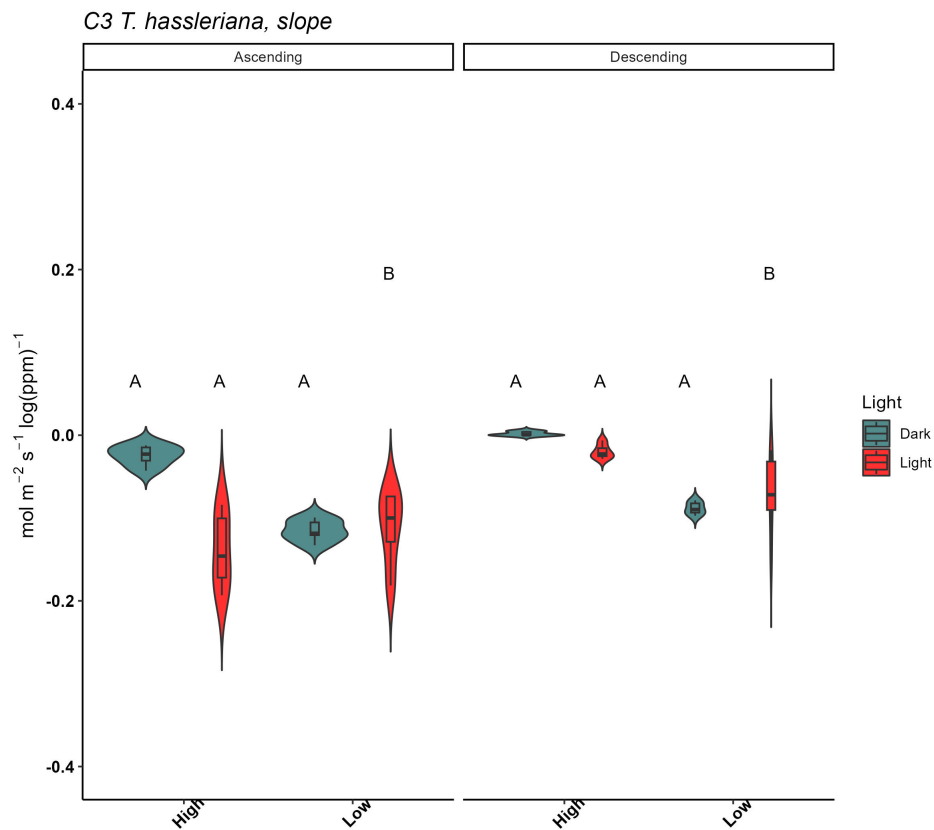


Fig. 3.6 Violin/box plots of the slope parameter from log-linear fits of the *C₃ T. hassleriana* CO_2 response curves.

Table 3.2 Mixed-effects ANOVA of the slope parameter in *C₃ T. hassleriana* in all light and CO_2 conditions.

Source	DF	F ratio	Pr(>F)
Light	1	9.93	0.0036
CO_2	1	31.25	<0.0001
Light* CO_2	1	18.21	0.00002
Range	1	33.42	<0.0001
Light*Range	1	8.33	0.0072
CO_2 *Range	1	4.61	0.0400
Light* CO_2 *Range	1	4.82	0.0360

Stomatal responses to CO_2 in *C₄ F. bidentis* showed significant two-way interaction between the effects of $[\text{CO}_2]$ and the range of $[\text{CO}_2]$ ($p=0.0050$) and between light and

Investigating stomatal responses to CO₂ in C₃ and C₄ pairs of congeneric dicot species

CO₂ ($p < 0.0001$) Table (3.3). At high CO₂, whether in darkness or illuminated, the slope parameter in C₄ *F. bidentis* were not significantly different at the ascending and descending parts of the treatment. However, at low CO₂, the presence or absence of light had a strong influence on the slope parameter which became significantly more negative in the presence of light. Furthermore, the slopes were significantly more negative for the ascending part of the experiment, indicating significant hysteresis due to more rapid closing than opening in the subambient range. In darkness, the slope was closer to zero (0.0001) than in the second portion (ascending) of the experiment (slope value). Similarly, when leaves were illuminated, the ascending portion of the CO₂ response was more negative (-0.1832) than the initial descending part (-0.1264). These differences were statistically significant and imply that decreasing CO₂ stimulated the stomatal opening response and that although there was also a marginally significant response to low CO₂ in darkness, the opening stimulus was substantially stronger when the leaves were illuminated.

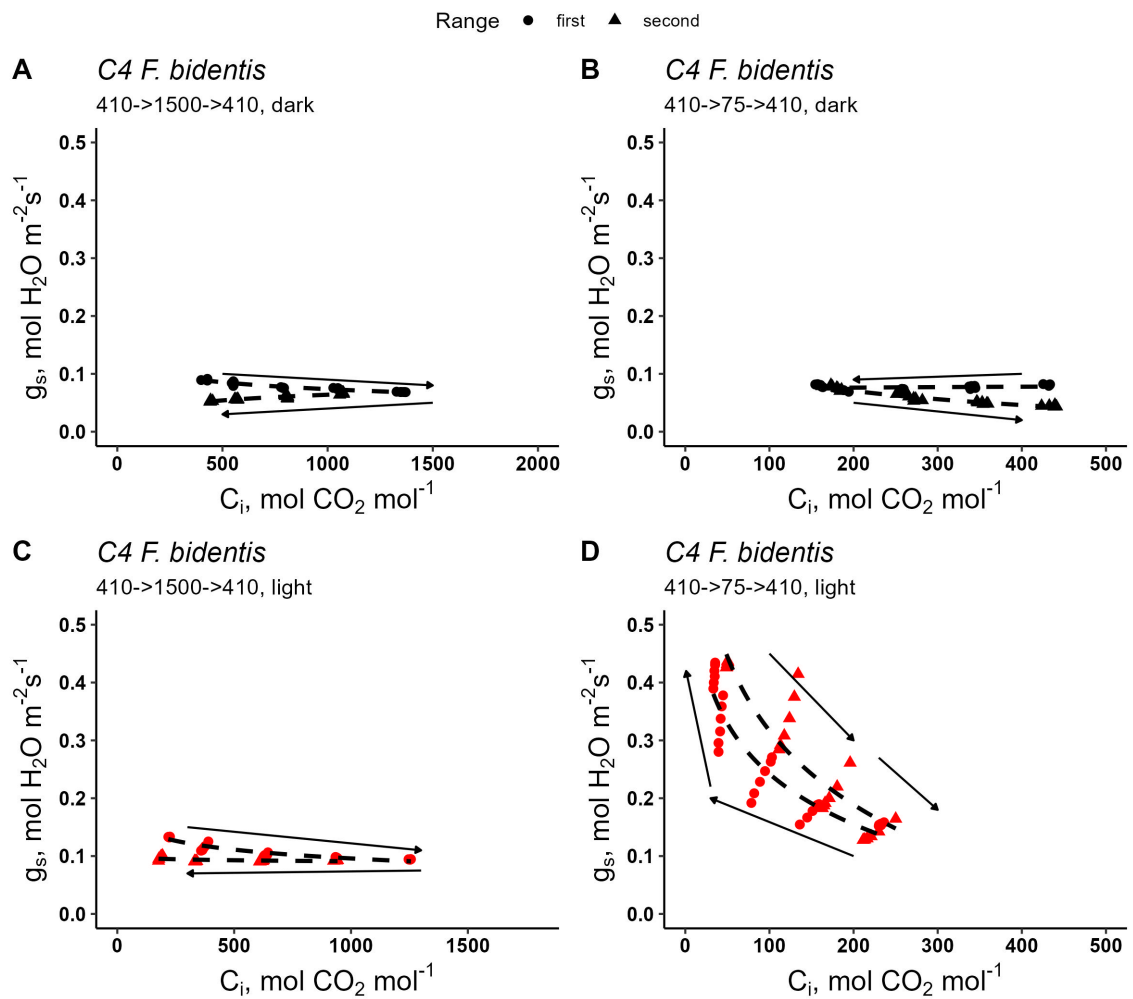


Fig. 3.7 Plots of g_s as a function of C_i in *C4 F. bidentis* for **A**) high CO_2 , darkness, **B**) low CO_2 , darkness, **C**) high CO_2 , light; and **D**) low CO_2 , light. First (circle) and second (triangle) portions of the CO_2 response curve indicate where CO_2 concentration was either increasing or decreasing. Arrows indicate the direction of the response. Data were taken from $n = 5-6$ biological replicates.

Investigating stomatal responses to CO₂ in C₃ and C₄ pairs of congeneric dicot species

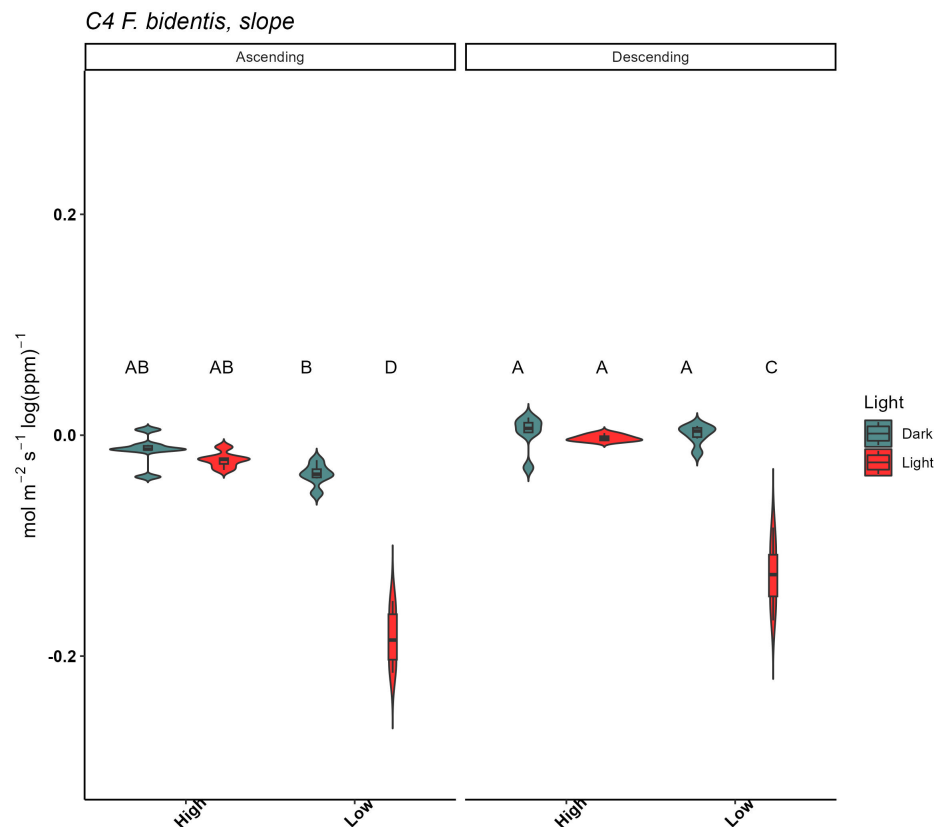


Fig. 3.8 Slope parameter from log-linear fits of C₄ *F. bidentis*

Table 3.3 Mixed-effects ANOVA of the slope parameter in C₄ *F. bidentis* in all light and CO₂ conditions.

Source	DF	F ratio	Pr(>F)
Light	1	222.4	<0.0001
CO ₂	1	255.0	<0.0001
Light*CO ₂	1	182.2	<0.0001
Range	1	44.22	<0.0001
Light*Range	1	1.637	0.2029
CO ₂ *Range	1	8.956	0.0050
Light*CO ₂ *Range	1	0.7093	0.4054

In C₃ *F. cronquistii* (Figure 3.9 and ??), a significant two-way interactions between light and range ($p=0.0226$) and light and CO₂ ($p=0.0308$) were detected Table (3.4). Slope values were more negative in tyhe ascending part of the CO₂ treatment than during the descending

part of the CO₂ response curve, but this difference was only significant under illumination. Additionally, slopes at low CO₂ were marginally more negative in the presence of light, whereas at high CO₂, slopes were not significantly different between illuminated leaves and those kept in darkness.

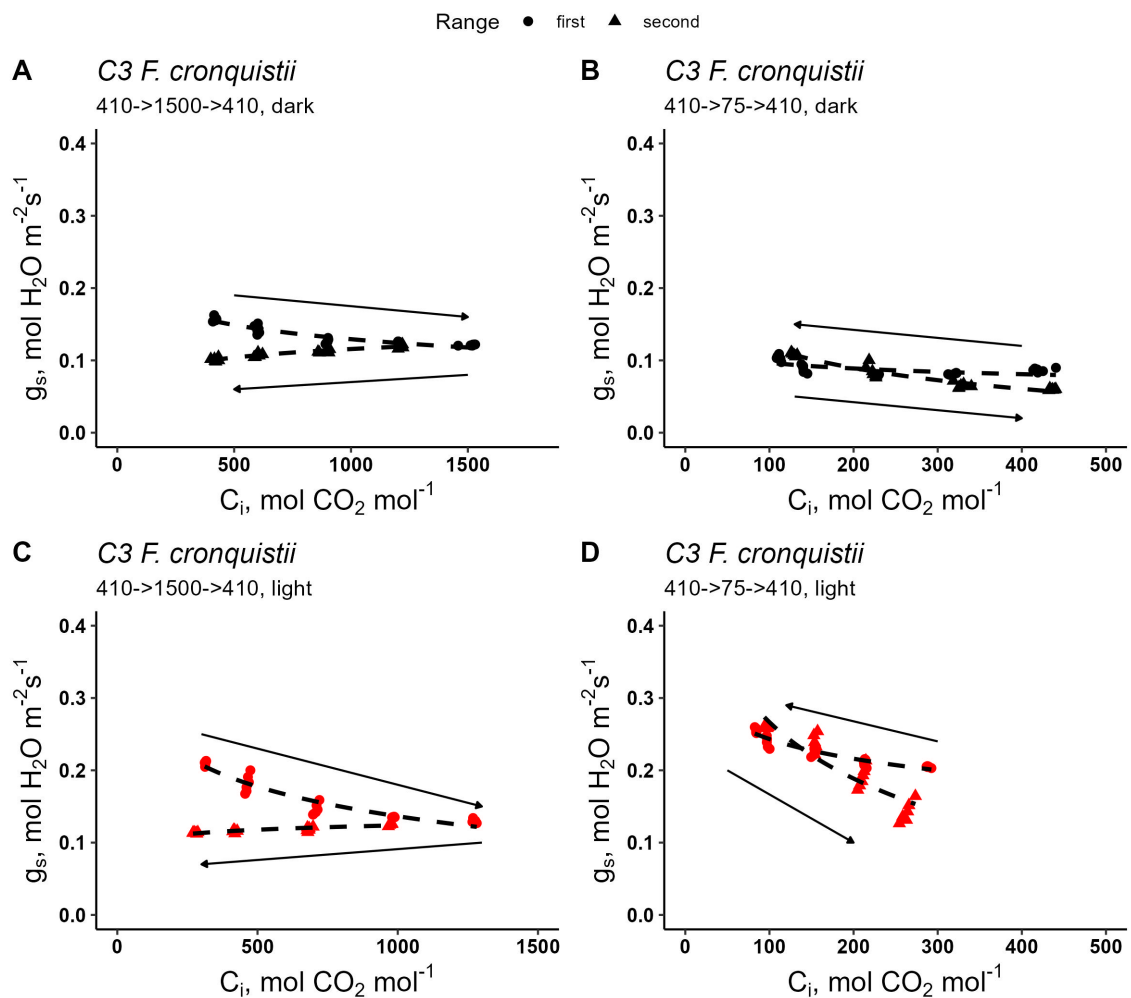


Fig. 3.9 Plots of g_s as a function of C_i in *C3 F. cronquistii* for **A**) high CO₂, darkness, **B**) low CO₂, darkness, **C**) high CO₂, light; and **D**) low CO₂, light. First (circle) and second (triangle) portions of the CO₂ response curve indicate where CO₂ concentration was either increasing or decreasing. Arrows indicate the direction of the response. Data were taken from $n = 5-6$ biological replicates.

Investigating stomatal responses to CO₂ in C₃ and C₄ pairs of congeneric dicot species

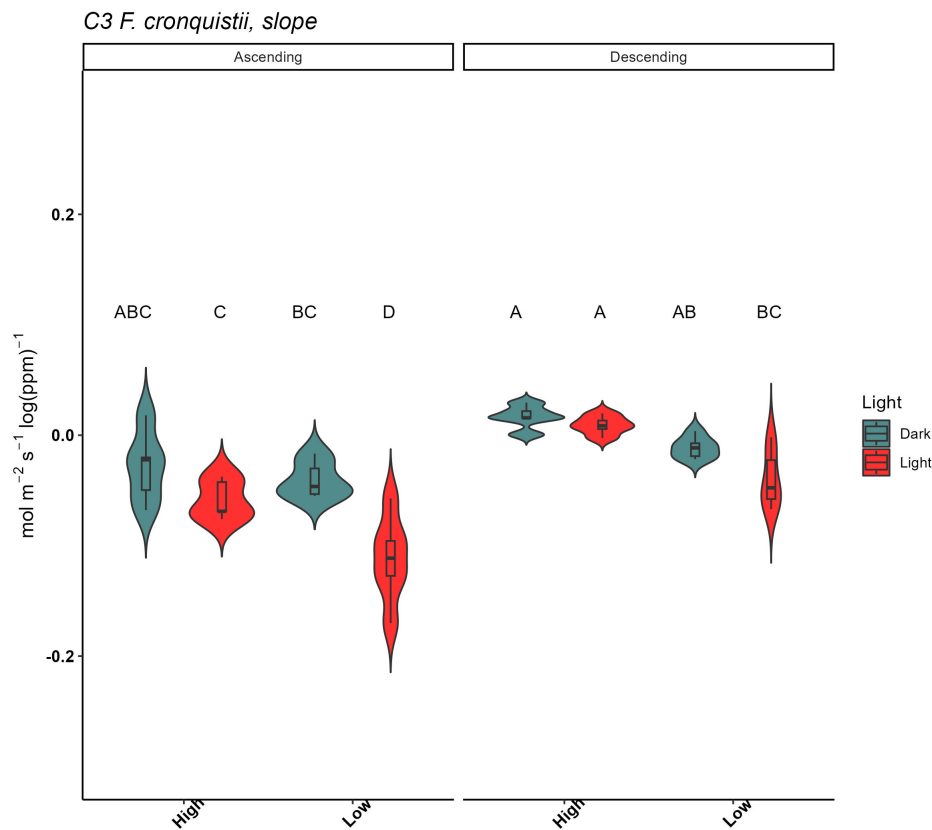


Fig. 3.10 Slope parameter from log-linear fits of C₃ *F. cronquistii*

Table 3.4 Mixed-effects ANOVA of the slope parameter in C₃ *F. cronquistii* in all light and CO₂ conditions.

Source	DF	F ratio	Pr(>F)
Light	1	25.43	0.0036
CO ₂	1	26.44	<0.0001
Light*CO ₂	1	5.111	0.0380
Range	1	61.35	<0.0001
Light*Range	1	5.746	0.0226
CO ₂ *Range	1	0.1629	0.6892
Light*CO ₂ *Range	1	0.5437	0.4663

3.4 Discussion

In this chapter, the stomatal sensitivities to CO₂ between the C₃ and C₄ species were examined. The experiments in this chapter assessed the stomatal movements in phylogenetically-linked C₃ and C₄ species of Cleomeaceae and *Flaveria*. These species belong to well-studied genera that are widely used to uncover the evolutionary history of C₄ photosynthesis. The choice of a pair of congeneric C₃ and C₄ species allowed a comparison between photosynthetic types while taking into account the possible confounding effect of evolution.

3.4.1 Investigating g_s responses to varying CO₂ concentrations

Experiments quantifying the response of net assimilation rate to CO₂ concentration are typically performed by employing CO₂ response curve protocols in which the concentration of CO₂ is changed every 2-3 min. However, such quick changes in CO₂ concentrations do not give enough time for full stomatal responses to occur. Instead, experiments testing the CO₂ response of stomata typically use a step-change approach wherein the leaf is allowed to achieve steady state g_s and then the concentration of CO₂ is either increased or decreased, monitored for at least 30 min or until steady-state condition is achieved at the new [CO₂], and then switched back to the original CO₂ level. These procedures are more appropriate for testing g_s responses to short-term changes in [CO₂] because it allows ample time for stomata to acclimate and achieve steady-state conditions in the new CO₂ environment. However, such protocols typically only quantify the stomatal response to two distinct CO₂ concentrations and do not provide information about differential sensitivities across supra- or sub-ambient CO₂ ranges as we hypothesised between C₃ and C₄ photosynthetic species.

In this chapter, we therefore pioneered an approach to test short-term responses of stomata to changes in CO₂. The new protocol involved step-wise progressive increase or decrease in CO₂ every 30 min from steady-state g_s at ambient CO₂ and then returning to ambient conditions following the same CO₂ sequence during the first half of the experiment, but then reversing the sequence during the second part of the protocol. Doing so allowed for constructing CO₂ response curves that captured short-term changes in stomatal responses and provided a systematic means to assess the sensitivity of stomatal movements in response to changes in CO₂ in the sub-ambient and supra-ambient range. Furthermore, the recursive design allowed a statistical assessment of hysteresis due to asymmetric rate constants of opening and closing.

Investigating stomatal responses to CO₂ in C₃ and C₄ pairs of congeneric dicot species

There are disadvantages following this protocol. First, the duration of the experiment was 6-7 h (including acclimation to steady state at the start to the experiment), which meant that only one plant could be measured per instrument during the photoperiod. Second, steady-state g_s was not achieved at every step-increase or -decrease in CO₂ was not observed in the experiment despite waiting for 30 min. This may have been confounded by the fact that changes in [CO₂] were directional, i.e., it was quite possible that the previous CO₂ level had a carry-over effect on the next CO₂ level. As such, the g_s response at every step-change was not truly independent. Despite these side-notes, converting the timeseries data into functional g_s/C_i curves followed by curve-fitting was able to address the specific hypotheses posed in this chapter.

3.4.2 C₄ stomata are relatively closed at ambient CO₂ and remain closed at supra-ambient CO₂

A fundamental response of C₃ plants to increasing CO₂ concentration is to minimise transpirational water loss by reducing g_s and simultaneously increasing assimilation rates [20]. Indeed, in C₃ *T. hassleriana*, illuminated leaves at elevated [CO₂] showed a dramatic reduction in g_s at rising [CO₂] which was also observed in C₃ *F. cronquistii* although somewhat less prominent. In both species, significant stomatal closing responses at high CO₂ were more clearly observed under illumination, since stomata were already largely closed at ambient CO₂ in the dark. Therefore, this pattern appears to correspond to expectations that stomatal movements primarily function to optimise water use efficiency.

C₄ species are typically CO₂-saturated because of the CCM, which reduces the need for C₄ stomata to be open at ambient CO₂ [69, 52]. Hence, C₄ stomata are predicted to be relatively closed (lower steady-state g_s) at ambient CO₂ compared to C₃ stomata, and could be expected to be closed (maintain ambient steady-state g_s) at higher than ambient CO₂ levels. Indeed, C₄ *G. gynandra* (Figure 3.1A) and C₄ *F. bidentis* (Figure 3.2A), consistently showed log-linear response slopes close to zero for any of the measurements at supra-ambient CO₂, regardless of background illumination or ascending or descending phase of the experiment. This suggests that the stomatal closing response to high CO₂ in these C₄ species is able to completely suppress the stimulus of red-light illumination in contrast to their C₃ relatives.

3.4.3 Stomata in C₄ dicots are more sensitive to CO₂ and showed limited stomatal movements in darkness than their C₃ counterparts

Under low CO₂, C₄ *G. gynandra* showed a strong opening response under red light, indicating that decreasing C_i is a strong signal for stomatal opening. Similarly, in C₄ *F. bidentis*, g_s was found to increase under decreasing CO₂. An alternative interpretation is that C₄ guard cells are more attuned to sensing CO₂ in order to maintain carbon flux to the CCM. C₄ species thus tend to have lower g_s and may have diminished BL response for the same reason, in addition to its thermoregulatory roles (Chapter 2).

As discussed in Chapter 2 of this thesis, stomatal guard cells in C₄ dicot species used in this chapter weakly respond to blue light, while their C₃ counterparts display strong stomatal opening responses. Surprisingly, stomatal movements were observed even in darkness. A significant increase in g_s was recorded for C₃ *T. hassleriana*, and smaller movements for C₃ and C₄ *Flaveria* under low CO₂ conditions. Vialet-Chabrand et al. (2021) concluded that blue light is responsible for providing energy for stomatal opening through ATP and NADPH generated via mitochondrial respiration. The finding that both blue light insensitive species show very little to no opening response to low CO₂ in darkness seem to support this conclusion.

The observed stomatal movements in the two C₄ dicots are entirely consistent with the hypothesis that stomatal opening responses would be more sensitive in subambient C_i. The immediate reason for this is the high affinity of PEPC for bicarbonate and the very high catalytic rate of carbonic anhydrase, which together allow the same CO₂ uptake flux at lower C_i than Rubisco. This results in significantly higher carboxylation efficiency, but therefore much steeper responses of CO₂ assimilation to C_i in the subambient range. The results imply that stomatal movements have adapted to these C₄ biochemical features to become especially responsive in this range of C_i.

This response is only seen with background illumination, while the two C₃ species also significantly respond to low CO₂ in darkness. This seems to be in line with a limited contribution from mitochondrial respiration in the C₄s and seems to suggest that stomatal opening in these C₄ species is more directly related to CO₂ assimilation than in their C₃ relatives. If this is a general C₄ feature, perhaps this also helps C₄ species limit water loss, considering that the C₄ syndrome is often suggested to have evolved in response to hot and dry conditions [105].

Investigating stomatal responses to CO₂ in C₃ and C₄ pairs of congeneric dicot species

An additional point to make is the need for an electron sink (i.e. CO₂ fixation) in the presence of background illumination, which requires sufficient stomatal opening when CO₂ supply starts to restrict CO₂ assimilation rates. Since the slope of the CO₂ response to the assimilation rate is much steeper in C₄ species, they may risk being photoinhibited more easily if C_i decreases too much. This might be another side of the coin both for the increased sensitivity at low CO₂ in C₄ and for the fact that this can only be observed with background illumination. This may also provide an alternative explanation for the findings by Pignon and Long (2020), that the CCM in C₄ species is stronger than would be predicted from an efficiency standpoint. The 'overinvestment' in initial carbon acquisition which was suggested by these authors may actually be a necessary safety feature to prevent severe photo-inhibitory conditions by maintaining CO₂ supply to light-independent reactions downstream of electron transfer.

3.5 Conclusion

This chapter assessed for the first time the differences in sub-ambient and supra-ambient CO₂ sensitivity between congeneric C₃ and C₄ species using a novel protocol. CO₂ sensitivity of stomatal conductance in C₄ species was found to be shifted to sub-ambient range relative to closely related C₃ species. In addition, C₄ species only showed significant responsiveness in the presence of light. Both differences suggest that stomatal conductance responses are more tightly linked with photosynthetic CO₂ assimilation in C₄ than in C₃ species.

Chapter 4

Investigating g_s regulation in *C₄ Flaveria bidentis* with a diminished C_4 cycle

4.1 Introduction

Stomatal pores, formed by a pair of specialised guard cells (GCs), regulate gas exchange between plants and the atmosphere. Stomata have the crucial role of balancing the uptake of CO_2 for photosynthesis and water loss via transpiration by adjusting its aperture. Stomatal conductance (g_s) to CO_2 and water depends on various environmental factors. Many of these factors that influence stomatal behaviour have been extensively studied and reported. Stomatal apertures widen when exposed to low CO_2 concentrations, high light, and high humidity but close under high CO_2 , darkness, low humidity, high temperature and drought [25, 75, 28].

Stomatal movements are frequently evaluated in relation to the concentration of CO_2 since the internal CO_2 concentration (C_i), regulated by both external CO_2 levels and photosynthetic carbon assimilation rates, is considered a crucial mechanism that connects stomatal behavior with mesophyll photosynthetic rates [86]. Scientific consensus is that CO_2 sensing takes place within the guard cells themselves. This is supported by evidence of CO_2 responses in epidermal peels [26]. Furthermore, it is widely accepted that guard cells sense C_i rather than atmospheric CO_2 concentration (C_a) [85]. However, research with transgenic plants seem to challenge this consensus view. g_s remained similar between the WT and transgenic plants, despite the fact that transgenic plants had elevated C_i concentrations due to reduced

Investigating g_s regulation in *C₄ Flaveria bidentis* with a diminished C_4 cycle

photosynthetic rates. In addition, stomata only appeared to close when C_a was elevated [136, 8].

One mechanism of high CO_2 sensing reported in *Arabidopsis* involves an elevated guard cell CO_2 /bicarbonate concentration, which enhances the interaction between MPK4 and MPK12, mitogen-activated protein (MAP) kinases, [131] with HIGH LEAF TEMPERATURE 1 (HT1) kinase [121]. This interaction leads to the down-regulation of HT1-dependent phosphorylation and activation of the downstream kinase CONVERGENCE OF BLUE LIGHT AND CO_2 (CBC1/2) [43]. The guard-cell located HT1 kinase thus acts as a negative regulator of CO_2 -induced stomatal closure.

The indirect feedback loop through changes in C_i through mesophyll photosynthesis is not the only signal that controls stomatal movement [78, 82]. A significant response to red light was observed in experiments where C_i was kept constant [82], suggesting that the stomatal opening induced by red light can also occur due to signals other than C_i . Furthermore, epidermal peel experiments have shown that the response of GCs to red light can be reversibly altered by the presence of the underlying mesophyll tissue. This suggests the involvement of a mesophyll-driven signal as part of the controlling mechanism for stomatal movement. Similarly, stomata in both WT and antisense SBPase tobacco plants opened when exposed to increasing red light when C_i was kept constant supporting a C_i -independent signal [62], in contrast to the earlier proposal that an increase in g_s was solely due to CO_2 depletion in the mesophyll [103]. Taken together, these findings suggest additional links between mesophyll photosynthesis and guard cell responses [63], in addition to the indirect feedback loop involving C_i .

Furthermore, the degree to which the stomata open or close (and therefore g_s changes) depends on the stomatal characteristics, including stomatal density (SD, the number of stomata per leaf area), which is influenced by the leaf growth environment and surrounding conditions. Species with C_4 photosynthesis are known to exhibit a reduction in SD as well as the size of the pore complex [10], however, not much is known about altered stomatal sensitivities under various environmental conditions.

C_4 plants, besides having a functional C_3 cycle, possess a carbon concentrating mechanism (CCM) that enhances photosynthesis by releasing CO_2 at the Rubisco site. The CCM involves two cell types, mesophyll cells (M) and bundle sheath cells (BS), working together to increase CO_2 concentration around Rubisco.

The CCM is compartmentalised between two morphologically different cell types, the mesophyll (M) and bundle sheath (BS) cells. Briefly, in the cytosol of M cells, carbonic anhydrases (CAs) catalyze the reversible interconversion of $\text{CO}_2 + \text{H}_2\text{O} \leftrightarrow \text{HCO}_3^- + 2\text{H}^+$. The addition of HCO_3^- to phospho-enol pyruvate produces the four-carbon compound oxaloacetic acid (OAA) along with inorganic phosphate via phospho-enol pyruvate carboxylase (PEPC). Malate dehydrogenase converts OAA into malate within the chloroplasts of mesophyll cells, after which it diffuses to BS cells. In BS chloroplasts, decarboxylases such as NADP-malic enzyme (NADP-ME) facilitates the decarboxylation of aspartate and malate leading to an increase in the concentration of CO_2 around Rubisco such that Rubisco is close to CO_2 saturation, effectively enhancing photosynthesis and suppressing photorespiration by eliminating the oxygenation reaction of Rubisco.

To work efficiently, the C_4 photosynthetic mechanism must balance the CO_2 supplied through the stomatal pores to the C_3 cycle and the photosynthetic demand for CO_2 of the C_4 cycle. However, the different response times of photosynthesis and g_s pose challenges in achieving efficient coordination between them, especially in fluctuating environmental conditions [63]. Although stomatal function and behaviour in C_4 plants share similarities with those of C_3 plants, some variations in magnitude and sensitivity to light and CO_2 have been observed between the two [46, 74, 146].

Several studies have manipulated the expression of key photosynthetic enzymes in C_4 *Flaveria bidentis* via RNA antisense. To date, Rubisco [31], NADP-malate dehydrogenase [132] and pyruvate phosphate dikinase [30], Rubisco activase [135], carbonic anhydrase [18], PEPC protein kinase [33], and NADP-ME have been targeted [94]. The approach has been valuable for understanding enzyme function and regulation, as well as carbon flux between C_3 and C_4 cycles. However, none of these studies was specifically designed to investigate the effect of a perturbed C_4 cycle on stomatal regulation. As a result, while many of these studies reported observations of g_s , the experiments were generally not designed to a) wait long enough for the stomatal responses to unfold and b) do not keep check of the pleiotropic effects on g_s such as increases in C_i when A decreases [61].

The chapter focusses on stomatal regulation in transgenic C_4 *F. bidentis* with reduced NADP-ME activity. While responses to red light and stomatal sensitivity to blue light appeared unaffected by the decrease in NADP-ME activity, the results showed that NADP-ME antisense lines of *F. bidentis* had higher operational C_i than WT. However, g_s remained unaltered, suggesting that the NADP-ME antisense construct used here may have had an impact on malate dynamics and that g_s responds to C_a , instead of C_i .

4.2 Materials and Methods

4.2.1 Plant materials

WT and T₁ seeds of NADP-ME antisense C_4 *F. bidentis* were a kind gift from Prof. Susanne von Caemmerer (Australian National University, Canberra, Australia). The transgenic construct contained a 845-bp fragment amplified by PCR, in antisense orientation, from the central coding region of ChlME1, the main chloroplastic C_4 isoform of NADP-ME identified in C_4 *F. trinervia* and C_4 *F. bidentis* (GenBank accession numbers X57142 and AY863144). The T-DNA consisted of a CaMV promoter, the NADP-ME antisense coding sequence, and the Nos terminator, as well as a cassette for resistance to kanamycin.

4.2.2 Growth conditions

WT and T₁ seeds from Prof. von Caemmerer were grown in plastic pots 10 cm H x 9 cm L x 9 cm W with M3 compost, in growth cabinets (Conviron) in a 12/12 h day and night cycle at 20°C, 65% RH and a PFD of 200 $\mu\text{mol m}^{-2} \text{s}^{-1}$. PCR-confirmed T₁ plants carrying a single copy number of the NADP-ME antisense cassette were allowed to set seed to obtain T₂ seeds. T₂ homozygous plants were grown under similar conditions as the T₁ parents, but with a slightly lower PFD of 150 $\mu\text{mol m}^{-2} \text{s}^{-1}$, since 200 $\mu\text{mol m}^{-2} \text{s}^{-1}$ was found to be stressful for the T₂ lines. All phenotyping was done on T₂ homozygous lines.

4.2.3 PCR confirmation and copy number estimation

T₁ antisense plants were confirmed for the presence of the NeoR/KanR selectable marker gene via PCR. Subsequently, copy number analysis was performed using RT-qPCR following Glowacka et al. (2016). RNA was extracted using Macherey-NagelTM NucleoSpinTM RNA Plant Kit (Thermo Fisher Scientific) following the manufacturer's instructions. RNA quality was determined using Nanodrop (Thermo Fisher Scientific). cDNA was synthesised using the iScriptTM cDNA Synthesis Kit (Bio-rad). Three independent single-insertion events were selected and allowed to set seed to generate the T₂ antisense plants.

4.2.4 SDS-PAGE and immunoblot analysis

Transblotting of proteins to polyvinylidene difluoride (PVDF) membranes was performed using Trans-Blot Turbo RTA Transfer Kit, PVDF (BIO-RAD Laboratories Inc.) according to the manufacturer's instructions. Before assembly, the PVDF membrane was briefly activated with absolute methanol, both the PVDF membrane and the filter paper were then soaked and equilibrated in 1x transfer buffer (diluted from the stock solution of Trans-Blot Turbo 5x transfer buffer, BIO-RAD Laboratories Inc.). Trans-blotting of western blot sandwich was performed using the Trans-Blot Turbo Transfer System (BIO-RAD Laboratories Inc.). All subsequent steps were performed on a horizontal shaker (Ultimax 1010, Heidolph Instruments, Schwabach, Germany) with gentle agitation (60-100 rpm). Transblotted membranes were first immersed in 1x Tris buffered saline (TBS) buffer (88 mM Tris base, 2.5 M NaCl, and adjusted to pH 7.5 with HCl) with sufficient volume covering the membrane. After washing, the membrane was blocked with 5% (w/v) non-fat milk in Tween-TBS (TTBS) buffer (1xTBS, 0.05% (v/v) Tween-20) for 60 min at room temperature. For the detection of phosphoproteins, milk was substituted by 5% (w/v) bovine serum albumin (BSA) to avoid high background noise. The membranes were then washed twice with TTBS for 5 min/wash, followed by primary antibody incubation (antibody concentration varied according to the manufacturer's recommendations, 1% (w/v) BSA / milk and TTBS) overnight at 4 ° C. The primary antibodies used was a maize-specific antibody (courtesy of Robert Sharwood, Western Sydney University, Australia) at 1:2000 dilution.

Upon completion of the primary antibody incubation, the membrane was washed 4 times with TTBS for 5 min/wash. The membrane was then incubated with secondary antibody (HRP conjugated antibody, 1% (w /v) BSA / milk and TTBS) for 1-2 hours, followed by washing with TTBS 3 times and TBS 2 times at 5 min/wash. Secondary antibodies used were goat anti-rabbit IgG (H&L), HRP conjugated (Product no AS09602, 1:10000 dilution, polyclonal antibody, Agrisera). Lastly, the membrane was incubated with 7 ml of Clarity Western ECL Substrate (1:1 luminol / enhancer solution: peroxide chemiluminescent detection reagent, BIO-RAD Laboratories Inc.) for 5 min before visualisation on the transilluminator (G: box, Syngene) using GeneSys software (Ver 1.7.2, Syngene). Subsequently, Coomassie blue staining (0.05% (w/v) Coomassie brilliant blue G-250, 50% (v/v) methanol, 10% (v/v) glacial acetic acid and adjusted with ultrapure water) was carried out on the same membrane for total protein quantification. The membrane was incubated with Coomassie blue staining solution for 5 min and stained with the staining solution (40% (v/v) methanol, 10% (v / v) glacial acetic acid, and destaining solution (40% (v/v) methanol, 10% (v/v) with ultra pure

Investigating g_s regulation in *C_4* *Flaveria bidentis* with a diminished C_4 cycle

water) for 5-10 min. For visualisation, the membrane was imaged with a transilluminator (G: box, Syngene) using GeneSys software (Ver 1.7.2, Syngene).

4.2.5 Gas exchange measurements

All gas exchange measurements were performed using LI-6400XT gas exchange system (LICOR Biosciences, Lincoln, NE, USA) on the youngest expanded leaf of 8-week old plants. CO_2 assimilation rate, A , and stomatal conductance, g_s were recorded.

Determination of the blue light response

To assess any possible impact of reduced NADP-ME leaf activity on stomatal movements the R→RB→R sequence was implemented as previously described in Chapter 2, Section 2.2.3.

Determination of the red light response

The red light response was quantified following the same procedure described in Chapter 2, Section 2.2.4.

RNA isolation

Frozen leaf samples were homogenized in liquid N_2 and total RNA was extracted using Macherey-Nagel™ NucleoSpin™ RNA Plant Kit (Thermo Fisher Scientific) according to the manufacturer's instructions.

RNA quality and quantity were determined using a NanoDrop (Thermo Fisher Scientific). 100 ng of total RNA was reverse transcribed into cDNA using a SuperScript III Reverse Transcriptase.

Primer design, selection and RT-qPCR conditions

The RT-qPCR experiment followed the guidelines of the Minimum Information for Publication of Quantitative Real-Time PCR Experiments (MIQE). The design of primers for RT-qPCR analysis was performed using the DNA Integrated Technologies' Primer Quest

4.2 Materials and Methods

Tool® program according to the following parameters: annealing temperature of 60–65°C, GC content of 40–60% and amplicon size of 75–120 bps.

The amplifications were performed on a CFX Connect Real-Time System cycler (Bio-Rad) using SYBR Green PCR Master Mix (Thermo Fisher Scientific) as a fluorescent reporter. Each PCR reaction mixed consisted of 5 μ L of SYBR Green PCR, 2 μ L of PCR reaction buffer, 1 μ L each of forward and reverse primers, and 1 μ L of 1:1 diluted cDNA template resulting in a total volume of 10 μ L. The PCR cycle was carried out as follows: 5 min at 94 °C followed by 40 rounds of 15 s at 94°C, 10 s at 60°C, 15 s at 72°C, and finally 1 round of 35 s at 60 °C. The melting curve cycle consisted of: 15 s at 95°C, 1 min at 60°C, 30 s at 95 °C and 15 s at 60 °C.

Relative transcript abundance was calculated using the Delta CT method. Δ Cq values were calculated by taking the Cq value for the gene of interest and subtracting the geometric mean for the Cq values from ACT7 and UBQ9. Two technical replicates were used for each sample. When the calculated Δ Cq values were not within one cycle, the samples were removed from the statistical analysis.

The sequences of primer pairs are listed in Table 4.1.

Table 4.1 Primers pairs used in phenotyping and copy number estimation, and in determining relative transcript abundance of selected CO₂ core signalling pathway genes.

Primer name	Direction	Sequence
FbACT7	Forward	AATGGAAGCTGCTGGTATTCA
	Reverse	CAACCACCTTGATCTTCATGC
FbEF1a	Forward	GATCAACGAGCCCAAGAGA
	Reverse	CAACCCAGATGGTCCAAAG
FbUBQ9	Forward	CACCACGCAGACGAAGCAC
	Reverse	CGCCGGATCAGCAGAGACTTA
FbNADP-ME1	Forward	AGCATATGAACTTGGTTTGGCG
	Reverse	CAACTGTCCTTTTTCCCCGC
FbCA1	Forward	TACGATGAGCTTGCTAAAGGC
	Reverse	AACGTTACGAACAACAAACGC
FbCA2	Forward	TTTGTACGGTGAGCTTGCG
	Reverse	ATGTTTCTGACCACGAAGGC
FbCA3	Forward	AGGAATTGGCACCTATGGC
	Reverse	CGACCGGGTCAAATCCG

Investigating g_s regulation in *C₄ Flaveria bidentis* with a diminished C_4 cycle

Primer name	Direction	Sequence
FbPEPC	Forward	GCTGAGCCGAGCAAACCA
	Reverse	TGATGCGTACAAACACTCAAGAAC
FbPPDK	Forward	TGAGTCGTGCTTACCGGCGA
	Reverse	CGGAGGAGACACCGGATTAAG
FbGASA9	Forward	ACCCATGGCCCTCAATATCA
	Reverse	TCTAACGCTTCTCCACCTTCTC
FbOST1	Forward	CAACTGTCCTTTTTCCCCGC
	Reverse	CAACTGTCCTTTTTCCCCGC
FbHT1	Forward	CGGGAAGATACTCCACAACAAC
	Reverse	GTTTGCTTCAGGTGCTCATAGT
FbMPK12	Forward	TCGAGCTCTGGAGATCACATT
	Reverse	CGAATCGGAGGCACATACTTTC

4.2.6 Leaf harvesting and protein and chlorophyll contents

Three replicate discs with a total area of 1.5 cm² were collected using metal cork borers from recently-expanded leaves from the same plants measured for gas exchange. Samples were flash-frozen in liquid N₂ and then stored at -80°C for further use.

Frozen leaf samples (1.5 cm²) were homogenized in ice-cold mortar and pestle into basic extraction buffer. The chlorophylls were extracted from 40 µl crude leaf extract in 960 µl 80% ethanol. The solution was incubated at 22°C (room temperature), in the dark for 2 hours, and the absorbance was determined spectrophotometrically at 649 nm and 665 nm allowing calculation of chlorophyll content following Winterman et al. (1965). Protein content was estimated against BSA standards using Bradford assay (Sigma, product no. B6916).

4.2.7 Enzyme activity assays

For all enzyme activity assays, the measured absorbance values on the microplate plate reader (Synergy HTX, Agilent Biotek) were normalised to a path length of 1 cm (the typical cuvette width used in spectrophotometers [14], using a factor of 5.47 mm, considering both the volume and dimensions of the well [113]). The reaction proceeded for at least 2 min to

4.2 Materials and Methods

obtain a clear slope of decreasing absorbance. The first minute of the linear range of the activity was used to calculate the activities.

The maximum NADP-ME activity was determined following Pengelly et al., 2012 and Sharwood et al., 2016. Briefly, frozen leaf samples (1.5 cm²) were homogenised using ice cold mortar and pestle in 900 μ l of basic ice cold extraction buffer containing 50 mM Bicine–NaOH, pH 8.2, 1 mM EDTA, 50 mM 2-mercaptoethanol, 1 mM dithiothreitol, 1% (v/v) protease inhibitor cocktail and 1% (w/v) polyvinylpyrrolidone in CO₂-sparged deionised H₂O).

The homogenate was centrifuged at 13,000 g for 1 min, and the supernatant was used in the assay. For each assay, 100 μ l of the supernatant was added to 900 μ l of the NADP-ME assay buffer [50 mM Bicine–NaOH, pH 8.2, 1 mM EDTA, 5 mM Malate] in 96-well microtiter plate. The reaction was initiated by adding 10 μ l of 200 mM MgCl₂. The activity of NADP-ME was calculated by monitoring the decrease in absorbance of NADPH at 340 nm using a diode array spectrophotometer plate reader (Synergy HTX, Agilent Biotek).

Maximal PEPC activity was measured using an NADH-linked assay as described in Sharwood et al., 2016. Frozen leaf samples (1.5 cm²) were homogenized in ice-cold mortar and pestle with 600 μ l of extraction buffer (50 mM Bicine–NaOH, pH 8.2, 1 mM EDTA, 50 mM 2-mercaptoethanol, 1 mM dithiothreitol, 1% (v/v) protease inhibitor cocktail, and 1% (w/v) polyvinylpyrrolidone, CO₂-sparged deionised H₂O). The homogenate was centrifuged for 1 min at 13,000 g and the supernatant was desalted on a Zeba™ spin desalting column (Thermo Scientific). To perform the assay, 5 μ l of supernatant was added to 195 μ l assay buffer (1 M HEPES–NaOH, pH 8.0, 1 M MgCl₂•6H₂O, 0.1 M EDTA, 0.5 M NaHCO₃, 0.1 M D-glucose 6-phosphate sodium salt, 8.5 KU mL⁻¹ malic dehydrogenase (MDH), 14 mM β -nicotinamide adenine dinucleotide (NADH, reduced disodium salt), and 0.2 M phospho(enol)pyruvic acid trisodium salt hydrate) and the reaction initiated by the addition of 5 μ l of 5 mM PEP. The activity was calculated by monitoring the decrease in NADH absorbance at 340 nm with a diode array spectrophotometer plate reader (Synergy HTX, Agilent Biotek) after initiating the reaction.

Rubisco activity was measured from leaf extracts after Sales et al. [112] with slight modifications. Leaf samples (1.5 cm²) were snap-frozen in liquid nitrogen and stored at -80°C until use were ground in an ice-cold mortar and pestle with 1500 μ l of extraction buffer containing 50 mM Bicine–NaOH, pH 8.2, 20 mM MgCl₂, 1 mM EDTA, 2 mM benzamidine, 5 mM ϵ -aminocaproic acid, 50 mM 2-mercaptoethanol, 10 mM dithiothreitol, 1% (v/v) protease inhibitor cocktail (Sigma-Aldrich) and 1 mM phenylmethylsulfonyl fluoride. The

Investigating g_s regulation in *C_4* *Flaveria bidentis* with a diminished C_4 cycle

homogenate was clarified by centrifugation at 14 000 g and 4°C for 1 min. The supernatant was immediately used for measuring Rubisco activity at 25°C. For initial activity, the reaction was started by adding 5 µl homogenate to 195 µl complete assay buffer. For total activity, Rubisco in leaf extracts was first activated by incubation in the assay buffer containing CO₂ and Mg²⁺ but in the absence of RuBP for 10 min in the dark, and then the reaction was initiated by adding 6 µl of 20 mM RuBP. The change in absorbance at 340 nm was monitored with a diode array spectrophotometer plate reader (Synergy HTX, Agilent Biotek) after initiating the reactions.

4.2.8 Extraction of epidermal peels for RT-qPCR

Abaxial and adaxial epidermal peels were obtained from the youngest recently expanded leaves of 8-week-old plants.

To obtain intact epidermal peels, leaves split in half were sandwiched between fast dissolving, water-soluble tape (L Liked Blank White, 1" x 2", Amazon UK). Two to three firm, stroking motions were applied using one side of a scalpel handle, or until the leaf surfaces were fully adhered to the tape. Afterwards, the exposed side of the leaf was scraped off using a scalpel blade until only the epidermis stuck on the tape is left. The process of removing the mesophyll should be done expediently so as not to desiccate the epidermis. Afterwards, the tape + epidermis was floated onto 0.5 M MES (pH 6.2) in deep Petri plates for 60 s to dissolve the tape. A single wash was enough to fully dissolve the tape leaving the epidermal layer. Two to three additional rinses in 0.5 M MES ensured that the epidermal peel was free from tape residues. The epidermal peel was then lightly blot dried on sterile filter paper and flash-frozen in liquid N₂ and stored at -80°C for further use.

4.2.9 Stomatal morphology and density using impressions

Stomatal impressions using nail varnish were collected from the youngest recently expanded leaf following the same procedure in Section 2.2.5.

4.2.10 Statistical analysis

To estimate the impact of light on stomatal conductance resulting from the shift from one light environment to the next, a linear mixed-effects model was used. To perform the analysis,

g_s and A at the introduction blue light ($t = 5$ min and $t = 65$ min, R→BR→R) and the final g_s at $t = 125$ min were extracted from the gas exchange time series. Light was the within-subject factor and species was the between-subject factor. Biological replicates were treated as random variables.

Linear mixed-effects model was fitted to the red light response data set. Genotype and red light PFD were assigned as within- and between-subject variables, respectively, while individual biological replicates were treated as random variables.

Linear mixed-effects model was used to analyse data from RT-qPCR experiments. Genotype and tissue-type were assigned as within- and between-subject variables, respectively, while individual biological replicates were treated as random variables.

NADP-ME activities were normally distributed, but the variances between groups were unequal, which could not be fixed by logarithmic transformation of the data. Hence, a one-way ANOVA assuming unequal variances (Welch's) was performed followed by a posthoc Tukey's test, where α was set at 0.05.

Values of PEPC activities did not show a normal distribution (but with equal variances), and a log-transformation was successfully used to satisfy the normality assumption.

Chlorophyll values also had a nonnormal distribution, but satisfied the equality of variance assumption. However, a log-transformation did not remedy non-normality, so a Kruskal-Wallis test (non-parametric one-way ANOVA) was instead used to analyse the data. Data on total soluble protein met the assumptions of a one-way ANOVA, and the analysis was carried out without performing any data transformation.

Stomatal morphology and density using impressions

The SD on the abaxial and adaxial surfaces was analysed using a two-way ANOVA, and Tukey's HSD ($\alpha = 0.05$) was used to separate the means if a significant difference was detected. Data on stomatal size were processed similarly.

4.3 Results

4.3.1 Transgenic *F. bidentis* with decreased NADP-ME activity

Transgenic *F. bidentis* plants with reduced NADP-ME activity were generated by the Von Caemmerer lab (see Pengelly et al. 2012) to investigate the impact on coordination between the C_3 and C_4 cycles. To generate these lines, Pengelly and co-workers used an antisense construct targeting the central coding region of ChlME1, the dominant isoform of NADP-ME at the mRNA and protein levels [77, 22]. A transgenic construct constitutively expressing the NADP-ME antisense sequence was introduced to *F. bidentis* via *Agrobacterium*-mediated transformation [94]. Eight lines were regenerated through tissue culture and coded as 1A-4, 1A-5, 1A-6, 1A-7, 1A-8, 2A-1 and 2A-2. Of these, segregating T_1 offspring of 1A-5, 1A-8, and 2A-1 formed the starting point in this study. Homozygous T_1 plants carrying a single integration event were identified based on RT-qPCR analysis using an amplicon in the KanR selectable marker. The resulting plants were allowed to self and set seed to obtain a T_2 homozygous population. Homozygous T_2 plants for these three lines were used for all the presented analyses. The effect of the construct on NADP-ME protein content was first assessed by immunoblotting Figure 4.1. The blots clearly show bands in the predicted size (65 kDa) for WT plants grown under regular (HL) or low light (LL, $150 \mu\text{mol m}^{-2} \text{s}^{-1}$), but strongly diminished bands for 1A-5, 1A-8 and 2A-1 plants, confirming the impact of the antisense construct on NADP-ME protein abundance.

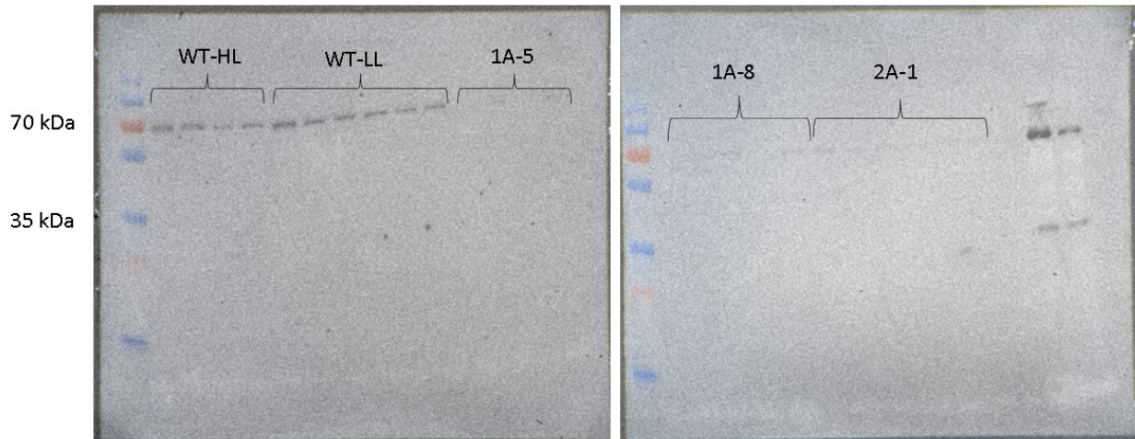


Fig. 4.1 NADP-ME protein expression in WT and antisense lines of *C₄ F. bidentis*. The relative expression level of NADP-ME was evaluated across WT-LL *C₄ F. bidentis* ($150 \mu\text{mol m}^{-2} \text{s}^{-1}$) and three independent antisense lines, 1A-5, 1A-8, and 2A-1, grown under the same light levels. A WT-HL *C₄ F. bidentis* cultivated at $350 \mu\text{mol m}^{-2} \text{s}^{-1}$ was included for comparison. NADP-ME protein was detected using a maize-specific antibody at 1:2000 dilution.

4.3.2 Enzyme activities and chlorophyll content

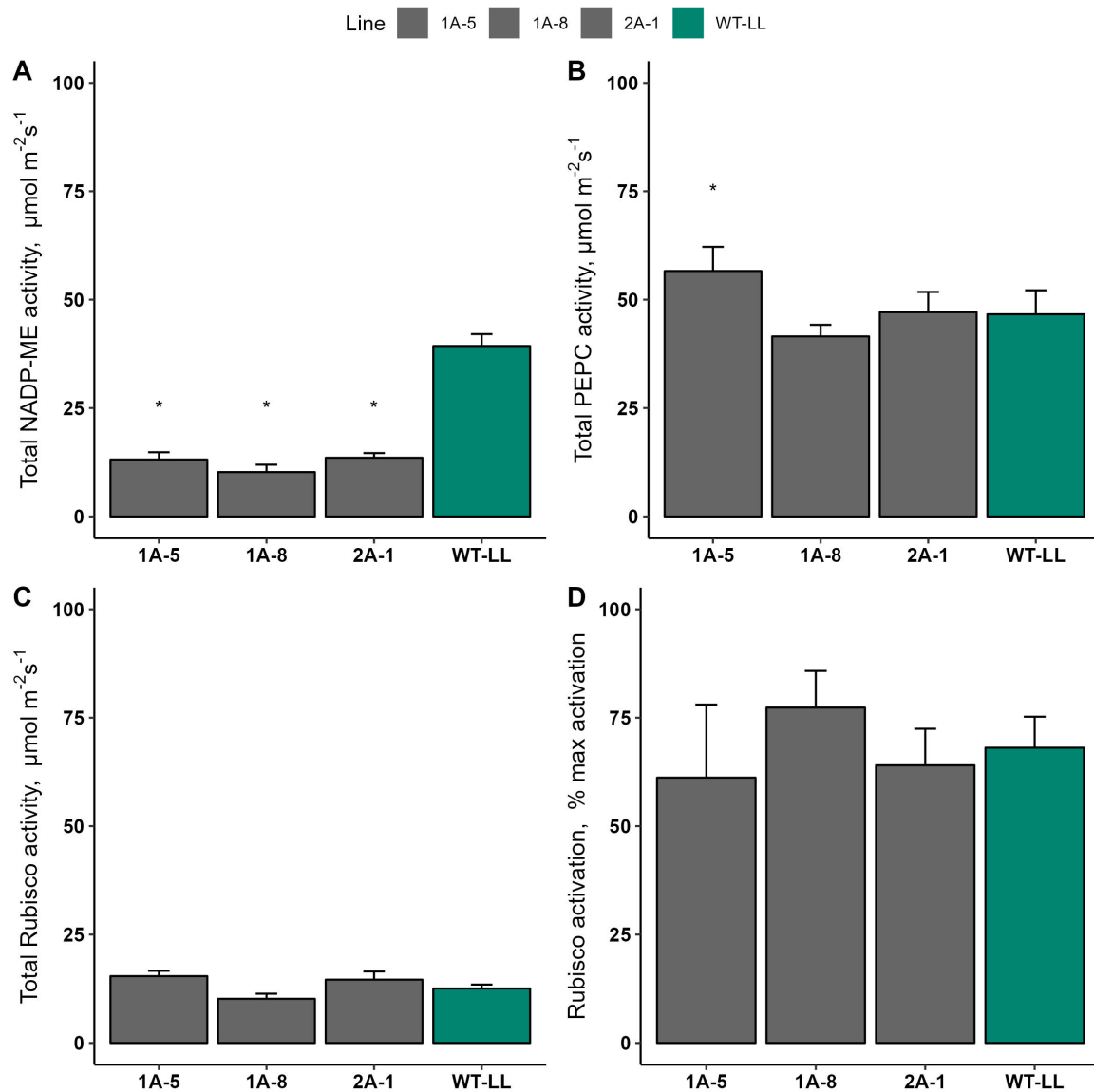


Fig. 4.2 Measurements were performed on soluble protein extracted youngest fully-expanded leaves of 8-week-old plants (n=4-6). (A) NADP-ME (malic enzyme) activity. (B) PEPC activity (C). Total Rubisco activity (D) Rubisco activation status. Values represent the mean \pm s.e.m. Asterisks indicate significant differences between antisense lines and wildtype (WT) control at $\alpha = 0.05$ using Dunnett's test.

To assess the impact of the decrease in NADP-ME protein content, total NADP-ME enzyme activity was assessed using a photometric assay. Total leaf activity of NADP-ME was significantly reduced ($p < 0.001$) in T_2 homozygous populations of antisense *F. bidentis* plants

(Figure 4.2A). On average, NADP-ME activity in the antisense lines was $12.4 \pm 0.9 \mu\text{mol m}^{-2} \text{s}^{-1}$, compared to WT which was $39.3 \pm 2.7 \mu\text{mol m}^{-2} \text{s}^{-1}$, or approximately 68% reduction in total NADP-ME leaf activity. The reductions in NADP-ME activity in the T₂ antisense lines varied from 66% to 73% which is less variable than the previously published values for in T₁ populations [94].

To find out if the significant decrease in NADP-ME activity had an impact on the activity of other key carbon assimilation enzymes, the activities of PEPC and Rubisco were also assayed on the same leaves. The measured levels of PEPC varied significantly between genotypes ($p < 0.007$). However, none of the PEPC activities in the antisense lines was significantly different from the WT control (Figure 4.2B). Rubisco activity (Figure 4.2C) and Rubisco activation state (Figure 4.2D) did not vary significantly between genotypes ($p = 0.075$ and $p = 0.634$, respectively).

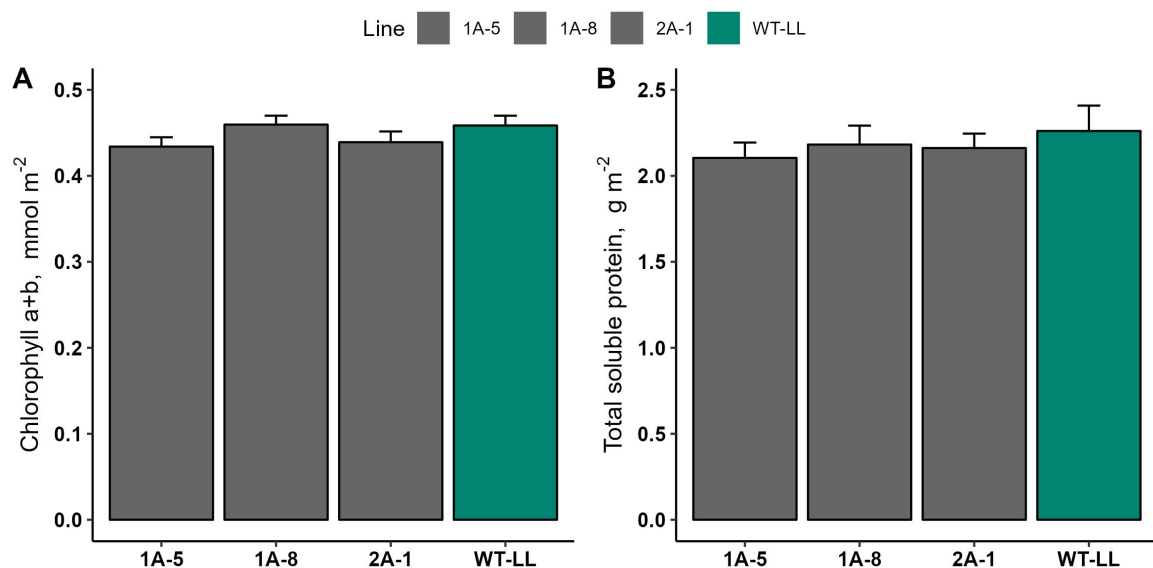


Fig. 4.3 Total chlorophyll (A) and total soluble protein (B) contents were measured spectrophotometrically from crude leaf extracts in 80%EtOH of 8-week-old plants. Protein content was estimated against BSA standards using Bradford assay. Values represent the mean \pm s.e.m of $n=4-6$.

Similarly, no significant genotype effects were detected for total chlorophyll content ($p=0.200$) and total soluble protein (Figure 4.3).

4.3.3 C_i is significantly increased in NADP-ME antisense lines of C_4 *F. bidentis*

To find out if the decrease in NADP-ME activity in antisense lines affected stomatal movements, g_s was assessed both under 100% red light and a mixture of 75% red and 25% blue light (Figure 4.4). As previously observed in wild-type *F. bidentis* plants (Chapter 2), blue light did not have a significant effect on stomatal opening in *F. bidentis* regardless of genotype. There was also no significant effect of genotype on the overall mean g_s throughout the experiment (mixed model analysis, $p = 0.18$), although the levels in WT plants were slightly lower at $0.125 \pm 0.017 \mu\text{mol CO}_2 \text{ m}^{-2} \text{ s}^{-1}$ than any of the mutants (1A-5 = $0.146 \pm 0.011 \text{ mol CO}_2 \text{ m}^{-2} \text{ s}^{-1}$; 1A-8 = $0.168 \pm 0.021 \text{ mol CO}_2 \text{ m}^{-2} \text{ s}^{-1}$, and: 2A-1 = $0.165 \pm 0.015 \text{ mol CO}_2 \text{ m}^{-2} \text{ s}^{-1}$). The analysis of C_i on the other hand (Figure 4.5), showed a significant genotype effect, with significantly higher values in antisense lines compared to the WT control (Dunnnett's test, $P < 0.05$). The mean WT C_i was $177 \pm 12 \text{ mol CO}_2 \text{ mol}^{-1}$, while the antisense lines, 1A-5, 1A-8, and 2A-1, on average, were 246 ± 29 , 295 ± 15 , and $264 \pm 20 \text{ mol CO}_2 \text{ mol}^{-1}$, respectively.

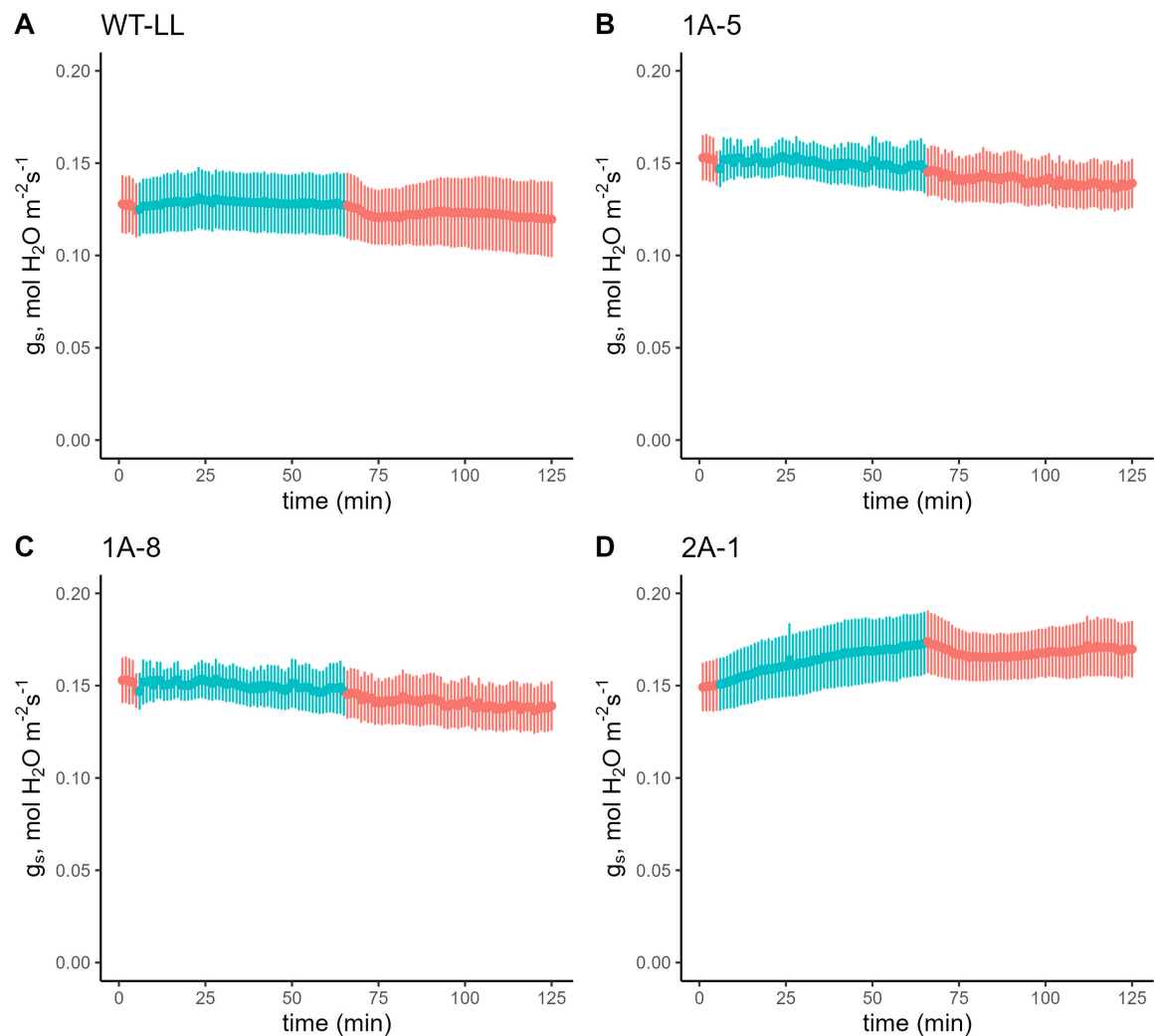


Fig. 4.4 Time course of g_s in WT (A) and antisense lines of *F. bidentis* (B, C, and D). The leaves were initially acclimated in 100% red light until steady state was achieved. Subsequently, the light environment was switched to 75% red + 25% blue while maintaining an intensity of $500 \mu\text{mol m}^{-2} \text{s}^{-1}$. The leaves were acclimated to the new light condition for 60 min before returning them back to the original condition for another 60 min before terminating the experiment. The light conditions were reversed at t_6 and t_{65} . Reference CO_2 was maintained at $410 \mu\text{mol mol}^{-1}$, block temperature was kept at 25°C and the mean VPD was 1.2 kPa. Data points represent $n=4 \pm \text{s.e.}$

Investigating g_s regulation in C_4 *Flaveria bidentis* with a diminished C_4 cycle

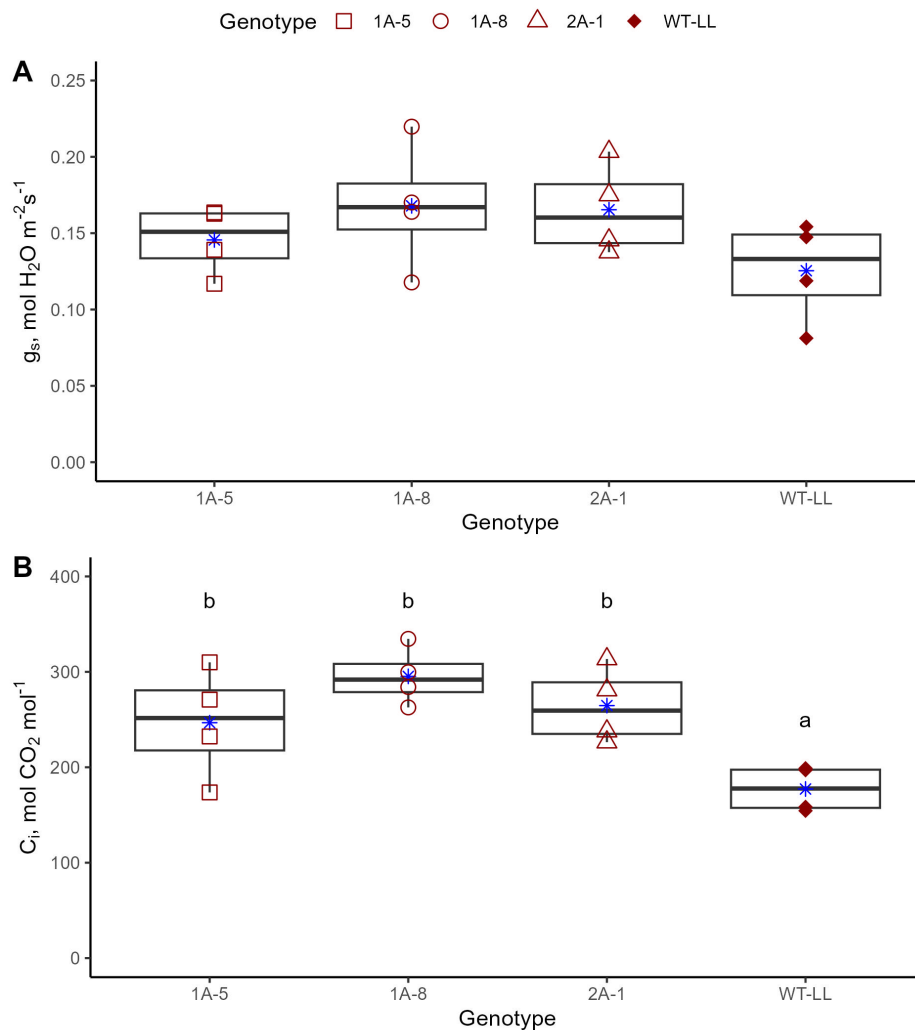


Fig. 4.5 Box plot of overall mean g_s (A) and C_i (B) in WT and three antisense lines of *F. bidentis*. Blue asterisks are the mean from t_0 to t_{125} , $n=4$. Box plots with the same asterisks are not significantly different from WT at $\alpha = 0.05$ using Dunnett's test.

4.3.4 g_s is elevated in NADP-ME antisense lines of C_4 *F. bidentis* at the C_i of the WT

While Figures 4.4 and 4.5 show that g_s under either red or RB light did not vary between the NADP-ME antisense lines and WT control plants, C_i during the measurements was markedly different and may have affected the measurements. Therefore, a follow up experiment was done under more equal conditions. To do so, C_i was kept constant at the operating level of WT plants at $120 \text{ mol } CO_2 \text{ mol}^{-1}$ for all lines.

When PFD was reduced from 800 to 200 $\mu\text{mol red photons m}^{-2} \text{ s}^{-1}$, overall g_s for the antisense lines did not change and ranged from $0.230 \pm 0.020 \text{ mol CO}_2 \text{ m}^{-2} \text{ s}^{-1}$ to $0.225 \pm 0.014 \text{ mol CO}_2 \text{ m}^{-2} \text{ s}^{-1}$. WT g_s was also constant across red light PFDs, but was significantly lower at $0.151 \pm 0.0127 \text{ mol CO}_2 \text{ m}^{-2} \text{ s}^{-1}$ to $0.131 \pm 0.0123 \text{ mol CO}_2 \text{ m}^{-2} \text{ s}^{-1}$ than the g_s of lines 1A-8 and 2A-1. Indeed, the interaction effect between genotype and red light PFD was not significant ($p = 0.6762$), nor was the effect of red light PFD ($p=0.2890$), but the g_s among the genotypes was significantly different ($p=0.0320$).

Not surprisingly, the CO_2 assimilation rate responded strongly to the intensity of red light in all genotypes but significantly less so in antisense plants compared to WT, reflecting the increased impact of decreased NADP-ME activity on CO_2 assimilation at higher light intensity (Figure 4.6B, genotype x red light PFD, $p=0.0031$).

Investigating g_s regulation in C_4 *Flaveria bidentis* with a diminished C_4 cycle

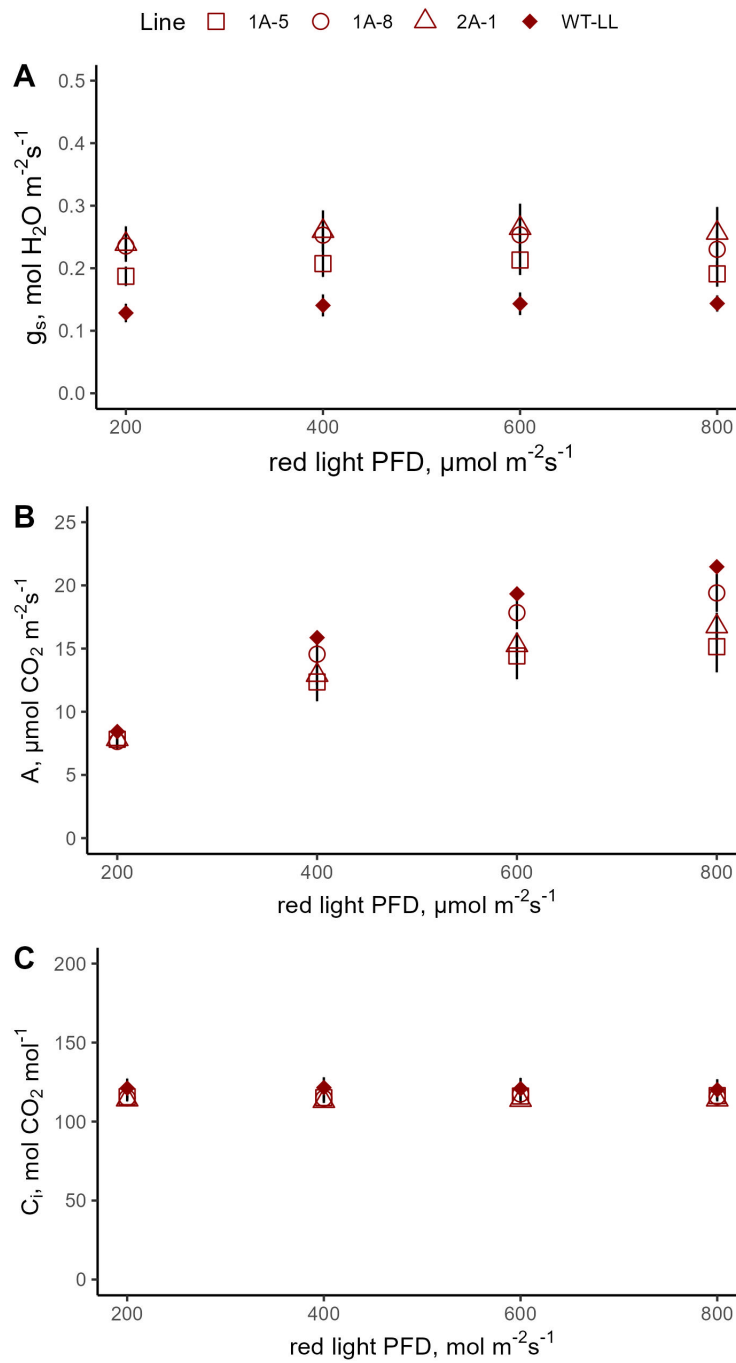


Fig. 4.6 Response of g_s (A) and A (B) in WT and independent NADP-ME antisense lines of *F. bidentis* at the C_i ($=120 \text{ mol CO}_2 \text{ mol}^{-1}$) of the WT (C) Each data point represents the mean and s.e. ($n = 4-6$).

4.3.5 Stomatal density and size remained unaltered in NADP-ME anti-sense lines

To determine if the g_s differences were due to stomatal patterning/morphology or regulation, stomatal density (SD) and size (SS) were collected. SD varied between leaf surfaces ($p < 0.0001$) with higher stomatal counts and larger stomatal size in the abaxial layer than in the adaxial layer (Figure 4.7). However, there was no consistent trend with respect to SD or SS between WT and mutant plants.

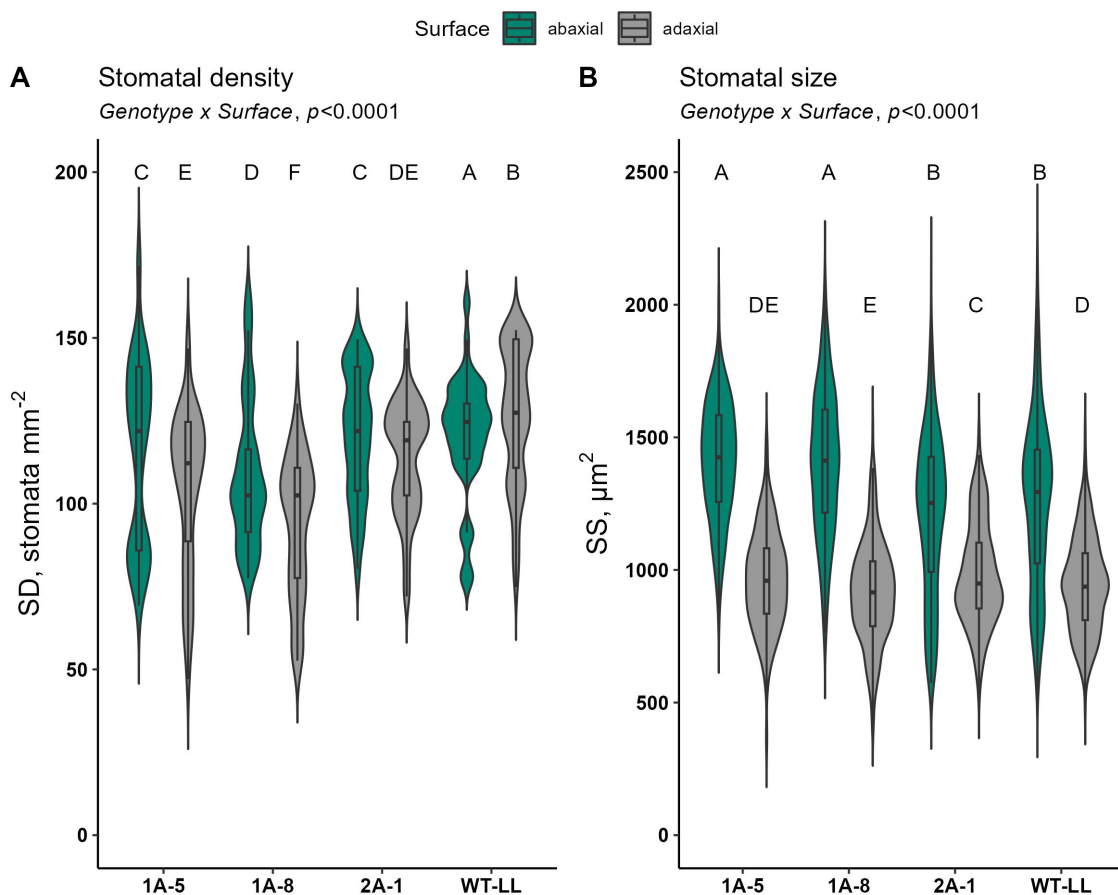


Fig. 4.7 Stomata density (SD, stomata mm⁻², **A**) and stomatal size (SS, μm², **B**) on the abaxial and adaxial leaf surfaces of WT and NADP-ME antisense lines of *F. bidentis*. Violin/box plots with the same letters are not significantly different at $\alpha = 0.05$ using Tukey's HSD test.

4.3.6 Gene expression analysis

The elevation of g_s in NADP-ME antisense lines at common C_i suggested that the CO_2 response of stomatal conductance were altered due to the antisense construct, allowing equal g_s at the higher operating C_i of the NADP-ME antisense lines. It is assumed that the CO_2 response is cell autonomous and that the components of the signal transduction and sensing pathway for these are located in guard cells [23]. If any of the components of the CO_2 -mediated sensing pathway were altered in NADP-ME antisense lines, they would be expected to appear in epidermal peels, which should be enriched in guard cells compared to whole leaf samples.

To investigate these questions, the abundance of transcripts of genes presumed to be strongly guard cell biased (GASA9, OST1, HT1, MPK12; Figure 4.8), as well as genes thought to be strongly expressed in the mesophyll as well as in the guard cell (NADP-ME, CA1, CA2, CA3, PEPC, PPDK; Figure 4.9) were quantified. Figure 4.8 shows ΔCq by subtracting the mean Cq of the GOI from the geometric mean Cq of two reference genes, thus giving lower ΔCq values for higher relative expression levels. The results of the RT-qPCR experiments showed that genes expected to be strongly enriched in guard cells, such as OST1 and HT1 and MPK12, were in fact not found to be contrasting between tissue fractions (Figure 4.8). At least at the transcript level, genes reported to be involved in the CO_2 -mediated response of guard cells in *Arabidopsis* and other C_3 species did not show higher transcript levels in the epidermal fractions of WT and antisense lines of C_4 *F. bidentis*. To ensure that the choice of reference genes did not affect the result, the expression levels of the reference genes were also analysed but did not show a significant tissue effect.

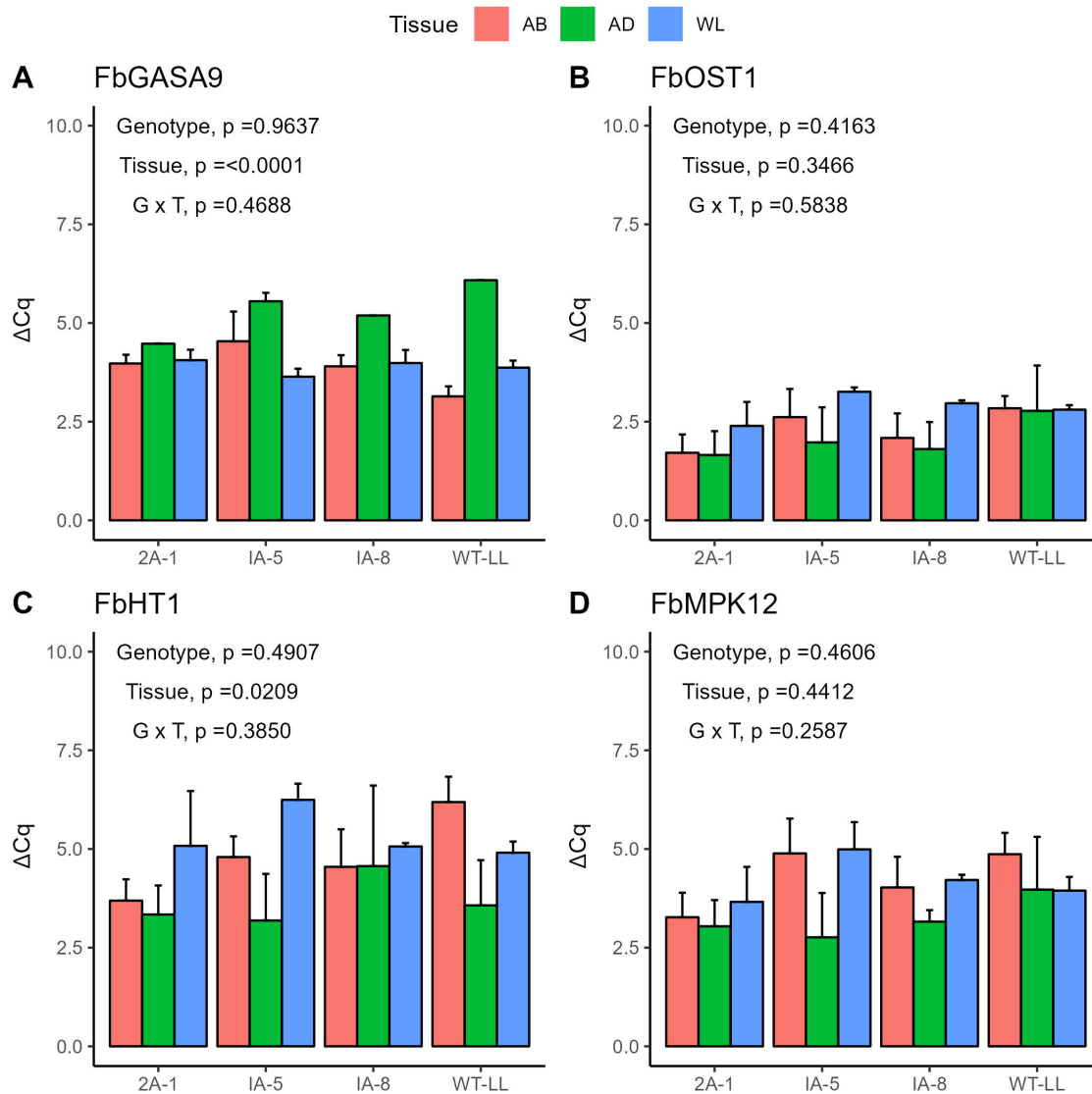


Fig. 4.8 Transcript levels of FbGASA9 (A), FbOST1 (B), FbHT1 (C), and FbMPK12 (D) in whole leaves, and abaxial and adaxial epidermises ($n=2-4$). Bars represent the mean and s.e.m. Bars without error bars are $n=2$. ACT7 and UBQ9 were used as reference genes.

Investigating g_s regulation in *C4* *Flaveria bidentis* with a diminished C_4 cycle

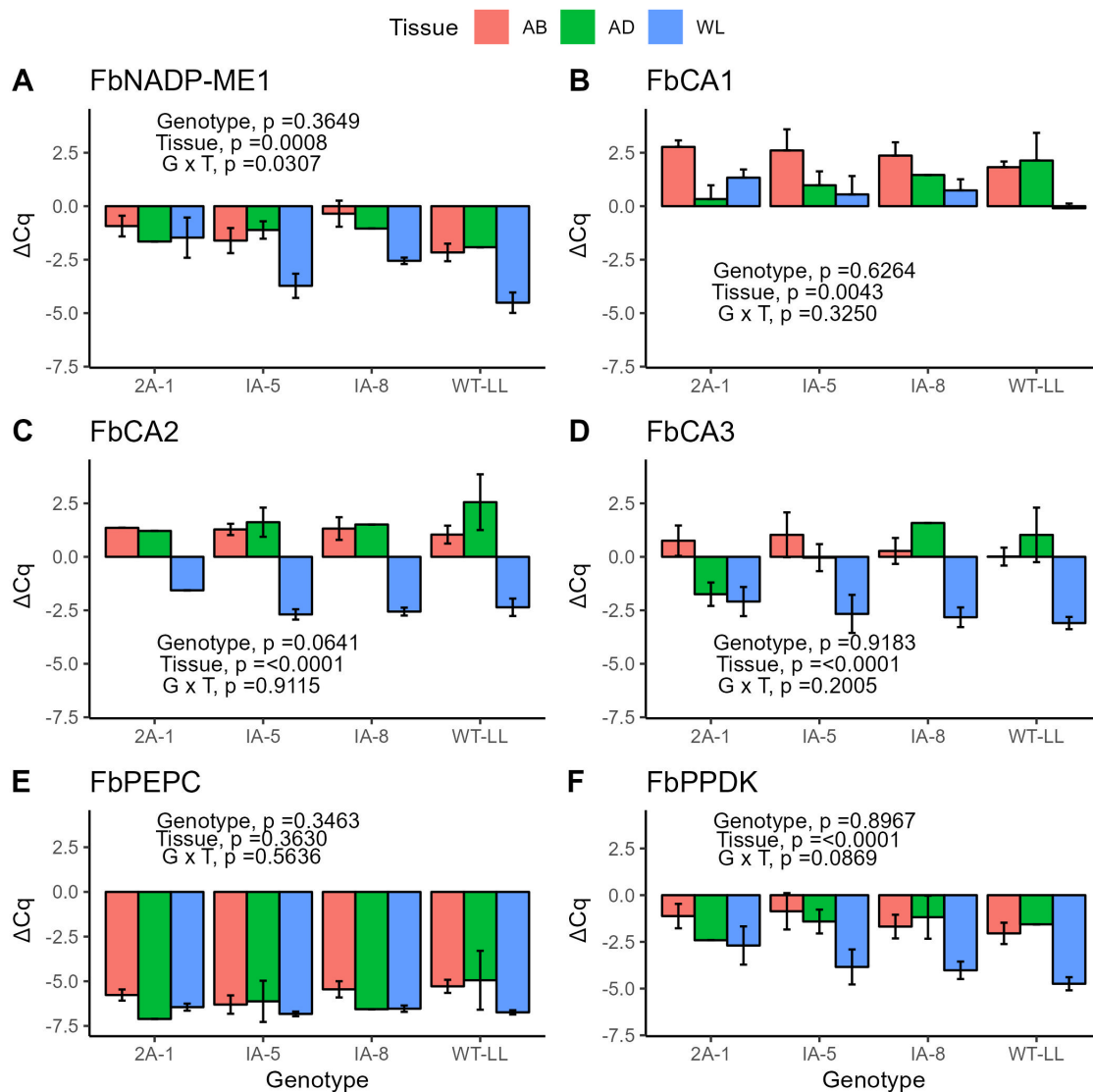


Fig. 4.9 Transcript abundance of key C_4 enzymes in whole leaves, and abaxial and adaxial epidermises ($n=2-4$). Bars represent the mean and s.e.m. Bars without error bars are $n=2$. ACT7 and UBQ9 were used as reference genes.

The orthologue of FbGASA9 is preferentially expressed in *Arabidopsis* guard cells [142]. FbGASA9 transcript levels were also found to differ in expression among tissue types ($p < 0.0001$). Transcript abundance in the adaxial layer was 5.6-fold higher than the abaxial layer (3.8-fold), which had similar expression levels with whole leaf samples (3.9-fold) (Figure 4.8A).

The OST1 encoding gene is expressed in guard cells and vascular tissues. In *Arabidopsis*, OST1 is responsible for controlling ABA-induced stomatal closure [88]. The orthologue of FbOST1 was not differentially expressed between tissue types or genotype (Figure 4.8B).

The protein kinase HT1 is predominantly expressed in guard cells [40]. FbHT1 varied by tissue type ($p = 0.0209$) but had a comparable abundance of transcripts in all genotypes ($p = 0.4997$). Whole leaf samples were 5.4-fold higher than abaxial fractions, and by 3.7-fold than the adaxial fractions. FbHT1 transcript abundance between whole leaf and abaxial samples (4.9-fold) were not statistically different. HT1 expression levels between abaxial and adaxial layers were also similar (Figure 4.8C). There were no significant differences in FbMPK12 transcripts (Figure 4.8D) across samples.

FbNADP-ME1, as expected, gave a significant genotype x tissue type interaction ($p=0.0307$). It should be mentioned that while the whole leaf samples showed significantly lower FbNADP-ME1 transcripts in the antisense lines, these were not found for the adaxial or abaxial epidermal fractions (Figure 4.9A).

All three of the C_4 *F. bidentis* CA isoforms [129] were strongly expressed in whole leaf samples (Figure 4.9B-D), consistent with their role of converting CO_2 to bicarbonate and protons in the mesophyll cytosol.

The FbPEPC transcripts did not show any differences in genotype or tissue levels (Figure 4.9E). Finally, FbPPDK had higher expression levels in whole leaves, than in either epidermal fractions (Figure 4.9F).

Thus, based on the RT-qPCR results, NADP-ME activity does not appear to be down-regulated in the epidermal layers as it is in the whole leaf and none of the selected CO_2 response genes showed altered patterns of expression in line with a decreased CO_2 sensitivity in the guard cells in the antisense lines.

4.4 Discussion

This study examined the effect of antisense reduction of NADP-ME, the major decarboxylating enzyme in C_4 *Flaveria*. It was hypothesised that perturbing the C_4 cycle, resulting in a reduced flux of carbon into the bundle sheath cells, may also alter stomatal regulation. Thus, the objective of this chapter was to investigate the coordination between mesophyll photosynthesis and g_s .

Investigating g_s regulation in C_4 *Flaveria bidentis* with a diminished C_4 cycle

Targeting key photosynthetic enzymes has been a useful strategy to gain insight into enzyme regulation and coordination of the C_3 and C_4 cycle. Previous studies in C_3 and C_4 transgenics with impaired photosynthesis demonstrated largely unaltered g_s [98, 118, 45, 60, 24]. Photosynthesis is well documented for its role in regulating stomatal apertures by lowering C_i in leaves. This has been referred to in the literature as the stomatal red light response. However, in addition to this indirect role through C_i reduction, a C_i -independent component is also recognized to be part of the red light response [82, 78]. When C_i was kept constant, the red light response becomes negligible between mutants and WT plants studied here, suggesting that this response is unlikely to underpin the difference in g_s between the transgenics and the control plants. Recent studies have also generated several hypotheses regarding the signal and / or the site of direct CO_2 detection, leading to contrasting findings in the published literature. Although some studies suggest a role for guard cells in CO_2 sensing, others indicate that mesophyll cells play a crucial role in directly sensing CO_2 through a "diffusible signal" [63, 23]. The point that previous mutant studies may have overlooked the confounding effect of C_i on g_s is crucial. If these studies had controlled for C_i , their conclusions might have differed, especially in cases where g_s is reported as unchanged in transgenic lines with lower assimilation rates compared to the WT. It is possible that under common C_i conditions, an increased g_s could have been observed, leading to a different interpretation of the results.

4.4.1 NADP-ME antisense construct did not have any pleiotropic effects.

Transgenic C_4 *F. bidentis* lines with reduced NADP-ME activity have previously been studied and have shown decreased CO_2 assimilation, yet similar g_s at increasing C_i or light intensities [94]. In the present study, when C_i was set at approximately WT levels, g_s in antisense plants was higher than in WT (Figure 4.6), suggesting that the stomatal opening in response to low C_i probably increased. CO_2 assimilation rate, on the other hand, was highest in the WT, which differed significantly from the three independent antisense lines. Hence, despite higher g_s values in the antisense lines, the mutants were unable to achieve higher assimilation rates, which may be attributed to the poor supply of carbon through the C_4 cycle. The observed differences in g_s at the common WT C_i may be explained by a) increased opening sensitivity at low C_i in the antisense lines, b) decreased closing sensitivity at elevated C_i in the antisense lines or c) g_s senses and responds to changes in ambient $[CO_2]$ rather than intercellular C_i .

The coordination between C₄ NADP-ME decarboxylation and Rubisco carboxylation rates is critical to maintaining flux through the C₄ pathway. Therefore, it was possible that the levels of PEPC and Rubisco were altered to compensate for the reduction in NADP-ME (Figure 4.8A). However, analysis of gene expression using RT-qPCR did not show changes in the transcript levels of the three CA isoforms (Figure 4.8B-D) in C₄ *F. bidentis* at the genotype level, suggesting that the reduction of NADP-ME activity did not directly impact the initial steps of CO₂ signal transduction [44]. The study also examined the transcripts of two other essential C₄ enzymes, PEPC (Figure 4.8E) and PPDK (Figure 4.8F), but no significant differences were found between the mutant lines and WT plants. Enzyme activity assays further demonstrated that PEPC and Rubisco (Figure 4.2C), as well as Rubisco activation status (Figure 4.2D), remained unaffected in transgenic plants. These findings are consistent with previous research, indicating that CO₂-regulated stomatal conductance operates independently of Rubisco activity [136] and other PCR cycle enzymes [45, 60, 87]. Similarly, PEPC levels were found to have no direct effect on high CO₂-induced stomatal closing [34, 19].

Contrasting results were reported by Pengelly et al. (2012), who observed an increase in PEPC and Rubisco activities in antisense lines compared to WT plants. They attributed this rise to a potential increase in the amount of nitrogen available for enzyme production [93]. However, the same study showed that the reduction in NADP-ME alone was not sufficient to explain the observed increase in leaf nitrogen. Furthermore, in this study, total chlorophyll and protein contents (Figure 4.3), remained consistent between antisense lines and WT, making out any off-target effects on light harvesting and electron transport, as previously seen in similar studies less likely [98].

4.4.2 Stomatal patterning and morphology can acclimate to CO₂, but do not explain the observed differences in g_s in NADP-ME antisense lines.

Plants adapt to changes in CO₂ levels by regulating their SD and stomatal index (SI, the number of guard cells relative to total epidermal cells). Light intensity and CO₂ concentration have been extensively studied in relation to their impacts on stomatal differentiation. Typically, plants grown in full sunlight or high light intensities exhibit a higher SD and SI compared to those grown in shaded conditions [28]. In response to elevated CO₂ levels, many species adapt by reducing their SD. To investigate whether changes in stomatal traits drove

Investigating g_s regulation in *C₄ Flaveria bidentis* with a diminished C_4 cycle

higher g_s between antisense lines, SD and SS were determined. While there were significant differences in SD, there was no apparent pattern that distinguished WT plants from mutants. These findings indicate that the higher operational g_s in antisense lines could not be due to changes in stomatal distribution or size.

4.4.3 Genes involved in stomatal CO_2 response and malate metabolism appear unchanged in NADP-ME mutants.

Guard cells have been suggested to indirectly sense changes in C_i through fluctuations in metabolites resulting from photosynthesis or by detecting bicarbonate with a CO_2 sensing module [121] involving HT1 and MPKs. Recent studies in *Arabidopsis* have identified the cellular and molecular components involved in CO_2 signaling and response highlighting key roles for HT1 and MPK12, which led us to hypothesize that the altered C_i response of g_s in the NADP-ME antisense plants could be due to altered expression levels of these gene products. However, RT-qPCR quantification showed that neither HT1 nor MPK12 transcripts were significantly different between the WT and mutant lines. Genes associated with stomatal movements, such as OPEN STOMATA 1 (OST1), were also investigated, but silencing of NADP-ME did not affect OST1 expression either. In general, these results indicate that the reduction of NADP-ME activity does not directly affect the initial steps of CO_2 signal transduction, at least at the transcript level in *C₄ F. bidentis*.

4.4.4 Could altered guard cell malate metabolism potentially explain the higher g_s observed in the antisense lines?

Malate is a powerful regulator of stomatal opening [12, 1], and the antisense construct in *C₄ F. bidentis* could have altered the pattern of malate flow and therefore affected g_s . During stomatal closure, malate is decarboxylated in the cell to pyruvate by NADP-malic enzyme, which is then completely oxidized in the mitochondrial tricarboxylic acid cycle. Alternatively, malate can be converted to PEP via NAD^+ -dependent malate dehydrogenase (MDH) and PEP carboxykinase (PEPCK) [114]. If the NADP-ME activity in guard cells decreased in antisense lines, then the malate that had been accumulating during stomatal opening could not be metabolically dissipated, leading to slower stomatal closure, which could be seen as an increased opening at common C_i .

Moreover, malate production is also linked to the C_4 cycle through OAA via PEPC [19]. An earlier study on *Amaranthus edulis* using PEPC knockdowns [19] suggested that PEPC is directly involved in the regulation of g_s . However, since PEPC deficiency also affects g_s due to shared enzymatic reactions controlling the dynamics of the malate pool with the C_4 cycle [114], the interpretation that g_s is directly regulated by PEPC may be dependent on how much the guard cell malate pools were affected. The same reservations apply to the mutants employed in this chapter.

4.4.5 Conclusion

This chapter has focused on the consequences of a disrupted C_4 cycle on the regulation of g_s . The results showed that NADP-ME antisense lines of C_4 *F. bidentis* had a higher operational C_i than WT. When measured at a common C_i , g_s was higher in the antisense lines than in the WT. Although this may imply altered guard cell C_i sensitivity in the antisense lines, or that guard cells sense C_a rather than C_i , the construct may have had an impact on the guard cell malate pool, which cannot be ruled out as an alternative explanation for the increase in g_s in common C_i .

Chapter 5

General Discussion

5.1 Thesis Summary

This thesis aimed to provide a detailed characterization of stomatal responses to light and CO₂ in congeneric C₃ and C₄ species. Chapter 1 synthesized current literature on the body of knowledge on stomatal responses to light and CO₂ and developed hypotheses that underpin the experimental chapters. This introductory chapter also included a discussion on the importance of using phylogenetically-controlled experiments to systematically compare photosynthetic types while minimising the confounding effects of evolution. The congeneric model species in studying the evolution of C₄ photosynthesis used in the study were also discussed. Finally, the chapter briefly reviewed the work on photosynthesis mutants in recent decades and how studying these mutants helped uncover the regulatory mechanisms underlying stomatal movements.

Chapter 2 investigated stomatal responses to light. Specifically, this chapter described the differential responses to blue and red light between C₃ and C₄ species using phylogenetically-controlled comparisons. A significant finding from this chapter is the insensitivity of C₄ dicots to blue light, contrasting with the corresponding C₃ species which were strongly responsive. Stomatal morphology differences were extensively characterized and shown to be largely species-specific, rather than follow previously postulated C₃-C₄ evolutionary trajectories.

Chapter 3 used a novel protocol to assess stomatal responses to CO₂. An important observation from this chapter is that C₄ dicots found to be insensitive to blue light in Chapter 2, were also found to be less responsive in the dark. In addition, stomatal opening in C₄ dicots

General Discussion

was more responsive to sub-ambient CO₂ than their corresponding C₃ dicots, but only in the presence of light. However, some stomatal opening also occurred in darkness, indicating that the energy used for stomatal opening was also sourced from products other than from photosynthesis. This is consistent with previous work in which respiratory processes were shown to contribute significantly to support energy demand of guard cell movements.

Chapter 4 examined the link between mesophyll photosynthesis and stomatal movements in mutant *C₄F. bidentis* with decreased NADP-ME activity. Three mutant lines were selected with moderate decreases in NADP-ME expression and activity. Gas exchange measurements showed a small decrease in CO₂ assimilation and an increase in C_i, yet similar g_s compared to control plants. When measured under common C_i, stomatal conductance was higher in the mutants, suggesting that the disruption of C₄ cycle activity led to a change in stomatal sensitivity to C_i or that guard cells of *C₄ F. bidentis* may be sensing C_a, rather than C_i. A method for extracting intact epidermal peels for physiological assays and downstream molecular biology applications was developed to look at expression of genes involved in CO₂ sensing, however no clear differences between WT and mutant plants were found.

Overall, this thesis used a powerful experimental design that allowed for controlling the confounding effects of evolutionary distance on comparisons between C₃ and C₄ photosynthesis by use of phylogenetically-controlled comparisons. The results show that, at least for the species tested here, the presence of C₄ photosynthesis indeed has implications for stomatal regulation beyond the commonly found decrease in maximal conductance. Regulation of movements in response to both light and to CO₂ were found to be affected, although distinct species-specific differences not associated with the photosynthetic pathway were also observed. Disrupting the C₄ cycle also seemed to affect stomatal responses to CO₂, demonstrating the strong link between stomatal regulation and the underlying mesophyll processes.

5.2 Discussion and Future work

5.2.1 Using phylogenetically-controlled comparisons is essential in understanding C₄ photosynthesis.

The C₄ syndrome evolved independently in more than 60 plant species from different evolutionary lineages [106], suggesting that the genomic changes associated with phenotypic

changes are not necessarily linked to the C₄ photosynthetic pathway [127]. For example, contrasting blue light responses in C₃ and C₄ were observed in crop species [146], but the findings could not be directly linked to photosynthetic type alone because the species examined were separated by considerable phylogenetic distance. Chapter 2 demonstrated the advantage of using phylogenetically-controlled comparisons to characterise differences between C₃ and C₄ comparisons while addressing the potential confounding effect of evolutionary distance. In addition to being representative of the three main decarboxylation subtypes [105], the individual genera allowed comparisons between C₃ and C₄ stomatal responses in the context of both the elliptic-shaped stomata common to the dicots and dumbbell-shaped stomata of the monocots. The findings also suggest that the evolution of C₄ photosynthesis in the dicots may have led to a change in light-regulated stomatal movements and challenge the general nature of previously observed stomatal morphological differences between C₃ and C₄ congeners. Similarities between C₃ and C₄ pairs were also highlighted, e.g., in *Alloteropsis*, where both the C₃ and C₄ subspecies had an increased stomatal aperture due to blue light, further strengthening the case for controlling for effects of evolution. Beyond this work, it is crucial to emphasise the impact of phylogenetic distance in studies attempting to characterise the evolution of C₄ pathway, the variety of traits associated with the C₄ syndrome, and their responses to wide ranging environmental variables.

5.2.2 Insensitivity to blue light and limited contributions from mitochondrial respiration may underlie stomatal movements in C₄ dicot stomata.

Blue light-induced stomatal opening is independent of photosynthesis [117] and involves the activation of guard cell PM H⁺-ATPase. The blue light photoreceptor, phototropin, via HT1 and CBC1/2 [43], promotes phosphorylation of the penultimate C-terminal residue of this enzyme. Chapter 2 compared pairs of C₃ and C₄ species from Cleomaceae, *Flaveria*, and *Alloteropsis* in terms of stomatal opening responses to blue light and found that C₄ dicots had diminished blue light-induced stomatal opening response while their C₃ cousins were more responsive. A hypothesis for the function of decreased response to blue light in C₄ dicots tested here could be related to achieving an optimal temperature for C₄ photosynthesis, which is higher by 5-10°C compared to C₃s [141]. Although this hypothesis should be confirmed in future work, low stomatal aperture affects evaporative cooling and conservation of leaf temperature in an optimal range. This is important for maintaining CO₂ assimilation

rates, which, in turn, affects the potential harvestable yield [101]. Interestingly, this is in line with the suggested role of PHOTs expression, given that PHOTs also serve thermosensory functions [29], while also promoting evapotranspiration and leaf cooling in high-temperature conditions in *Arabidopsis* [54]. In addition, Chapter 3 used a pioneering approach to investigate CO₂ responses in C₃ and C₄ dicot pairs from Cleomaceae and *Flaveria*. We found that C₄ dicots responded to low CO₂ but only under red light. The findings in the chapter also seem to confirm the hypothesis that stomata in C₄ dicots may have evolved to be more sensitive to sub-ambient C_i. This feature of C₄ photosynthesis seems to suggest that stomatal opening in C₄ dicots relies more on CO₂ assimilation rate rather than their C₃ counterparts. Taken together, the insensitivity to blue light, when considered alongside the findings from Chapter 3 of the sensitivity of C₄ dicot guard cells to sub-ambient CO₂, appear to be a feature common to the C₄ dicots studied here as a strategy to increase efficiency of water use, the amount of carbon gained per unit water lost, both by limiting water loss and optimising CO₂ assimilation rate. This seems to be consistent with the evolutionary origins of the C₄ syndrome which is often suggested to have evolved as an adaptation to hot and arid conditions [91, 105].

5.2.3 The interaction between red light-induced stomatal opening and the CO₂ response pathway is mediated both by C_i-dependent and C_i-independent mechanisms.

In *Arabidopsis*, red light induces photosynthesis-dependent phosphorylation of threonine, the penultimate residue of PM H⁺-ATPase, leading to stomatal opening [2]. In contrast, in the presence of red light, elevated CO₂ induces guard cell PM H⁺-ATPase dephosphorylation as well as stomatal closure [4]. As the phosphorylation of PM H⁺-ATPase in guard cells is mediated by both red and blue light [48], leaves in Chapter 3 were illuminated with red light only or kept in darkness while being subjected to sub- or supra-ambient [CO₂]. While the mesophyll contributes to red light-induced stomatal opening there is also evidence supporting that red light triggers stomatal opening in detached epidermal peels, suggesting a direct guard cell response to red light [82]. In whole leaves, the red light-induced stomatal opening response was found to be dependent on photosynthesis [2]. Chapter 3's findings demonstrated that C₄ dicots guard cells exhibit heightened sensitivity to sub-ambient C_i levels, specifically when exposed to background red light. This observation implies that stomatal opening in C₄ dicots is finely tuned to CO₂ assimilation or its byproducts, in contrast to C₃ dicots.

Interestingly, Chapter 3 also reports stomatal opening even in darkness, at low CO₂, which raises the question: where do guard cells derive the energy that drives stomatal opening in the dark? In the absence of photosynthesis, the ATP and NADPH required to power stomatal opening could be supplied from GC mitochondria [117, 134].

The responsiveness of C₄ dicots to sub-ambient CO₂ levels could possibly be modulated by K⁺. Olsen et al. (2002) observed that when CO₂ levels were low, there was a reduced uptake of K⁺ by *V. faba* guard cells in response to red light. This implies that the role of K⁺ as an osmotic regulator in guard cells under red light conditions may vary depending on CO₂ levels. The addition of K⁺ also had no discernible influence on the stomatal response to red light in epidermal peels of *Arabidopsis* [147] and *V. faba* [124]. Therefore, relevant research questions could be: does sub-ambient C_i stimulate PM H⁺-ATPase phosphorylation under red light? Can K⁺ modulate g_s in C₄? If so, this could indicate a mechanism distinct from the established CO₂ signalling pathway, which should be investigated in future studies.

5.2.4 Do C₄ dicot guard cells exhibit altered sensitivity to C_i, or do they perceive C_a instead of C_i?

Chapter 4 investigated the link between mesophyll photosynthesis and stomatal movements in mutant C₄ *F. bidentis* with decreased NADP-ME activity. The gas exchange measurements were performed under red light, as blue light drives stomatal opening independent of photosynthesis. (Though Chapter 2 unequivocally demonstrated the absence or diminished blue light response in C₄ *F. bidentis*, the same red/blue light switchover experiment was performed among the antisensed lines, which also confirmed the weak blue light response in C₄ *Flaveria* species [data not shown].)

Results from Chapter 4 showed a slight reduction in CO₂ assimilation and an elevation in internal CO₂ levels (C_i) were observed in the mutant plants, while their stomatal conductance (g_s) remained comparable to that of the control plants. When assessed at common C_i levels, the mutants exhibited higher g_s, suggesting that the perturbation in the C₄ cycle activity may have altered stomatal responsiveness to C_i or possibly indicated that the guard cells in C₄ *F. bidentis* might be perceiving ambient CO₂ (C_a) rather than (C_i).

An alternative hypothesis for the increased g_s at a common C_i is that the antisense construct altered the pattern of malate flow in antisense lines, resulting to higher g_s. Malate is one of the counterions of K⁺, and the accumulation of malate may be due to the degradation of starch in guard cells, or import from mesophyll cells [21, 66]. However, in Chapter

General Discussion

4, while the whole leaf samples showed significantly lower FbNADP-ME1 transcripts in the antisense lines, these were not found for the adaxial or abaxial epidermal fractions, suggesting that guard cell metabolism was unaffected by the antisense construct. It does seem possible that guard cells in the antisense lines could have been over-accumulating malate, leading to slower closing and interpreted as increased stomatal opening at a common C_i . However, a metabolomics study suggested that malate does not participate as an osmolyte in red-light-induced stomatal opening [147]. Clearly, the subcellular compartmentation of malate needs to be studied to provide additional insight on the modulatory role of malate in guard cell function.

5.2.5 What is the functional role of CBC1/2 in CO_2 sensing in Cleomeaceae and *Flaveria* species?

Guard cells have been suggested to indirectly sense changes in C_i through fluctuations in metabolites resulting from photosynthesis or by detecting bicarbonate with a CO_2 sensing module [121], involving interactions between HT1 and MPKs, which led us to hypothesise that the altered C_i response of g_s in the NADP-ME antisense plants could be due to altered expression levels of these gene products. In *Arabidopsis*, when the atmospheric CO_2 concentration is low, the intracellular HCO_3^- concentration is also low. In this case, HT1 interacts with and phosphorylates OST1, inhibiting OST1 activity. SLAC1 is inactive and thus stomata remain open [130]. However, RT-qPCR quantification showed that neither HT1 nor MPK12 transcripts were significantly different between the WT and mutant lines. OPEN STOMATA 1 (OST1), a kinase which is essential for the activation of the SLAC1 anion channel [90] and stomatal closing [130], was also investigated, but silencing of NADP-ME did not affect expression of OST1 either. In general, these results indicate that the reduction of NADP-ME activity does not directly affect the initial steps of CO_2 signal transduction, at least at the transcript level in C_4 *F. bidentis*.

CONVERGENCE OF BLUE LIGHT AND CO_2 1/2 (CBC1/2) link blue light and concentrations of low CO_2 in guard cells of C_3 *Arabidopsis* [43]. AtCBC1/2 have homologues in C_4 *F. bidentis*, with 77 and 82% homology, respectively (Munekage, email comm.). CBC1/2 were part of the original panel of transcripts that we set out to investigate, but for practical reasons, had to be dropped from the list. It remains relevant, however, in the discussion of CO_2 sensing because CBCs integrate low C_i signals with that of the action of BL. Since BL sensitivity is diminished in C_4 dicots tested in Chapters 2 and 4, it would be

insightful to ascertain the sequence of CBCs in C_4 *F. bidentis* and characterise their functional role in the core CO_2 response pathway.

Defining a model for CO_2 -dependent stomatal responses in C_4 would help uncover underlying mechanisms and would be valuable in identifying targets for improving WUE and sustainability. Studying how plants have adapted to low CO_2 can also help to understand plant responses to future high CO_2 [128] (and references therein). Finally, further work focused on stomatal responses to CO_2 would benefit from CO_2 signaling mutants which is feasible because reproducible transformation protocols for C_4 model dicot and monocot species are available.

References

- [1] Allaway, W. (1973). Accumulation of malate in guard cells of *Vicia faba* during stomatal opening. *Planta*, 110:63–70.
- [2] Ando, E. and Kinoshita, T. (2018). Red light-induced phosphorylation of plasma membrane H⁺-ATPase in stomatal guard cells. *Plant Physiology*, 178(2):838–849.
- [3] Ando, E. and Kinoshita, T. (2019). Fluence rate dependence of red light-induced phosphorylation of plasma membrane h⁺-ATPase in stomatal guard cells. *Plant signaling & behavior*, 14(2):1561107.
- [4] Ando, E., Kollist, H., Fukatsu, K., Kinoshita, T., and Terashima, I. (2022). Elevated CO₂ induces rapid dephosphorylation of plasma membrane H⁺-ATPase in guard cells. *New Phytologist*, 236(6):2061–2074.
- [5] Arce Cubas, L., Vath, R. L., Bernardo, E. L., Sales, C. R. G., Burnett, A. C., and Kromdijk, J. (2023). Activation of CO₂ assimilation during photosynthetic induction is slower in C₄ than in C₃ photosynthesis in three phylogenetically controlled experiments. *Frontiers in Plant Science*, 13.
- [6] Arrivault, S., Obata, T., Szecówka, M., Mengin, V., Guenther, M., Hoehne, M., Fernie, A. R., and Stitt, M. (2017). Metabolite pools and carbon flow during C₄ photosynthesis in maize: ¹³CO₂ labeling kinetics and cell type fractionation. *Journal of Experimental Botany*, 68(2):283–298.
- [7] Aubry, S., Aresheva, O., Reyna-Llorens, I., Smith-Unna, R. D., Hibberd, J. M., and Genty, B. (2016). A specific transcriptome signature for guard cells from the C₄ plant *Gynandropsis gynandra*. *Plant physiology*, 170(3):1345–1357.
- [8] Baroli, I., Price, G. D., Badger, M. R., and von Caemmerer, S. (2008). The contribution of photosynthesis to the red light response of stomatal conductance. *Plant physiology*, 146(2):737.
- [9] Bauer, H., Ache, P., Wohlfart, F., Al-Rasheid, K. A., Sonnewald, S., Sonnewald, U., Kneitz, S., Hetherington, A. M., and Hedrich, R. (2013). How do stomata sense reductions in atmospheric relative humidity? *Molecular Plant*, 6(5):1703–1706.
- [10] Bertolino, L. T., Caine, R. S., and Gray, J. E. (2019). Impact of stomatal density and morphology on water-use efficiency in a changing world. *Frontiers in plant science*, 10:225.

References

- [11] Bläsing, O. E., Westhoff, P., and Svensson, P. (2000). Evolution of C₄ phosphoenolpyruvate carboxylase in *Flaveria*, a conserved serine residue in the carboxyl-terminal part of the enzyme is a major determinant for C₄-specific characteristics. *Journal of Biological Chemistry*, 275(36):27917–27923.
- [12] Bowling, D. (1976). Malate-switch hypothesis to explain the action of stomata. *Nature*, 262(5567):393–394.
- [13] Bowyer, J. and Leegood, R. (1997). 2 - photosynthesis. In Dey, P. and Harborne, J., editors, *Plant Biochemistry*, pages 49–p4. Academic Press, London.
- [14] Burnett, R. W. (1972). Accurate measurement of molar absorptivities. *Journal of Research of the National Bureau of Standards. Section A, Physics and Chemistry*, 76(5):483.
- [15] Chen, Z.-H., Chen, G., Dai, F., Wang, Y., Hills, A., Ruan, Y.-L., Zhang, G., Franks, P. J., Nevo, E., and Blatt, M. R. (2017). Molecular evolution of grass stomata. *Trends in Plant Science*, 22(2):124–139.
- [16] Cheng, S., van den Bergh, E., Zeng, P., Zhong, X., Xu, J., Liu, X., Hofberger, J., de Bruijn, S., Bhide, A. S., Kuelahoglu, C., et al. (2013). The *tarenaya hassleriana* genome provides insight into reproductive trait and genome evolution of Crucifers. *The Plant Cell*, 25(8):2813–2830.
- [17] Christie, J. M. (2007). Phototropin blue-light receptors. *Annu. Rev. Plant Biol.*, 58:21–45.
- [18] Cousins, A. B., Badger, M. R., and von Caemmerer, S. (2006). Carbonic anhydrase and its influence on carbon isotope discrimination during C₄ photosynthesis. insights from antisense RNA in *Flaveria bidentis*. *Plant physiology*, 141(1):232–242.
- [19] Cousins, A. B., Baroli, I., Badger, M. R., Ivakov, A., Lea, P. J., Leegood, R. C., and von Caemmerer, S. (2007). The role of phospho enol pyruvate carboxylase during C₄ photosynthetic isotope exchange and stomatal conductance. *Plant Physiology*, 145(3):1006–1017.
- [20] Cowan, I. R. and GD, F. (1977). Stomatal function in relation to leaf metabolism and environment. *Sym. Soc. Exper. Biol.*, (31):471–505.
- [21] Daloso, D. M., Antunes, W. C., Pinheiro, D. P., Waquim, J. P., Araújo, W. L., Loureiro, M. E., Fernie, A. R., and Williams, T. C. (2015). Tobacco guard cells fix CO₂ by both Rubisco and PEPcase while sucrose acts as a substrate during light-induced stomatal opening. *Plant, Cell & Environment*, 38(11):2353–2371.
- [22] Drincovich, M. F., Casati, P., Andreo, C. S., Chessin, S. J., Franceschi, V. R., Edwards, G. E., and Ku, M. S. (1998). Evolution of C₄ photosynthesis in *Flaveria* species: isoforms of NADP-malic enzyme. *Plant Physiology*, 117(3):733–744.
- [23] Engineer, C. B., Hashimoto-Sugimoto, M., Negi, J., Israelsson-Nordström, M., Azoulay-Shemer, T., Rappel, W.-J., Iba, K., and Schroeder, J. I. (2016). CO₂ sensing and CO₂ regulation of stomatal conductance: advances and open questions. *Trends in plant science*, 21(1):16–30.

- [24] Evans, J. R., Caemmerer, S., Setchell, B. A., and Hudson, G. S. (1994). The relationship between CO₂ transfer conductance and leaf anatomy in transgenic tobacco with a reduced content of rubisco. *Functional Plant Biology*, 21(4):475–495.
- [25] Farquhar, G. D. and Sharkey, T. D. (1982). Stomatal conductance and photosynthesis. *Annual review of plant physiology*, 33(1):317–345.
- [26] Fitzsimons, P. J. and Weyers, J. D. (1986). Volume changes of *Commelina communis* guard cell protoplasts in response to K⁺, light and CO₂. *Physiologia plantarum*, 66(3):463–468.
- [27] Flütsch, S. and Santelia, D. (2021). Mesophyll-derived sugars are positive regulators of light-driven stomatal opening. *New Phytologist*, 230(5):1754–1760.
- [28] Fricker, M. and Willmer, C. (2012). *Stomata*. Springer Science & Business Media.
- [29] Fujii, Y., Tanaka, H., Konno, N., Ogasawara, Y., Hamashima, N., Tamura, S., Hasegawa, S., Hayasaki, Y., Okajima, K., and Kodama, Y. (2017). Phototropin perceives temperature based on the lifetime of its photoactivated state. *Proceedings of the National Academy of Sciences*, 114(34):9206–9211.
- [30] Furbank, R. T., Chitty, J. A., Jenkins, C. L., Taylor, W. C., Trevanion, S. J., von Caemmerer, S., and Ashton, A. R. (1997). Genetic manipulation of key photosynthetic enzymes in the C₄ plant *Flaveria bidentis*. *Functional Plant Biology*, 24(4):477–485.
- [31] Furbank, R. T., Chitty, J. A., Von Caemmerer, S., and Jenkins, C. L. (1996). Antisense RNA inhibition of RbcS gene expression reduces Rubisco level and photosynthesis in the C₄ plant *Flaveria bidentis*. *Plant Physiology*, 111(3):725–734.
- [32] Furbank, R. T., Hatch, M. D., and Jenkins, C. L. (2000). C₄ photosynthesis: mechanism and regulation. *Photosynthesis: physiology and metabolism*, pages 435–457.
- [33] Furumoto, T., Izui, K., Quinn, V., Furbank, R. T., and von Caemmerer, S. (2007). Phosphorylation of phosphoenol pyruvate carboxylase is not essential for high photosynthetic rates in the C₄ species *Flaveria bidentis*. *Plant Physiology*, 144(4):1936–1945.
- [34] Gehlen, J., Panstruga, R., Smets, H., Merkelbach, S., Kleines, M., Porsch, P., Fladung, M., Becker, I., Rademacher, T., Häusler, R. E., et al. (1996). Effects of altered phosphoenol pyruvate carboxylase activities on transgenic C₃ plant *Solanum tuberosum*. *Plant Molecular Biology*, 32:831–848.
- [35] Goh, C.-H. (2009). Phototropins and chloroplast activity in plant blue light signaling. *Plant signaling & behavior*, 4(8):693–695.
- [36] Gowik, U. and Westhoff, P. (2011). The path from C₃ to C₄ photosynthesis. *Plant Physiology*, 155(1):56–63.
- [37] Hall, J. C., Sytsma, K. J., and Iltis, H. H. (2002). Phylogeny of capparaceae and brassicaceae based on chloroplast sequence data. *American Journal of Botany*, 89(11):1826–1842.

References

- [38] Hanson, D. T., Stutz, S. S., and Boyer, J. S. (2016). Why small fluxes matter: the case and approaches for improving measurements of photosynthesis and (photo) respiration. *Journal of Experimental Botany*, 67(10):3027–3039.
- [39] Harrison, E. L., Arce Cubas, L., Gray, J. E., and Hepworth, C. (2020). The influence of stomatal morphology and distribution on photosynthetic gas exchange. *The Plant Journal*, 101(4):768–779.
- [40] Hashimoto, M., Negi, J., Young, J., Israelsson, M., Schroeder, J. I., and Iba, K. (2006). *Arabidopsis* HT1 kinase controls stomatal movements in response to CO₂. *Nature cell biology*, 8(4):391–397.
- [41] Heckmann, D., Schulze, S., Denton, A., Gowik, U., Westhoff, P., Weber, A. P., and Lercher, M. J. (2013). Predicting C₄ photosynthesis evolution: modular, individually adaptive steps on a Mount Fuji fitness landscape. *Cell*, 153(7):1579–1588.
- [42] Hetherington, A. M. and Woodward, F. I. (2003). The role of stomata in sensing and driving environmental change. *Nature*, 424(6951):901–908.
- [43] Hiyama, A., Takemiya, A., Munemasa, S., Okuma, E., Sugiyama, N., Tada, Y., Murata, Y., and Shimazaki, K.-i. (2017). Blue light and CO₂ signals converge to regulate light-induced stomatal opening. *Nature communications*, 8(1):1284.
- [44] Hu, H., Boisson-Dernier, A., Israelsson-Nordström, M., Böhmer, M., Xue, S., Ries, A., Godoski, J., Kuhn, J. M., and Schroeder, J. I. (2010). Carbonic anhydrases are upstream regulators of CO₂-controlled stomatal movements in guard cells. *Nature cell biology*, 12(1):87–93.
- [45] Hudson, G. S., Evans, J. R., von Caemmerer, S., Arvidsson, Y. B., and Andrews, T. J. (1992). Reduction of ribulose-1,5-bisphosphate carboxylase/oxygenase content by antisense RNA reduces photosynthesis in transgenic tobacco plants. *Plant Physiology*, 98(1):294–302.
- [46] Huxman, T. E. and Monson, R. (2003). Stomatal responses of C₃, C₃-C₄ and C₄ *Flaveria* species to light and intercellular CO₂ concentration: implications for the evolution of stomatal behaviour. *Plant, Cell & Environment*, 26(2):313–322.
- [47] Iltis, H. H. and Cochrane, T. S. (2007). Studies in the Cleomaceae V: A new genus and ten new combinations for the flora of North America. *Novon: A Journal for Botanical Nomenclature*, 17(4):447–451.
- [48] Inoue, S.-i. and Kinoshita, T. (2017). Blue light regulation of stomatal opening and the plasma membrane H⁺-ATPase. *Plant Physiology*, 174(2):531–538.
- [49] Inoue, S.-i., Kinoshita, T., Matsumoto, M., Nakayama, K. I., Doi, M., and Shimazaki, K.-i. (2008). Blue light-induced autophosphorylation of phototropin is a primary step for signaling. *Proceedings of the National Academy of Sciences*, 105(14):5626–5631.
- [50] Jezek, M. and Blatt, M. R. (2017). The membrane transport system of the guard cell and its integration for stomatal dynamics. *Plant Physiology*, 174(2):487–519.

- [51] Kassambara, A. (2023). *ggpubr: 'ggplot2' Based Publication Ready Plots*. R package version 0.6.0.
- [52] Knapp, A. K. and Medina, E. (1999). Success of C₄ photosynthesis in the field: lessons from communities dominated by C₄ plants. *C₄ plant biology*, pages 251–283.
- [53] Kollist, H., Nuhkat, M., and Roelfsema, M. R. G. (2014). Closing gaps: linking elements that control stomatal movement. *New Phytologist*, 203(1):44–62.
- [54] Kostaki, K.-I., Coupel-Ledru, A., Bonnell, V. C., Gustavsson, M., Sun, P., McLaughlin, F. J., Fraser, D. P., McLachlan, D. H., Hetherington, A. M., Dodd, A. N., et al. (2020). Guard cells integrate light and temperature signals to control stomatal aperture. *Plant Physiology*, 182(3):1404–1419.
- [55] Koteyeva, N. K., Voznesenskaya, E. V., Roalson, E. H., and Edwards, G. E. (2011). Diversity in forms of C₄ in the genus *Cleome* (cleomaceae). *Annals of Botany*, 107(2):269–283.
- [56] Kromdijk, J., Głowacka, K., and Long, S. P. (2019). Predicting light-induced stomatal movements based on the redox state of plastoquinone: theory and validation. *Photosynthesis research*, 141(1):83–97.
- [57] Kromdijk, J., Ubierna, N., Cousins, A. B., and Griffiths, H. (2014). Bundle-sheath leakiness in C₄ photosynthesis: a careful balancing act between CO₂ concentration and assimilation. *Journal of Experimental Botany*, 65(13):3443–3457.
- [58] Kwak, J. M., Murata, Y., Baizabal-Aguirre, V. M., Merrill, J., Wang, M., Kemper, A., Hawke, S. D., Tallman, G., and Schroeder, J. I. (2001). Dominant negative guard cell K⁺ channel mutants reduce inward-rectifying K⁺ currents and light-induced stomatal opening in *Arabidopsis*. *Plant physiology*, 127(2):473–485.
- [59] Lambers, H. and Oliveira, R., editors (2019). *Plant Physiological Ecology*. Springer Nature, Switzerland.
- [60] Lauerer, M., Saftic, D., Quick, W., Labate, C., Fichtner, K., Schulze, E. D., Rodermeil, S., Bogorad, L., and Stitt, M. (1993). Decreased ribulose-1,5-bisphosphate carboxylase-oxygenase in transgenic tobacco transformed with “antisense” rbcS: Vi. effect on photosynthesis in plants grown at different irradiance. *Planta*, 190:332–345.
- [61] Lawson, T. (2009). Guard cell photosynthesis and stomatal function. *New Phytologist*, 181(1):13–34.
- [62] Lawson, T., Lefebvre, S., Baker, N. R., Morison, J. I., and Raines, C. A. (2008). Reductions in mesophyll and guard cell photosynthesis impact on the control of stomatal responses to light and CO₂. *Journal of Experimental Botany*, 59(13):3609–3619.
- [63] Lawson, T., Simkin, A. J., Kelly, G., and Granot, D. (2014). Mesophyll photosynthesis and guard cell metabolism impacts on stomatal behaviour. *New Phytologist*, 203(4):1064–1081.
- [64] Lawson, T., von Caemmerer, S., and Baroli, I. (2011). Photosynthesis and stomatal behaviour. *Progress in botany* 72, pages 265–304.

References

- [65] Lee, J. and Bowling, D. (1992). Effect of the mesophyll on stomatal opening in *Commelina communis*. *Journal of Experimental Botany*, 43(7):951–957.
- [66] Lee, M., Choi, Y., Burla, B., Kim, Y.-Y., Jeon, B., Maeshima, M., Yoo, J.-Y., Martinoia, E., and Lee, Y. (2008). The ABC transporter AtABCB14 is a malate importer and modulates stomatal response to CO₂. *Nature Cell Biology*, 10(10):1217–1223.
- [67] Leegood, R. C. and von Caemmerer, S. (1988). The relationship between contents of photosynthetic metabolites and the rate of photosynthetic carbon assimilation in leaves of *Amaranthus edulis* L. *Planta*, 174(2):253–262.
- [68] Leigh, A., Sevanto, S., Close, J., and Nicotra, A. (2017). The influence of leaf size and shape on leaf thermal dynamics: does theory hold up under natural conditions? *Plant, Cell & Environment*, 40(2):237–248.
- [69] Long, S. P. (1999). Environmental responses. *C₄ plant biology*, pages 215–249.
- [70] Lundgren, M. R., Besnard, G., Ripley, B. S., Lehmann, C. E., Chatelet, D. S., Kynast, R. G., Namaganda, M., Vorontsova, M. S., Hall, R. C., Elia, J., et al. (2015). Photosynthetic innovation broadens the niche within a single species. *Ecology Letters*, 18(10):1021–1029.
- [71] Lundgren, M. R., Christin, P.-A., Escobar, E. G., Ripley, B. S., Besnard, G., Long, C. M., Hattersley, P. W., Ellis, R. P., Leegood, R. C., and Osborne, C. P. (2016). Evolutionary implications of C₃–C₄ intermediates in the grass *Alloteropsis semialata*. *Plant, Cell & Environment*, 39(9):1874–1885.
- [72] Lundgren, M. R., Dunning, L. T., Olofsson, J. K., Moreno-Villena, J. J., Bouvier, J. W., Sage, T. L., Khoshravesh, R., Sultmanis, S., Stata, M., Ripley, B. S., et al. (2019). C₄ anatomy can evolve via a single developmental change. *Ecology letters*, 22(2):302–312.
- [73] Lyu, M.-J. A., Gowik, U., Kelly, S., Covshoff, S., Mallmann, J., Westhoff, P., Hibberd, J. M., Stata, M., Sage, R. F., Lu, H., et al. (2015). RNA-seq based phylogeny recapitulates previous phylogeny of the genus *Flaveria* (asteraceae) with some modifications. *BMC evolutionary biology*, 15(1):1–14.
- [74] Maherali, H., Reid, C., Polley, H., Johnson, H., and Jackson, R. (2002). Stomatal acclimation over a subambient to elevated CO₂ gradient in a C₃/C₄ grassland. *Plant, Cell & Environment*, 25(4):557–566.
- [75] Mansfield, T., Hetherington, A., and Atkinson, C. (1990). Some current aspects of stomatal physiology. *Annual review of plant biology*, 41(1):55–75.
- [76] Marshall, D. M., Muhaidat, R., Brown, N. J., Liu, Z., Stanley, S., Griffiths, H., Sage, R. F., and Hibberd, J. M. (2007). *Cleome*, a genus closely related to *Arabidopsis*, contains species spanning a developmental progression from C₃ to C₄ photosynthesis. *The Plant Journal*, 51(5):886–896.
- [77] Marshall, J. S., Stubbs, J. D., and Taylor, W. C. (1996). Two genes encode highly similar chloroplastic NADP-malic enzymes in *Flaveria* (implications for the evolution of C₄ photosynthesis). *Plant Physiology*, 111(4):1251–1261.

- [78] Matrosova, A., Bogireddi, H., Mateo-Peñas, A., Hashimoto-Sugimoto, M., Iba, K., Schroeder, J. I., and Israelsson-Nordström, M. (2015). The ht1 protein kinase is essential for red light-induced stomatal opening and genetically interacts with ost1 in red light and CO₂-induced stomatal movement responses. *New Phytologist*, 208(4):1126–1137.
- [79] Matthews, J. S., Violet-Chabrand, S., and Lawson, T. (2020). Role of blue and red light in stomatal dynamic behaviour. *Journal of Experimental Botany*, 71(7):2253–2269.
- [80] McAusland, L., Violet-Chabrand, S., Davey, P., Baker, N. R., Brendel, O., and Lawson, T. (2016). Effects of kinetics of light-induced stomatal responses on photosynthesis and water-use efficiency. *New Phytologist*, 211(4):1209–1220.
- [81] McKown, A. D., Moncalvo, J.-M., and Dengler, N. G. (2005). Phylogeny of Flaveria (asteraceae) and inference of C₄ photosynthesis evolution. *American Journal of Botany*, 92(11):1911–1928.
- [82] Messinger, S. M., Buckley, T. N., and Mott, K. A. (2006). Evidence for involvement of photosynthetic processes in the stomatal response to CO₂. *Plant physiology*, 140(2):771–778.
- [83] Michaletz, S. T., Weiser, M. D., McDowell, N. G., Zhou, J., Kaspari, M., Helliker, B. R., and Enquist, B. J. (2016). The energetic and carbon economic origins of leaf thermoregulation. *Nature plants*, 2(9):1–9.
- [84] Monson, R. K. (1996). The use of phylogenetic perspective in comparative plant physiology and development biology. *Annals of the Missouri Botanical Garden*, pages 3–16.
- [85] Mott, K. A. (1988). Do stomata respond to CO₂ concentrations other than intercellular? *Plant physiology*, 86(1):200–203.
- [86] Mott, K. A. (2009). Opinion: stomatal responses to light and CO₂ depend on the mesophyll. *Plant, Cell & Environment*, 32(11):1479–1486.
- [87] Muschak, M., Willmitzer, L., and Fisahn, J. (1999). Gas-exchange analysis of chloroplastic fructose-1,6-bisphosphatase antisense potatoes at different air humidities and at elevated CO₂. *Planta*, 209:104–111.
- [88] Mustilli, A.-C., Merlot, S., Vavasseur, A., Fenzi, F., and Giraudat, J. (2002). *Arabidopsis* OST1 protein kinase mediates the regulation of stomatal aperture by abscisic acid and acts upstream of reactive oxygen species production. *The Plant Cell*, 14(12):3089–3099.
- [89] Nations, U. (2023). Our growing population. Accessed: November 2, 2023.
- [90] Negi, J., Hashimoto-Sugimoto, M., Kusumi, K., and Iba, K. (2014). New approaches to the biology of stomatal guard cells. *Plant and Cell Physiology*, 55(2):241–250.
- [91] Osborne, C. P. and Sack, L. (2012). Evolution of C₄ plants: a new hypothesis for an interaction of CO₂ and water relations mediated by plant hydraulics. *Philosophical Transactions of the Royal Society B: Biological Sciences*, 367(1588):583–600.

References

- [92] Patchell, M. J., Roalson, E. H., and Hall, J. C. (2014). Resolved phylogeny of Cleomeaceae based on all three genomes. *Taxon*, 63(2):315–328.
- [93] Pengelly, J. J., Sirault, X. R., Tazoe, Y., Evans, J. R., Furbank, R. T., and Von Caemmerer, S. (2010). Growth of the C₄ dicot *Flaveria bidentis*: photosynthetic acclimation to low light through shifts in leaf anatomy and biochemistry. *Journal of Experimental Botany*, 61(14):4109–4122.
- [94] Pengelly, J. J., Tan, J., Furbank, R. T., and von Caemmerer, S. (2012). Antisense reduction of NADP-malic enzyme in *Flaveria bidentis* reduces flow of CO₂ through the C₄ cycle. *Plant Physiology*, 160(2):1070–1080.
- [95] Posit team (2022). *RStudio: Integrated Development Environment for R*. Posit Software, PBC, Boston, MA.
- [96] Powell, A. M. (1978). Systematics of *Flaveria* (flaveriinae–asteraceae). *Annals of the Missouri Botanical Garden*, pages 590–636.
- [97] Price, G. D., von Caemmerer, S., Evans, J. R., Siebke, K., Anderson, J. M., and Badger, M. R. (1998). Photosynthesis is strongly reduced by antisense suppression of chloroplastic cytochrome b6 complex in transgenic tobacco. *Functional Plant Biology*, 25(4):445–452.
- [98] Quick, W., Schurr, U., Scheibe, R., Schulze, E.-D., Rodermel, S., Bogorad, L., and Stitt, M. (1991). Decreased ribulose-1,5-bisphosphate carboxylase-oxygenase in transgenic tobacco transformed with “antisense” rbcS: I. impact on photosynthesis in ambient growth conditions. *Planta*, 183:542–554.
- [99] R Core Team (2022). *R: A Language and Environment for Statistical Computing*. R Foundation for Statistical Computing, Vienna, Austria.
- [100] Ritz, C., Baty, F., Streibig, J. C., and Gerhard, D. (2015). Dose-response analysis using R. *PLOS ONE*, 10(e0146021).
- [101] Roberts, J., Tranbarger, T., Wagstaff, C., Wingler, A., Dijkwel, P., Stewart, D., Zhang, J., Rasmussen, A., and Lu, C. (2018). *Annual Plant Reviews online*, volume 926. Wiley Online Library.
- [102] Rodríguez, M. and Larqué-Saavedra, A. (1983). Abscisic acid accumulation in *Phaseolus vulgaris* L. with different growth habits. *Journal of Plant Growth Regulation*, 2(1-4):225.
- [103] Roelfsema, M. R. G., Hanstein, S., Felle, H. H., and Hedrich, R. (2002). CO₂ provides an intermediate link in the red light response of guard cells. *The Plant Journal*, 32(1):65–75.
- [104] Roelfsema, M. R. G., Konrad, K. R., Marten, H., Psaras, G. K., Hartung, W., and Hedrich, R. (2006). Guard cells in albino leaf patches do not respond to photosynthetically active radiation, but are sensitive to blue light, CO₂ and abscisic acid. *Plant, Cell & Environment*, 29(8):1595–1605.
- [105] Sage, R. F. (2004). The evolution of C₄ photosynthesis. *New phytologist*, 161(2):341–370.

- [106] Sage, R. F. (2016). Tracking the evolutionary rise of C₄ metabolism. *Journal of Experimental Botany*, 67(10):2919–2922.
- [107] Sage, R. F., Christin, P.-A., and Edwards, E. J. (2011). The C₄ plant lineages of planet Earth. *Journal of Experimental Botany*, 62(9):3155–3169.
- [108] Sage, R. F. and McKown, A. D. (2006). Is C₄ photosynthesis less phenotypically plastic than C₃ photosynthesis? *Journal of Experimental Botany*, 57(2):303–317.
- [109] Sage, R. F., Monson, R. K., Ehleringer, J. R., Adachi, S., and Pearcy, R. W. (2018). Some like it hot: the physiological ecology of C₄ plant evolution. *Oecologia*, 187:941–966.
- [110] Sage, T. L., Busch, F. A., Johnson, D. C., Friesen, P. C., Stinson, C. R., Stata, M., Sultmanis, S., Rahman, B. A., Rawsthorne, S., and Sage, R. F. (2013). Initial events during the evolution of C₄ photosynthesis in C₃ species of *Flaveria*. *Plant physiology*, 163(3):1266–1276.
- [111] Sakamoto, K. and Briggs, W. R. (2002). Cellular and subcellular localization of phototropin 1. *The Plant Cell*, 14(8):1723–1735.
- [112] Sales, C. R., da Silva, A. B., and Carmo-Silva, E. (2020). Measuring Rubisco activity: challenges and opportunities of NADH-linked microtiter plate-based and 14C-based assays. *Journal of Experimental Botany*, 71(18):5302–5312.
- [113] Sales, C. R., Degen, G. E., da Silva, A. B., and Carmo-Silva, E. (2018). Spectrophotometric determination of Rubisco activity and activation state in leaf extracts. *Photosynthesis: methods and protocols*, pages 239–250.
- [114] Santelia, D. and Lawson, T. (2016). Rethinking guard cell metabolism. *Plant Physiology*, 172(3):1371–1392.
- [115] Schindelin, J., Arganda-Carreras, I., Frise, E., Kaynig, V., Longair, M., Pietzsch, T., Preibisch, S., Rueden, C., Saalfeld, S., Schmid, B., et al. (2012). Fiji: an open-source platform for biological-image analysis. *Nature methods*, 9(7):676–682.
- [116] Sharkey, T. D. and Raschke, K. (1981). Separation and measurement of direct and indirect effects of light on stomata. *Plant physiology*, 68(1):33–40.
- [117] Shimazaki, K.-i., Doi, M., Assmann, S. M., and Kinoshita, T. (2007). Light regulation of stomatal movement. *Annual review of plant biology*, 58(1):219–247.
- [118] Stitt, M., Quick, W., Schurr, U., Schulze, E.-D., Rodermeil, S., and Bogorad, L. (1991). Decreased ribulose-1, 5-bisphosphate carboxylase-oxygenase in transgenic tobacco transformed with ‘antisense’ rbcS: II. flux-control coefficients for photosynthesis in varying light, CO₂, and air humidity. *Planta*, 183:555–566.
- [119] Stitt, M. and Schulze, D. (1994). Does rubisco control the rate of photosynthesis and plant growth? an exercise in molecular ecophysiology. *Plant, cell & environment*, 17(5):465–487.

References

- [120] Suetsugu, N., Takami, T., Ebisu, Y., Watanabe, H., Iiboshi, C., Doi, M., and Shimazaki, K.-i. (2014). Guard cell chloroplasts are essential for blue light-dependent stomatal opening in *Arabidopsis*. *PLOS one*, 9(9):e108374.
- [121] Takahashi, Y., Bosmans, K. C., Hsu, P.-K., Paul, K., Seitz, C., Yeh, C.-Y., Wang, Y.-S., Yarmolinsky, D., Sierla, M., Vahisalu, T., et al. (2022). Stomatal CO₂/bicarbonate sensor consists of two interacting protein kinases, raf-like HT1 and non-kinase-activity requiring MPK12/MPK4. *Science Advances*, 8(49):eabq6161.
- [122] Takemiya, A., Sugiyama, N., Fujimoto, H., Tsutsumi, T., Yamauchi, S., Hiyama, A., Tada, Y., Christie, J. M., and Shimazaki, K.-i. (2013). Phosphorylation of BLUS1 kinase by phototropins is a primary step in stomatal opening. *Nature communications*, 4(1):1–8.
- [123] Talbott, L. D. and Zeiger, E. (1996). Central roles for potassium and sucrose in guard-cell osmoregulation. *Plant physiology*, 111(4):1051–1057.
- [124] Tallman, G. and Zeiger, E. (1988). Light quality and osmoregulation in *Vicia* guard cells: evidence for involvement of three metabolic pathways. *Plant physiology*, 88(3):887–895.
- [125] Taylor, S., Franks, P., Hulme, S., Spriggs, E., Christin, P., Edwards, E., Woodward, F., and Osborne, C. (2012). Photosynthetic pathway and ecological adaptation explain stomatal trait diversity amongst grasses. *New Phytologist*, 193(2):387–396.
- [126] Taylor, S. H., Aspinwall, M. J., Blackman, C. J., Choat, B., Tissue, D. T., and Ghannoum, O. (2018). CO₂ availability influences hydraulic function of C₃ and C₄ grass leaves. *Journal of Experimental Botany*, 69(10):2731–2741.
- [127] Taylor, S. H., Hulme, S. P., Rees, M., Ripley, B. S., Ian Woodward, F., and Osborne, C. P. (2010). Ecophysiological traits in C₃ and C₄ grasses: a phylogenetically controlled screening experiment. *New Phytologist*, 185(3):780–791.
- [128] Temme, A., Cornwell, W., Cornelissen, J., and Aerts, R. (2013). Meta-analysis reveals profound responses of plant traits to glacial CO₂ levels. *Ecology and Evolution*, 3(13):4525–4535.
- [129] Tetu, S. G., Tanz, S. K., Vella, N., Burnell, J. N., and Ludwig, M. (2007). The *Flaveria bidentis* β-carbonic anhydrase gene family encodes cytosolic and chloroplastic isoforms demonstrating distinct organ-specific expression patterns. *Plant Physiology*, 144(3):1316–1327.
- [130] Tian, W., Hou, C., Ren, Z., Pan, Y., Jia, J., Zhang, H., Bai, F., Zhang, P., Zhu, H., He, Y., et al. (2015). A molecular pathway for CO₂ response in *Arabidopsis* guard cells. *Nature Communications*, 6(1):6057.
- [131] Töldsepp, K., Zhang, J., Takahashi, Y., Sindarovska, Y., Hōrak, H., Ceciliato, P. H., Koolmeister, K., Wang, Y.-S., Vaahtera, L., Jakobson, L., et al. (2018). Mitogen-activated protein kinases MPK4 and MPK12 are key components mediating CO₂-induced stomatal movements. *The Plant Journal*, 96(5):1018–1035.

- [132] Trevanion, S. J., Furbank, R. T., and Ashton, A. R. (1997). NADP-malate dehydrogenase in the C₄ plant *Flaveria bidentis* (cosense suppression of activity in mesophyll and bundle-sheath cells and consequences for photosynthesis). *Plant physiology*, 113(4):1153–1165.
- [133] United Nations (2023). Sustainable development goals.
- [134] Violet-Chabrand, S., Matthews, J. S., and Lawson, T. (2021). Light, power, action! interaction of respiratory energy-and blue light-induced stomatal movements. *New Phytologist*, 231(6):2231–2246.
- [135] von Caemmerer, S., Hendrickson, L., Quinn, V., Vella, N., Millgate, A., and Furbank, R. T. (2005). Reductions of rubisco activase by antisense RNA in the C₄ plant *Flaveria bidentis* reduces Rubisco carbamylation and leaf photosynthesis. *Plant Physiology*, 137(2):747–755.
- [136] von Caemmerer, S., Lawson, T., Oxborough, K., Baker, N. R., Andrews, T. J., and Raines, C. A. (2004). Stomatal conductance does not correlate with photosynthetic capacity in transgenic tobacco with reduced amounts of Rubisco. *Journal of Experimental Botany*, 55(400):1157–1166.
- [137] Watcharamongkol, T., Christin, P.-A., and Osborne, C. P. (2018). C₄ photosynthesis evolved in warm climates but promoted migration to cooler ones. *Ecology Letters*, 21(3):376–383.
- [138] Wickham, H. (2016). *Ggplot2: Elegant graphics for data analysis*. Use R! Springer International Publishing, Cham, Switzerland, 2 edition.
- [139] Williams, B. P., Johnston, I. G., Covshoff, S., and Hibberd, J. M. (2013). Phenotypic landscape inference reveals multiple evolutionary paths to C₄ photosynthesis. *Elife*, 2:e00961.
- [140] Xu, Z., Jiang, Y., Jia, B., and Zhou, G. (2016). Elevated-CO₂ response of stomata and its dependence on environmental factors. *Frontiers in plant science*, 7:657.
- [141] Yamori, W., Hikosaka, K., and Way, D. A. (2014). Temperature response of photosynthesis in C₃, C₄, and CAM plants: temperature acclimation and temperature adaptation. *Photosynthesis research*, 119(1):101–117.
- [142] Yang, Y., Costa, A., Leonhardt, N., Siegel, R. S., and Schroeder, J. I. (2008). Isolation of a strong *Arabidopsis* guard cell promoter and its potential as a research tool. *Plant Methods*, 4(1):1–15.
- [143] Zeiger, E., Farquhar, G., and Cowan, I. (1987). *Stomatal Function*. Stanford University Press.
- [144] Zhang, J., De-oliveira Ceciliato, P., Takahashi, Y., Schulze, S., Dubeaux, G., Hauser, F., Azoulay-Shemer, T., Töldsepp, K., Kollist, H., Rappel, W.-J., et al. (2018). Insights into the molecular mechanisms of CO₂-mediated regulation of stomatal movements. *Current Biology*, 28(23):R1356–R1363.

References

- [145] Zhao, Y.-Y., Lyu, M. A., Miao, F., Chen, G., and Zhu, X.-G. (2022). The evolution of stomatal traits along the trajectory toward C₄ photosynthesis. *Plant Physiology*, 190(1):441–458.
- [146] Zhen, S. and Bugbee, B. (2020). Steady-state stomatal responses of C₃ and C₄ species to blue light fraction: Interactions with CO₂ concentration. *Plant, Cell & Environment*, 43(12):3020–3032.
- [147] Zhu, M., Geng, S., Chakravorty, D., Guan, Q., Chen, S., and Assmann, S. M. (2020). Metabolomics of red-light-induced stomatal opening in *Arabidopsis thaliana*: Coupling with abscisic acid and jasmonic acid metabolism. *The Plant Journal*, 101(6):1331–1348.